

IDENTIFICATION OF A  $Mg^{2+}/Ca^{2+}$ -SENSING SYSTEM IN  
MOUSE DISTAL CONVOLUTED TUBULE CELLS AND CHARACTERIZATION OF  
ITS ROLE IN HORMONE-STIMULATED MAGNESIUM TRANSPORT

by

BRIAN WALTER BAPT

B.Sc., The University of British Columbia, 1992

A THESIS SUBMITTED IN PARTIAL FULFILLMENT OF  
THE REQUIREMENTS FOR THE DEGREE OF  
DOCTOR OF PHILOSOPHY

in

THE FACULTY OF GRADUATE STUDIES

DEPARTMENT OF MEDICINE

EXPERIMENTAL MEDICINE,  
NEPHROLOGY

We accept this thesis as conforming  
to the required standard

THE UNIVERSITY OF BRITISH COLUMBIA

April 30, 1999

© Brian W. Bapt 1999.

In presenting this thesis in partial fulfilment of the requirements for an advanced degree at the University of British Columbia, I agree that the Library shall make it freely available for reference and study. I further agree that permission for extensive copying of this thesis for scholarly purposes may be granted by the head of my department or by his or her representatives. It is understood that copying or publication of this thesis for financial gain shall not be allowed without my written permission.

Department of Medicine: (Experimental Medicine) - MEDX.

The University of British Columbia  
Vancouver, Canada

Date May 4, 1999.

## ABSTRACT

Distal convoluted tubule cells of the kidney play a crucial role in the determination of the final urinary magnesium excretion. In addition to responding to changes in local divalent cation concentrations, magnesium absorption in these cells is also under the influence from a number of hormones. Immortalized mouse distal convoluted tubule cells (MDCT) retain a number of the properties of *in vivo* distal convoluted tubule cells. This study was performed to identify polyvalent-cation sensing mechanisms in MDCT cells and to describe the co-ordinated response to hormones that control magnesium reabsorption. The presence of  $\text{Ca}^{2+}$ -sensing receptor ( $\text{Ca}^{2+}$ -SR) was confirmed by sequencing a MDCT RT-PCR product that had greater than 92% identity with the published rat clone. Western blot analysis demonstrated the presence of the  $\text{Ca}^{2+}$ -SR protein. Microfluorescence studies and analysis of hormone-induced cAMP generation, were used to determine changes in the cell's physiological response to stimulation of the polyvalent cation-sensing receptor. MDCT cells respond to extracellular  $\text{Mg}^{2+}$ ,  $\text{Ca}^{2+}$ ,  $\text{Gd}^{3+}$ , and neomycin with a transient increase in  $[\text{Ca}^{2+}]_i$ . With respect to  $\text{Mg}^{2+}$  and  $\text{Ca}^{2+}$ , MDCT cells can differentiate between small concentration changes in  $\text{Mg}^{2+}$  and  $\text{Ca}^{2+}$ , even in the presence of an excess of the other cation. Evidence is provided for a separate mechanism that responds to extracellular  $\text{Mg}^{2+}$ . Parathyroid hormone (PTH), arginine vasopressin (AVP), calcitonin (CT), glucagon, and prostaglandin  $\text{E}_2$ , stimulate cAMP generation and increased the  $\text{Mg}^{2+}$  uptake rate in MDCT cells. Aldosterone potentiates this hormonal stimulation. Hormone-stimulated  $\text{Mg}^{2+}$  uptake and cAMP generation are inhibited with stimulation of the  $\text{Mg}^{2+}/\text{Ca}^{2+}$ -SR. Pre-treatment of MDCT cells with  $1,25,(\text{OH})_2 \text{D}_3$  (16 hr,  $10^{-7}$  M) increased  $\text{Mg}^{2+}$  uptake by  $78 \pm 4\%$ . Stimulation of the cation-sensing mechanism did not inhibit  $1,25,(\text{OH})_2 \text{D}_3$  stimulated  $\text{Mg}^{2+}$  transport. Accordingly, the polyvalent cation-sensing receptor present in MDCT cells has differential effects on hormone mediated transport. We conclude further still that a specific  $\text{Mg}^{2+}$ -sensing mechanism is present in MDCT cells and that this mechanism inhibits hormone mediated  $\text{Mg}^{2+}$  uptake in these cells. We infer from these studies that a cation-sensing mechanism is located in the distal convoluted tubule and plays a role in the control of distal  $\text{Mg}^{2+}$  absorption.



	0.7	Determination of $[Mg^{2+}]_i$	15
	0.8	cAMP Determination	16
	0.9	Creating and Screening a cDNA Library	16
	0.10	<i>Xenopus</i> oocyte isolation, preparation, and injection	16
	0.11	Statistical analysis	17
III		Results	17
	0.1	RT-PCR analysis of $Ca^{2+}$ -SR mRNA in MDCT cells	18
	0.2	Western Analysis of the $Ca^{2+}$ -SR in MDCT cells	18
	0.3	Intracellular $Ca^{2+}$ signaling in MDCT cells by $Ca^{2+}$ -SR activation	18
	0.4	$Ca^{2+}$ -SR activation inhibits hormone-stimulated cAMP release	29
IV		Discussion	29
Chapter 2: ATTEMPTS TO ISOLATE A SPECIFIC $Mg^{2+}$ -SENSING RECEPTOR			32
I		Background	32
III		Results	32
	0.1	Intracellular $Ca^{2+}$ signaling in MDCK, but not HEK cells, in response to $Mg^{2+}_o$	32
	0.2	Expression of the <i>Palaemon serratus</i> $Mg^{2+}$ response in <i>Xenopus</i> oocytes	33
	0.3	A $Ca^{2+}$ -SR cDNA, or related transcript, was not identified by screening a <i>Palaemon serratus</i> oocyte or MDCK cDNA library	33
IV		Discussion	34
Chapter 3. CHARACTERIZATION OF MAGNESIUM UPTAKE INFLUENCED BY PEPTIDE HORMONES ACTING THROUGH G-PROTEIN LINKED RECEPTORS.			37
I		Background	37
III		Results	39

0.1	Glucagon, arginine vasopressin, parathyroid hormone, and calcitonin stimulate cAMP release in $Mg^{2+}$ -depleted MDCT cells	39
0.2	$Mg^{2+}$ uptake in MDCT cells.	40
0.3	Glucagon stimulates $Mg^{2+}$ uptake in MDCT cells.	41
0.4	AVP stimulates $Mg^{2+}$ uptake in MDCT cells	46
0.5	Calcitonin and PTH have similar effects on $Mg^{2+}$ uptake as glucagon and AVP	46
0.6	Glucagon- and AVP-stimulated $Mg^{2+}$ entry does not require protein synthesis	46
0.7	cAMP stimulates $Mg^{2+}$ uptake in MDCT cells	48
0.8	The effect of protein kinase A and protein kinase C inhibition on hormone-stimulated $Mg^{2+}$ uptake.	50
0.9	Glucagon and calcitonin stimulated $Mg^{2+}$ uptake is inhibited with phospholipase-C inhibition	53
IV	Discussion	53
Chapter 4. THE INHIBITION OF HORMONE STIMULATED $Mg^{2+}$ UPTAKE WITH ACTIVATION OF THE POLYVALENT CATION-SENSING RECEPTOR		57
I	Background	57
III	Results	57
0.1	Activation of the $Mg^{2+}/Ca^{2+}$ -sensing mechanism inhibits hormone-stimulated cAMP release	57
0.2	Activation of $Mg^{2+}/Ca^{2+}$ -sensing diminishes hormone-stimulated $Mg^{2+}$ uptake into $Mg^{2+}$ -depleted MDCT cells.	58
0.3	Activation of $Mg^{2+}/Ca^{2+}$ -sensing does not affect cAMP stimulation of $Mg^{2+}$ uptake	64
0.4	Activation of $Mg^{2+}/Ca^{2+}$ -sensing does not inhibit amiloride-stimulated $Mg^{2+}$ uptake	67
IV	Discussion	67
Chapter 5. MINERAL CORTICOID HORMONES EFFECT $Mg^{2+}$ UPTAKE IN MDCT CELLS		70

I	Background	70
III	Results	71
0.1	Aldosterone potentiates hormone-stimulated $Mg^{2+}$ uptake	71
0.2	Aldosterone potentiates hormone-stimulated cAMP accumulation in MDCT cells.	75
0.3	Aldosterone potentiates hormone-stimulated $Mg^{2+}$ uptake and cAMP generation through de novo protein synthesis	75
0.4	Stimulation of the $Ca^{2+}$ -SR inhibits Aldosterone stimulated $Mg^{2+}$ uptake	81
IV	Discussion	87
Chapter 6. 1,25-DIHYDROXYVITAMIN $D_3$ STIMULATES $Mg^{2+}$ UPTAKE INTO MOUSE DISTAL CONVOLUTED TUBULE CELLS		82
I	Background	82
III	Results	83
0.1	1,25(OH) $_2D_3$ stimulates $Mg^{2+}$ entry in MDCT cells	83
0.2	1,25(OH) $_2D_3$ and PTH stimulate $Mg^{2+}$ uptake by separate pathways	84
0.3	Stimulation of the $Ca^{2+}$ -SR does not inhibit 1,25(OH) $_2D_3$ stimulated $Mg^{2+}$ uptake.	89
IV	Discussion	91
GENERAL CONCLUSIONS		92
GENERAL DISCUSSION		92
FUTURE RESEARCH		105
BIBLIOGRAPHY		106

## LIST OF FIGURES

Fig. 1	Model of polyvalent cation sensing receptor	2
Fig. 2	Summary of calcium and magnesium absorption along the nephron	4
Fig. 3	Agarose gel of RT-PCR products from MDCT cells	19
Fig. 4	Nucleotide sequence of MDCT RT-PCR product	20
Fig. 5	Western analysis of the $\text{Ca}^{2+}$ -SR	22
Fig. 6	External polyvalent cations stimulate transient cytosolic calcium increase	22
Fig. 7	MDCT $\text{Ca}^{2+}$ -SR is sensitive to small changes in $[\text{Mg}^{2+}]_o$ and $[\text{Ca}^{2+}]_o$ in the presence of elevated divalent cation concentrations	27
Fig. 8	The polyvalent cation sensing receptor of MDCT cells responds sensitively to $[\text{Mg}^{2+}]$ and $[\text{Ca}^{2+}]$	27
Fig. 9	Repetitive stimulation of MDCT- $\text{Ca}^{2+}$ -SR with $[\text{Mg}^{2+}]_o$ and $[\text{Ca}^{2+}]_o$	28
Fig. 10	External polyvalent cations transiently increase cytosolic $\text{Ca}^{2+}$ in MDCK but not HEK 293 cells	35
Fig. 11	Extracellular $\text{Mg}^{2+}$ (15 mM), but not $\text{Ca}^{2+}$ , evokes increases in $\text{Cl}^-$ currents in <i>Xenopus</i> oocytes injected with 50 ng prawn mRNA	36
Fig. 12	Glucagon and arginine vasopressin (AVP) stimulate cAMP accumulation in MDCT cells	43
Fig. 13	Glucagon and arginine vasopressin (AVP) stimulate $\text{Mg}^{2+}$ uptake in $\text{Mg}^{2+}$ -depleted mouse distal convoluted tubule (MDCT) cells	44
Fig. 14	Concentration-dependence of glucagon-stimulation of $\text{Mg}^{2+}$ entry in MDCT cells	45
Fig. 15	Concentration-dependence of AVP stimulation of $\text{Mg}^{2+}$ uptake in MDCT cells	46
Fig. 16	Summary of hormone induced stimulation of $\text{Mg}^{2+}$ uptake and cAMP generation in MDCT cells	49
Fig. 17	Exogenous cAMP stimulates $\text{Mg}^{2+}$ entry in MDCT cells	51
Fig. 18	The phospholipase inhibitor U73122 inhibits hormone stimulated $\text{Mg}^{2+}$ uptake	52

Fig. 19	Concentration-dependence of extracellular $Mg^{2+}$ or $Ca^{2+}$ inhibition of glucagon-stimulated cAMP	60
Fig. 20	Activation of the $Mg^{2+}/Ca^{2+}$ -sensing mechanism diminishes hormone-stimulated $Mg^{2+}$ uptake into MDCT cells	62
Fig. 21	Summary of the effects of $Mg^{2+}/Ca^{2+}$ -sensing mechanism activation on hormone-stimulated $Mg^{2+}$ uptake	63
Fig. 22	Glucagon-stimulation of $Mg^{2+}$ uptake is dependent on the concentration of extracellular $Mg^{2+}$ used to determine $d([Mg^{2+}]_i)/dt$	65
Fig. 23	Activation of $Mg^{2+}/Ca^{2+}$ sensing does not alter exogenous cAMP-mediated $Mg^{2+}$ uptake	66
Fig. 24	Activation of $Mg^{2+}/Ca^{2+}$ sensing does not alter amiloride-stimulated $Mg^{2+}$ uptake	68
Fig. 25	Aldosterone potentiates glucagon- and AVP- stimulated $Mg^{2+}$ uptake in $Mg^{2+}$ -depleted mouse distal convoluted tubule (MDCT) cells	72
Fig. 26	Aldosterone potentiates glucagon-stimulated $Mg^{2+}$ entry in MDCT cells	73
Fig. 27	Aldosterone potentiates AVP-stimulated $Mg^{2+}$ uptake in MDCT cells	74
Fig. 28	Aldosterone potentiation of hormone-stimulated $Mg^{2+}$ entry is through dihydropyridine-sensitive pathways	78
Fig. 29	Aldosterone potentiates glucagon-stimulated intracellular cAMP accumulation in a concentration-dependent manner	79
Fig. 30	Aldosterone and glucagon stimulated $Mg^{2+}$ uptake are inhibited by stimulation of the $Ca^{2+}$ -SR	80
Fig. 31	$1,25(OH)_2D_3$ stimulates $Mg^{2+}$ uptake in $Mg^{2+}$ -depleted (MDCT) cells	85
Fig. 32	Concentration-dependence of $1,25(OH)_2D_3$ -stimulation of $Mg^{2+}$ entry in MDCT cells	86
Fig. 33	Summary of $1,25(OH)_2D_3$ -stimulated $Mg^{2+}$ uptake in MDCT cells	87
Fig. 34	PTH stimulates cAMP formation and $Mg^{2+}$ entry into MDCT cells	88
Fig. 35	Summary of the effects of activation of $Mg^{2+}/Ca^{2+}$ -sensing on hormone-stimulated $Mg^{2+}$ uptake	90
Fig. 36	Model of the inhibitory effects of $Mg^{2+}/Ca^{2+}$ sensing on hormone-stimulated $Mg^{2+}$ uptake in the DCT	104

## LIST OF TABLES

Table 1	Polyvalent cations stimulate cytosolic $\text{Ca}^{2+}$ transients in MDCT cells	23
Table 2	Activation of $\text{Ca}^{2+}$ -SR inhibits hormone-stimulated cAMP release	30
Table 3	Glucagon and AVP stimulate cAMP release in magnesium-depleted MDCT cells	41
Table 4	Hormone-stimulated $\text{Mg}^{2+}$ uptake in MDCT cells is dihydropyridine sensitive	42
Table 5	Role of protein synthesis on glucagon stimulated $\text{Mg}^{2+}$ uptake in MDCT cells	48
Table 6	Glucagon and AVP act, in part, through protein kinase A-mediated pathway	50
Table 7	Activation of $\text{Mg}^{2+}/\text{Ca}^{2+}$ -sensing inhibits hormone-stimulated cAMP accumulation	59
Table 8	Aldosterone potentiates hormone-stimulation of cAMP accumulation in MDCT cells	70
Table 9	Role of protein synthesis on glucagon-stimulated $\text{Mg}^{2+}$ uptake and cAMP release in MDCT cells	77
Table 10	$1,25(\text{OH})_2\text{D}_3$ does not stimulate $\text{Mg}^{2+}$ uptake through a protein kinase A pathway	89
Table 11	Comparison of data obtained from MDCT cells and data from intact distal tubules	103

### LIST OF ABBREVIATIONS:

General	$\text{Ca}^{2+}$ -SR	$\text{Ca}^{2+}$ -sensing receptor outside the parathyroid gland
	$\text{Mg}^{2+}$ -SR	putative $\text{Mg}^{2+}$ -sensing receptor
	$\text{Mg}^{2+}/\text{Ca}^{2+}$ -SR	$\text{Mg}^{2+}$ and $\text{Ca}^{2+}$ sensing system where one or both may be present
	Casr	$\text{Ca}^{2+}$ -sensing receptor in the parathyroid gland as defined by Brown <i>et al</i> (4)
	total RNA, RNA	total ribonucleic acid isolated from a cell
	mRNA	RNA isolated containing a poly-adenosine tail
	cDNA	single strand deoxy-ribonucleic acid complementary to mRNA
	PCR	polymerase chain reaction
	RT-PCR	reverse transcribed polymerase chain reaction; amplification from cDNA strand
	$\text{Mg}^{2+}, \text{Ca}^{2+}, \text{Cl}^{-}, \dots$	ionic (unbound) state of specific element
	$[\text{Mg}^{2+}]_i, [\text{Ca}^{2+}]_i, [\text{Cl}^{-}]_i, \dots$	concentration of specified ion within the cell
	$[\text{Mg}^{2+}]_o, [\text{Ca}^{2+}]_o, [\text{Cl}^{-}]_o, \dots$	concentration of specified ion outside the cell
Anatomical	TAL	thick ascending limb
	DCT	distal convoluted tubule
	CNT	connecting tubule
	CCD	cortical collecting duct
	mCD	medullary collecting duct
	TPTXed	thyroparathyroid ectomized
Cell lines	MDCT	mouse distal convoluted tubule

	MDCK	Madin Darby canine kidney
	AtT-20	mouse pituitary cell line
	HEK	human embryonic kidney
	CHO	Chinese hamster ovary
hormones	Aldo	aldosterone
	AVP	arginine vasopressin
	CT	calcitonin
	Glu	glucagon
	PTH	parathyroid hormone (bovine PTH,1-34)
messengers	GDP	guanosine diphosphate
	GTP	guanosine triphosphate
	cAMP	cyclic adenosine monophosphate
	IP <sub>3</sub> , PIP <sub>2</sub>	inositol tri-phosphate
	G-protein	heterotrimeric GTP/GDP binding protein, contains $\alpha$ , $\beta$ , and $\gamma$ subunits
	G <sub>i</sub>	G $\alpha_i$ (inhibitory) subunit released from G-protein
	G <sub>s</sub>	G $\alpha_s$ (stimulatory) subunit released from the G-protein
	G <sub>o</sub>	any of a number of other identified type of G $\alpha$ subunit
	20-HETE	20-hydroxyeicosatetraenoic acid
	PLA <sub>2</sub>	phospholipase A <sub>2</sub>
	PKA	protein kinase A
	PKC	protein kinase C
	PLC	phospholipase C
toxins, blockers,	Neo	neomycin
and agonists	Rp-cAMP	cyclic adenosine monophosphate Rp-isomer
	PMA	Phorbol 12-myristate 14-acetate
	IBMX	3-isobutyl-1-methylxanthine

**ACKNOWLEDGMENT:**

I would like to thank Dr. Peter A. Freidman for providing the MDCT cell line. Dr. Allen Spiegel and Dr. Paul Goldsmith (Metabolic Diseases Branch, NIDDK/NIH, Bethesda, MD, USA) for the ADD antibody. Dr.'s Marie and Henrie Goudeau for the prawn oocytes, and Lucie Canaff and Dr. Geoffrey Hendy (Departments of Medicine, Physiology and Human Genetics, McGill University and Royal Victorian Hospital, Montreal Quebec,) for Western blot contributions and independent PCR data corroboration. In addition I would like to thank Dr. Gary Quamme for his guidance, patience, and support throughout this work. I am grateful also for the efforts and friendship of Dr. Long-Jun Dai, Gordon Ritchie, and Don Huysmans.

## General Introduction

The epithelial cells of the kidney are intrinsically responsive to their changing environment and yet are under hormonal control. In the epithelium of the nephron, where the apical membrane is in contact with the tubular fluid and the basolateral membrane is in contact with the blood, the cells are in contact with two different environments. The body's nutrient requirements are coordinated as dictated by hormonal signals, in the face of a changing environment. Accordingly the epithelium must detect these changes and respond appropriately. One class of extracellular sensors that cells can use for detecting changes in their environment, and hormonal signals from other cells, are G-protein coupled receptors.

### *I. The $\text{Ca}^{2+}$ -Sensing receptor ( $\text{Ca}^{2+}$ -SR) and its Localization Along the Nephron.*

The G-protein coupled receptor superfamily of proteins are seven predicted hydrophobic trans membrane segments. With associated G-protein alpha subunits they have the ability to stimulate the exchange of bound GDP for GTP in response to agonist binding [1]. The superfamily is subdivided into six families (A-F) which are again subdivided into groups. Families of receptors contain 20% or more sequence identity over the predicted transmembrane segments. Sub-groups share common biochemical properties. Only families A, B, and C occur in vertebrates with family C further restricted to mammals [2,3]. Families D, E, and F are restricted to fungi and slime molds [2,3].

The  $\text{Ca}^{2+}$ -SR, which responds to polyvalent cations such as magnesium, gadolinium and neomycin, was first cloned by Brown *et al.* from bovine parathyroid gland where it is involved with the control of parathyroid hormone (PTH) secretion [4]. This is a family C receptor is related to metabotropic receptors and a newly identified multigene family of pheromone receptors [5]. The  $\text{Ca}^{2+}$ -SR contains three major domains: 1) a large extracellular amino-terminal domain consisting of 613 amino acids which is thought to possess the cation binding sites, 2) a 250 amino acid domain with seven predicted membrane spanning segments characteristic of the superfamily of G protein-coupled receptors, and 3) a carboxyl

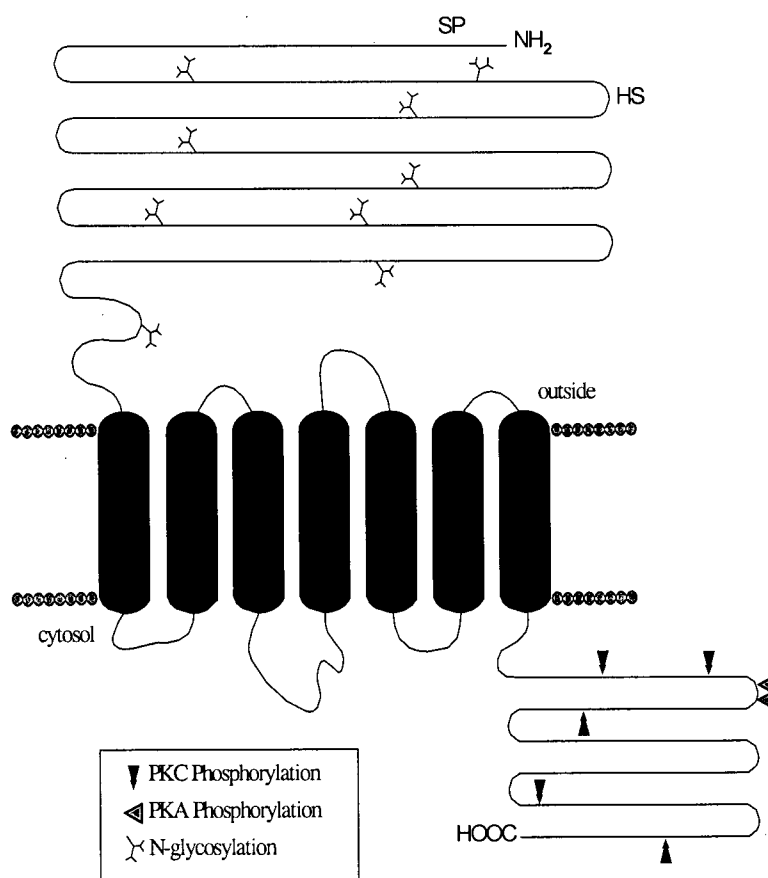


Fig. 1 Model of the  $\text{Ca}^{2+}$ -SR [4]. SP, predicted signal peptide; HS, hydrophobic segment.

terminal domain of 222 amino acids that likely resides within the cytoplasm and is involved with intracellular signalling processes [4] (Fig. 1). There is evidence that extracellular polyvalent cations bind to the extracellular domain initiating a number of intracellular signals [5,6,7,8].

The human receptor is coded for by a single gene located at chromosome 3q13.3-q21 [9]. The  $\text{Ca}^{2+}$ -SR found in the parathyroid gland has been shown to be present in bovine, rat, mouse, and human kidneys [4,10,11,12,13]. The  $\text{Ca}^{2+}$ -SR has been localized along the nephron with immuno-fluorescence, in situ hybridization, Northern analysis, as well as RT-PCR techniques [10-16]. Relative abundance, apical or basolateral orientation, and mechanism of action vary along the nephron (Fig. 2) [14].

Using RT-PCR the  $\text{Ca}^{2+}$ -SR receptor has been identified in the glomerulus [11,17]. Immuno-fluorescence, however, failed to support this finding in rats, suggesting very low expression in these cells [15]. In the rat the  $\text{Ca}^{2+}$ -SR is present on the luminal border of the proximal convoluted and straight tubule with decreasing intensity from the SI to SIII segments [15]. The highest expression of the  $\text{Ca}^{2+}$ -SR is detected at the basolateral border of cortical thick ascending limb (TAL) cells and to a lesser extent in the medullary TAL [15,16]. Basolaterally located  $\text{Ca}^{2+}$ -SR was also detected in the macula densa, distal convoluted tubule (DCT) and type A intercalated cells [15]. Within the DCT cells, Riccardi *et al.* [10,15] have also reported some sub-membranous apical staining suggesting the presence of the  $\text{Ca}^{2+}$ -SR in intracellular vesicles. In the inner medullary collecting duct  $\text{Ca}^{2+}$ -SR expression was localized to the apical membrane as in the proximal tubule [10,15]. The mechanism by which the  $\text{Ca}^{2+}$ -SR affects transport in the kidney has not been fully characterized.

## II. Function of the $\text{Ca}^{2+}$ -SR:

The function of the  $\text{Ca}^{2+}$ -SR is to induce a suitable cellular response to changes in extracellular divalent cation concentrations. The complete nature of this response is not uniform and is still undefined in many of the tissues which express the  $\text{Ca}^{2+}$ -SR. When the bovine *Casr* (*Casr* used specifically for bovine parathyroid  $\text{Ca}^{2+}$ -SR) was expressed in *Xenopus leavis* oocytes the binding of agonist resulted in activation

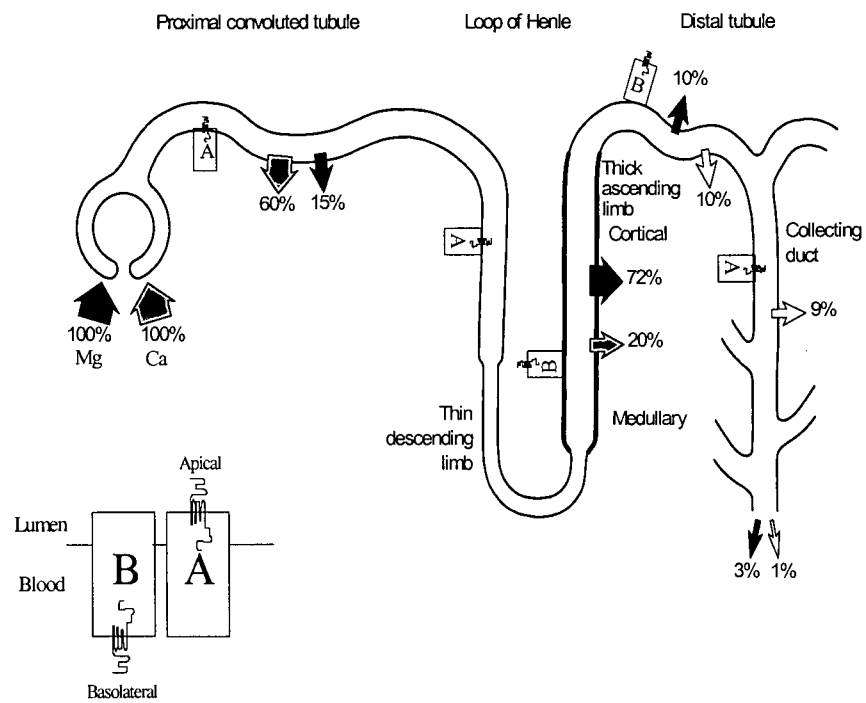


Fig. 2. Calcium and magnesium absorption (as a percent of that filtered at the glomerulus) and distribution of the calcium sensing receptors along the nephron. Insert indicated apical or basolateral presentation on the cell surface.

of phospholipase C and mobilization of intracellular  $\text{Ca}^{2+}$ , and the opening of  $\text{Ca}^{2+}$ -activated  $\text{Cl}^-$  channels [4]. This was the physiological assay used to test for expression and the method by which the receptor was originally cloned by Brown and colleagues [4].

To date, expression studies of  $\text{Ca}^{2+}$ -SR transfected into human embryonic kidney cells (HEK) have implicated a number of second messengers including  $\text{G}_i$ ,  $\text{G}_q$ ,  $\text{G}_{11}$ , G-protein stimulated phospholipase C,  $\text{A}_2$ , and D, as well as some down-stream metabolites such as arachadonic acid. [6,7]. Similar responses to this was also seen when the  $\text{Ca}^{2+}$ -SR was expressed in Chinese hamster ovary (CHO) cells [18]. When expressed in HEK cells there is evidence of a negative feedback whereby PKC phosphorylates Thr<sup>888</sup> of the  $\text{Ca}^{2+}$ -SR leading to a diminished response to  $\text{Ca}^{2+}_o$  [19]. In these studies, as well as expression studies in *Xenopus* oocytes, the hallmark of  $\text{Ca}^{2+}$ -SR stimulation an increase or and oscillation of  $[\text{Ca}^{2+}]_i$ . In vivo, however, stimulation of the  $\text{Ca}^{2+}$ -SR must be linked to appropriate physiological response from the cell. There are no endogenous  $\text{Ca}^{2+}$ -SR's in HEK, CHO cells, or *Xenopus* oocytes.

Characterization of the native  $\text{Ca}^{2+}$ -SR's response to agonists in three microdissected regions of the kidney has generated some physiological data. Previous to the cloning of the  $\text{Ca}^{2+}$ -SR, Mathias and Brown noted that an elevation of  $[\text{Ca}^{2+}]_o$  decreased PTH-dependant cAMP production in dispersed rat proximal tubule cells [8] and increasing extracellular polyvalent cations in bovine parathyroid cells lead to an increase in  $[\text{Ca}^{2+}]_i$ . In the TAL, Takaichi *et al.* noted that increasing  $\text{Ca}^{2+}_o$  results in diminished hormone-dependant cAMP production [20]. Cloning of the  $\text{Ca}^{2+}$ -SR helped to explain these observations. In TAL cells, where the highest expression of  $\text{Ca}^{2+}$ -SR in the kidney is identified, two theories have been suggested to link stimulation of the  $\text{Ca}^{2+}$ -SR with reduction in cation reabsorption. Wang *et al.* have provided compelling evidence that 20-hydroxyeicosatetraenicoic acid (20-HETE), the phospholipase  $\text{A}_2$  ( $\text{PLA}_2$ ) liberated arachadonic acid break-down product, directly inhibits the 70pS  $\text{K}^+$  channel [7]. This apically located channel contributes significantly to  $\text{K}^+$  recycling and maintenance of the lumen positive environment which is the

driving force for the movement of calcium and magnesium. In contrast, using isolated perfused tubules, Celeste *et al.*, suggest the  $\text{Ca}^{2+}$ -SR acts to inhibit  $\text{Cl}^-$  conductance through an inhibition of the cAMP pathway which does not involve protein kinase C (PKC),  $\text{PLA}_2$ , or metabolic derivatives [21]. This  $\text{Cl}^-$  current is associated with maintenance of the transepithelial voltage gradient. The characterization of a  $\text{Ca}^{2+}$ -inhibitable (Type 6) adenylate cyclase in the rat TAL [23] lends some support for this theory.

In isolated rat inner medullary collecting ducts stimulation of the apical  $\text{Ca}^{2+}$ -SR leads to a reduction in vasopressin-elicited water permeability [10]. In this case the  $\text{Ca}^{2+}$ -SR has been co-localized with  $\text{Ca}^{2+}$  dependant PKC's as well as gprotein alpha subunits  $G_q/G_{11}$ , and  $G_{i3}$ . The physiologically important affect is a reduction in insertion of aquaporin 2 into the apical membrane likely through the effect of  $G_i$  on membrane trafficking [10]. This leads to diminished water uptake and a more dilute urine. Sands and Hebert *et al* postulate that diuresis induced by hypercalciuria and hypermagnesuria in this segment inhibits renal stone formation [10].

### *III. Genetic disorders arising from mutations in the $\text{Ca}^{2+}$ -SR:*

Some insight into the role of the  $\text{Ca}^{2+}$ -SR can be inferred from familial diseases arising from mutations of the  $\text{Ca}^{2+}$ -sensing receptor. Two disorders arising from inactivating mutations in the  $\text{Ca}^{2+}$ -SR have been identified. Familial hypocalciuric hypercalcemia (FHH, also known as FBH, and FBHH), an autosomal dominant heterozygous inactivating mutation with 100% penetrance, and neonatal severe hyperparathyroidism (NSHPT, also known as NHPT), the homozygous form of FHH [24-33, and reviewed in 34,35]. FHH is generally an asymptomatic disorder, exhibiting mild hypercalcemia, mild hypermagnesemia, relative hypocalciuria, and inappropriately normal levels of PTH [34,35]. In contrast, NSHPT is life threatening without parathyroidectomy and is characterized by very high serum  $\text{Ca}^{2+}$  concentrations, hypotonia, skeletal

demineralization, respiratory distress, and parathyroid hyperplasia [34,35]. With disruption of the  $\text{Ca}^{2+}$ -SR gene, Ho *et al.* developed a transgenic mouse model for FHH and NSHPT which closely mirrors the human clinical condition of both disorders [26]. Of significant note in this study is that the elevation of serum  $\text{Mg}^{2+}$  was not significantly different in the heterozygous and homozygous mouse indicating additional mechanisms must also be present for control of serum  $\text{Mg}^{2+}$ .

Familial hypocalcemic hypercalciuria is a dominant, heterozygous, gain-of-function mutation in the *Casr* gene [31,32]. Patients demonstrate mild to severe symptoms similar to hypoparathyroidism with the exception of hypercalciuria even at low serum calcium concentrations [34,35]. The hypercalciuria is the result of the defective cation-sensing receptor in the kidney. Both activating and inactivating mutations cluster around the first third of the amino terminal, the region associated with  $\text{Ca}^{2+}$  binding, or within the transmembrane domain, likely resulting in defective G-protein coupling [29,32]. These observations have provided insight into the importance and function of the receptor in the kidney with respect to calcium balance and offer new questions as to the contributing role it may play in magnesium balance.

#### *IV. Summary of Renal Magnesium and Calcium Handling*

Control of body magnesium homeostasis principally resides within the kidney nephron. The proximal tubule reabsorbs 5-15%, the thick ascending limb of the loop of Henle absorbs 70-80% passively through the paracellular pathway, and the distal tubule actively reclaims some 5-10% of the filtered magnesium. Although the distal tubule normally reabsorbs up to 10% of the magnesium filtered through the glomerulus this amount is significant as it represents 60-70% of the magnesium delivered to this segment from the loop of Henle [36] (Fig.2). As there is little magnesium reabsorption beyond the distal tubule in the collecting ducts, the tubule segments comprising this portion of the nephron play

an important role in determining the final urinary excretion of magnesium and are, therefore, the focus of current research.

The majority of filtered calcium (60-70%) is passively reabsorbed in the proximal tubule across the paracellular pathway down its concentration gradient as salt and water are removed [37]. About 20% of the filtered calcium is absorbed in the cortical TAL segment [37]. The relatively high luminal positive voltage across the TAL epithelial cells drives cations through the paracellular pathway. About 10% of the filtered  $\text{Ca}^{2+}$  is extracted in the distal tubule (Fig. 2). Calcium absorption within the distal tubule is thought to be trans cellular and active in nature[37]. The distal tubule is composed of the distal convoluted tubule (DCT), connecting tubule (CNT), cortical connecting duct (CCD), and medullary connecting duct (CD)[38].

Little is known about the cellular mechanisms of absorption in the distal convoluted tubule because this segment is difficult to isolate for in vivo microperfusion studies. Accordingly, isolated cell lines have been used to study functional responses. We have used an immortalized mouse distal convoluted tubule (MDCT) cell line to characterize cation transport in this nephron segment. The MDCT cell line possesses amiloride-inhibitable  $\text{Na}^+$  conductance, chlorothiazide-sensitive  $\text{NaCl}$  cotransport, and hormone stimulated magnesium and calcium transport [39,40,41]. Accordingly, this established cell line has proven to be very useful in describing functions of the intact tubule.

#### *V. Objectives:*

1. To identify and characterize extracellular  $\text{Mg}^{2+}/\text{Ca}^{2+}$  sensing in an immortalized distal tubule cell line.
2. To determine the function of extracellular  $\text{Mg}^{2+}/\text{Ca}^{2+}$  sensing on hormone actions within mouse distal convoluted tubule cells.

## *VI. Experimental Rational*

The MDCT cell line has proven to be a very useful model of the in vivo distal convoluted tubule. Preliminary experiments indicated that an extracellular polyvalent cation-sensing receptor is present in MDCT cells. My experiments showed that this polyvalent cation-sensing receptor present in MDCT cells is more sensitive to extracellular  $Mg^{2+}_o$  than  $Ca^{2+}_o$ .  $Mg^{2+}$ -sensing receptors have been reported in the number of tissues including prawn oocytes so that they may be a good source in which to identify such receptors. Activation of the  $Ca^{2+}$ -sensing receptor did not inhibit basal  $Mg^{2+}$  uptake in MDCT cells but preliminary evidence suggested that it influenced hormone-dependent cAMP formation. Accordingly, we characterized hormone (PTH, calcitonin, glucagon, AVP) actions within the MDCT cells. Finally, the actions of the  $Ca^{2+}$ -SR were determined on hormone-stimulated  $Mg^{2+}$  uptake in MDCT cells. The steroid hormones, mineralocorticoids and vitamin D metabolites, were shown to stimulate  $Mg^{2+}$  entry rates by different intracellular signaling pathways. Accordingly, it was of interest to examine  $Ca^{2+}$ -SR actions on these hormones. These studies clearly demonstrate the importance of polyvalent cation-sensing receptor(s) in the MDCT cell line and by inference in the intact distal convoluted tubule.

## Chapter 1. Identification of a kidney $\text{Ca}^{2+}$ -SR in MDCT Cells.

### I. Background

The distal convoluted tubule plays an important role in salt conservation. This segment reabsorbs as much as 10% of the filtered  $\text{Mg}^{2+}$  and  $\text{Ca}^{2+}$  that are under control of many hormones including PTH, calcitonin, glucagon, and vasopressin [37]. Accordingly, isolated cell lines have been used to study functional responses. An immortalized mouse distal convoluted cell line (MDCT) has been extensively used to characterize cation transport in this nephron segment [42,43]. In the initial study, we show that a polyvalent cation-sensing mechanism is present in MDCT cells that responds sensitively and equipotently to extracellular  $\text{Mg}^{2+}$  and  $\text{Ca}^{2+}$ . The presence of polyvalent cation-sensitive receptors in this established cell line will facilitate study of their function in control of magnesium and calcium absorption within the DCT [44].

### II. *Materials and Methods*. Includes materials and methods used throughout the present study.

#### II.1. *Materials*.

Basal Dulbecco's minimal essential medium (DMEM) and Ham's F-12 media were purchased from GIBCO. Customized magnesium-free media was purchased from Stem Cell Technologies Inc. (Vancouver, BC). Fetal calf serum was from Flow Laboratories (McLean, VA). Mag-fura-2/AM was obtained from Molecular Probes (Eugene, OR). Hormones, vitamin-D, and other chemicals were purchased from Sigma (St. Louis Mo.) unless otherwise mentioned.

#### II.2. *Methods*:

##### II.2.1 *Cell Culture*:

The MDCT cell line was generated by Pizzonia *et al.* [42]. Cortical thick ascending limb and distal convoluted tubule cells were isolated from mice and established in primary culture. Transformation was

accomplished with chimeric adenovirus 12-simian virus 40 (AD12/SV40)[42]. The MDCT cell line was cultured in Dulbecco's modified Eagle's medium (DMEM)/Ham's F-12, 1:1, media supplemented with 10% fetal calf serum, 1 mM glucose, 5 mM L-glutamine, 50 U/ml penicillin, and 50 U/ml streptomycin in a humidified environment of 5% CO<sub>2</sub> and 95% air at 37°C. For the hybridization studies, MDCT cells were grown to confluence on plastic supports and harvested by scraping into buffered solution. For the fluorescent studies confluent cells were washed three times with phosphate buffered saline (PBS) containing 5mM ethylene glycol-bis(B-aminoenolyl ether) N,N,N',N',- tetraacetic acid (EGTA), trypsinized, and seeded on glass coverslips. Aliquots of harvested cells were allowed to settle onto sterile glass coverslips in 100-mm Corning tissue culture dishes, and the cells were grown to confluence over one or two days in media supplemented as described above.

#### II.2.2. RNA preparation:

Total RNA was extracted from confluent MDCT cells using TRIzol (GIBCO BRL). Briefly, cells from a 150 cm<sup>2</sup> flask were rinsed in 5 ml cold PBS, centrifuged and lysed with a 5 min incubation in TRIzol reagent. Then, 0.4 ml chloroform was added and the mixture shaken vigorously for 15 seconds. After two minutes at room temperature the mixture was centrifuged at 12,000 X g for 15 minutes and the upper aqueous phase containing the extracted RNA removed to a separated tube. RNA was precipitated from the aqueous phase with addition of an equal volume of isopropanol and centrifuged at 12,000 X g for 10 minutes at 4°C. The RNA precipitate was washed twice with 75% ice-cold ethanol, dried under vacuum, and taken up in diethyl-pyrocabonate (DEPC)-treated water. Ten micrograms of RNA were incubated with RNase free DNase (134 U) in the presence of 5 mM MgCl<sub>2</sub> at 37°C for 10 minutes. The DNase was heat inactivated with a five minute incubation at 99°C. Isolated RNA was stored in 70% ethanol at -80°C until use. For isolation of mouse cortical kidney RNA an adult mouse was euthanised with cervical dislocation and the

kidney was immediately removed and put on ice. While on ice the kidney cortex was dissected then placed in liquid nitrogen. The sample was pulverized in liquid nitrogen before TRIzol extraction.

Messenger RNA used for the creation of the cDNA library was derived from the total RNA using the Poly-Atract™ system for mRNA isolation from total RNA (Promega Madison, WI.) according to kit instructions.

### II.2.3. *Reverse Transcription-polymerase chain reaction analysis.*

Reverse-transcription-polymerase chain reaction (RT-PCR) was carried out as follows. One  $\mu\text{g}$  total RNA was taken up to 12  $\mu\text{l}$  in DEPC treated water, heated to 70°C then quickly chilled on ice. Four  $\mu\text{l}$  5 $\times$  first strand buffer (GIBCO-BRL), 2  $\mu\text{l}$  0.1 M DTT, 1  $\mu\text{l}$  10 mM dNTP mix, and 1  $\mu\text{l}$  (50  $\mu\text{M}$ ) random hexamers were added at room temperature and incubated for 5 min. The temperature was raised to 42°C and 1  $\mu\text{l}$  (200 units) of Superscript II RNase H<sup>-</sup> reverse transcriptase (GIBCO-BRL) was added and the reaction allowed to proceed for 90 min at 42°C. The reaction was heat inactivated at 70°C over 15 min. Five microliters of the RT reaction mixture was electrophoresed in 1% agarose gels, stained with ethidium bromide, to check for quantity and quality of cDNA.

One  $\mu\text{l}$  of the cDNA reaction mixture, or for the negative control 1  $\mu\text{l}$  (0.5  $\mu\text{g}/\mu\text{l}$ ) non-reverse transcribed RNA, was used as the template for PCR. The 50  $\mu\text{l}$  PCR mix included 0.5  $\mu\text{l}$  Taq Polymerase (Perkin-Elmer-Cetus), 5  $\mu\text{l}$  10 $\times$  PCR buffer, 2.5  $\mu\text{l}$  (50 mM)  $\text{MgCl}_2$ , 2  $\mu\text{l}$  10 mM dNTP mix, 36.25  $\mu\text{l}$  distilled  $\text{H}_2\text{O}$ , 1.5  $\mu\text{l}$  of each primer (15 mM). A cDNA fragment of 509 bp corresponding to the mRNA sequence encoding the majority of the transmembrane-spanning segment was amplified using the primer pair, sense 5'-GTTCCGAAACACACCTATCGTCAAG-3' and antisense 5'-TGAACCTGGCTTCGTTGAAGTTCTC-3'. The PCR amplification consisted of 32 cycles of denaturation at 94°C for 40 seconds, annealing at 55°C for 30 seconds, and polymerization at 72°C for 45 seconds, using a GeneAmp PCR system thermocycler Model 9600 (Perkin-Elmer-Cetus, Branchburg, Nj, USA).

Sequence analysis of PCR-amplified  $\text{Ca}^{2+}$ -SR product was performed after subcloning the amplified fragment into pCRII TA-cloning vector (Invitrogen, San Diego, Ca. USA) according to kit instruction. The insert was sequenced on an Applied Biosystems Model 373A gene sequencing system.

#### II.2.4. *Southern Hybridization:*

In a screw cap vial, 100ng of full length human kidney  $\text{Ca}^{2+}$ -sensing receptor DNA was made up to 9  $\mu\text{l}$ , boiled for 5 minutes, spun briefly, and stored on ice. To this was added 2  $\mu\text{l}$  10 X Klenow buffer, 2  $\mu\text{l}$  d(A,T,G,)TP (10 mM), 1  $\mu\text{l}$  random hexamer (100 pmol/ $\mu\text{l}$ ), 1  $\mu\text{l}$  Klenow, 5  $\mu\text{l}$   $^{32}\text{P}$ -dCTP (50  $\mu\text{Ci}$ ). The reaction was carried out at 37°C for 30 minutes. Unincorporated nucleotide is removed by a Sephadex G-50 spin column, equilibrated with 10 mM Tris/HCl, 1 mM EDTA (pH 7.6), and the probe collected. The probe was boiled for 5 minutes before use.

The PCR products were separated by agarose gel (1% in 1X TAE) electrophoresis and transferred by downward alkaline capillary transfer to GeneScreen. The blot was crosslinked in a UV Stratalinker (Stratagene San Diego, Ca, USA.). Membranes were pre-hybridized for 1 hour at 55°C in 30 ml hybridization buffer (0.3 g fatty acid free BSA, 10.5 ml sodium phosphate buffer, 9.0 ml de-ionized formamide, 10.5 ml 20% SDS). For hybridization, the pre-hybridization solution was removed and fresh buffer, with boiled probe was added. Hybridization proceeded overnight in a 50°C hybridization carousel. Membranes were washed 2 X 10 minutes in 250 ml 150 mM NaP/0.1% SDS. Washing was continued at 55°C with intermittent monitoring of membrane counts. When counts were sufficiently reduced the membranes were removed and exposed overnight at -70°C on Kodak X-OMAT film (Eastman Kodak, Rochester NY, USA) .

#### II.2.5. *Western blots:*

Cells were lysed in triple detergent buffer [50 mM Tris-HCl (pH 8.0), 150 mM NaCl, 0.02%  $\text{NaN}_3$ ,

0.1% SDS, 1 mM EDTA, 100  $\mu$ g/ml PMSF, 2  $\mu$ l/ml leupeptin, 2  $\mu$ g/ml aprotinin, 0.15 NP-40, 0.5% sodium deoxycholate) for five minutes on ice. The cell lysates were spun at 1200 X g, two minutes, 4°C and the supernatants stored at -80°C. Aliquotes were electrophoresed through 8% SDS-polyacrylamide gels and blotted onto polyvinylidene difluoride (PVDF) membranes (BioRad). Membranes were rinsed in TBS-Tween 20 (10 mM Tris-HCL, pH 8.0, 150 mM NaCl, 0.05% Tween 20), blocked with 5% dried milk powder in TBS-Tween 20 for 2 hours and incubated in  $\text{Ca}^{2+}$ -SR antiserum. A mouse monoclonal antibody (ADD) raised against the peptide comprising residues 214 to 236 of the  $\text{Ca}^{2+}$ -SR was used [45]. This antibody, as well as the peptide against which it was raised, was provided by Drs. P.K. Goldsmith and A.M. Spiegel (NIH, Bethesda, MD, USA) and K.V. Rodgers (NPS Pharmaceuticals, UT, USA) and has been extensively characterized with respect to specificity for the  $\text{Ca}^{2+}$ -SR [45]. As the control, immuno-blotting was carried out as above with the antiserum pre-absorbed for one hour with the peptide (10  $\mu$ g/ml) against which it was raised.

#### II.2.6. Determination of $[\text{Ca}^{2+}]_i$ .

Epifluorescence microscopy was used to monitor changes in the fura-2 fluorescence of the MDCT cells. Glass cover slips, with cells loaded with fura-2, were mounted in a plexiglass chamber containing 500  $\mu$ l buffer. The chamber was mounted on an inverted Nikon Diaphot-TMD microscope, with a Fluor x100 objective, and fluorescence was monitored under oil immersion within a single cell over the course of study. Fluorescence was recorded at 1-s intervals using a dual-excitation wavelength spectrofluorometer (Delta-scan, Photon Technologies, Princeton, NJ) with excitation at 335 and 385 nm (chopper speed set at 100 Hz) and emission at 505 nm. All experiments were performed at 23°C. Solution changes were made without an interruption in recording.

The intracellular  $\text{Ca}^{2+}$  concentration  $[\text{Ca}^{2+}]_i$  was calculated, assuming a dissociation constant of 224

nM for the Fura-2- $\text{Ca}^{2+}$  complex after correction for extracellular fura-2 and autofluorescence. The final concentration is as described by Gynkyewicz *et al* [46] and Malgaroli *et al* [47] based on the equation:

$$[\text{Ca}]_i = K_d (R - R_{\min} / R_{\max} - R) \text{Sf2/Sb2}$$

Where  $K_d$  is the disassociation constant;  $R_{\min}$  is the fluorescence ratio at the excitation wavelengths 335/385 nm for uncomplexed fura-2 (zero calcium);  $R_{\max}$  is the ratio of fluorescence at 335/385 nm for fura-2 saturated with  $\text{Ca}^{2+}$ ; Sf2 and Sb2 are the fluorescence intensities at 385 nm with zero  $\text{Ca}^{2+}$  and excess  $\text{Ca}^{2+}$ , respectfully;  $R$  is the ratio of fluorescence at wave lengths 335/385 of the sample to be measured. Dye content and instrument sensitivity are free to change between ratio measurements as they cancel.  $R$ ,  $R_{\min}$ , and  $R_{\max}$  must be measured without changing instrumentation so a bias does not occur during an experiment.

Fura-2/AM and mag-fura-2-AM are hydrophobic and thus pass easily into cells across the plasma membrane. Once inside the cell cytosolic esterases cleave the acetoxymethyl groups from the dye rendering a highly charged compound which is incapable of crossing the cell membrane. The dyes must be allowed to de-esterify as incomplete de-esterification of the dye interferes with measurements. Loaded cells were, therefore, washed twice with buffered salt solution (145 mM NaCl, 4.0 mM KCl, 1 mM  $\text{CaCl}_2$ , 0.5 mM  $\text{MgCl}_2$ , 0.8 mM  $\text{Na}_2\text{HPO}_4$ , 0.1 mM  $\text{KH}_2\text{PO}_4$ , 5 mM glucose, and 20 mM HEPES-Tris, pH 7.4 (depending on the experiment divalent cation may be removed). The cells were incubated a further 20 min to ensure complete de-esterification and finally washed once with fresh buffer solution.

In all experiments involving  $[\text{Ca}^{2+}]_i$  analysis, single traces are shown, but similar results were obtained in at least four separate experiments from independent cell preparations.

## II.2.7 Determination of $[\text{Mg}^{2+}]_i$

Coverslips were mounted into a perfusion chamber, and  $[\text{Mg}^{2+}]_i$  determined with the use of the  $\text{Mg}^{2+}$ -sensitive fluorescent dye, mag-fura-2 [48]. The cell-permeant acetoxymethyl ester (AM) form of the

dye was dissolved in dimethyl sulfoxide (DMSO) to a stock concentration of 5 mM and then diluted to 5  $\mu$ M mag-fura-2/AM in media for 20 min at 19 °C.

The free  $[Mg^{2+}]_i$  was calculated from the ratio of the fluorescence at the two excitation wavelengths as described using a dissociation constant ( $K_d$ ) of 1.4 mM for the mag-fura-2• $Mg^{2+}$  complex [48]. The minimum ( $R_{min}$ ) and maximum ( $R_{max}$ ) ratios were determined for the cells at the end of each experiment using 20  $\mu$ M digitonin.  $R_{max}$  for mag-fura-2 was determined by the addition of 50 mM  $MgCl_2$  in the absence of  $Ca^{2+}$ , and  $R_{min}$  was obtained by removal of  $Mg^{2+}$  and addition of 100 mM EDTA, pH 7.2.

#### II.2.8. *cAMP measurements*

3',5'-Cyclic adenosine monophosphate (cAMP) was determined in confluent MDCT cell monolayers cultured in 24-well plates in DMEM-Ham F-12 media without serum. After addition of various hormones, MDCT cells were incubated at 37°C for 5 min in the presence of 0.1 mM isobutylmethylxanthine (IBMX). The cAMP was extracted with 5% trichloroacetic acid that was removed with diethyl ether acidified with 0.1 N HCl. The aqueous phase was dried, dissolved in Tris-EDTA buffer, and cAMP measured with a radioimmunoassay kit (Diagnostic Products Corporation, Los Angeles, Ca, USA).

#### II.2.9. *cDNA Library*

cDNA libraries were constructed using SuperScript™ Lambda System for cDNA Synthesis and  $\lambda$  Cloning (GibcoBRL) according to kit instructions.

#### II.2.10. *Xenopus oocyte isolation, preparation, and injection*

Ovarian lobes were surgically removed from adult female *Xenopus laevis* toads anesthetized with 5.7 mM tricaine buffered to pH 7.4 with Tris base. Portions of ovarian lobes were incubated for 120 min in  $Ca^{2+}$  free buffer (5mM HEPES, 83 mM NaCl, 2 mM KCl, and 1.06 mM  $MgCl_2$  containing 0.2% collagenase

type II). Stage 5 or 6 oocytes were separated manually and washed extensively and stored overnight in buffer (96 mM NaCl, 2 mM KCl, 1.8 mM  $\text{CaCl}_2$ , 1.0 mM  $\text{Na}_2\text{HPO}_4$ , 2.5 mM Na-Pyruvate, 5.0 mM HEPES, 0.8 mM  $\text{MgCl}_2$ , titrated to 7.4 pH with NaOH, 10  $\mu\text{g}/\text{ml}$  Penicillin/Streptomycin).

Oocytes were injected using a WPI Nanolitre injector (A203XV4) with a glass pipette (5-7  $\mu\text{m}$ ). Standard injected volumes were 50 nl of water (negative control) or 50 nl mRNA (1  $\mu\text{g}/\mu\text{l}$ ) in water. oocytes were then incubated 2-3 days at 19° C in buffer.

Chloride currents were measured using standard two electrode voltage clamp techniques. Glass microelectrodes had a tip resistance of 1.5-3 M $\Omega$  when filled with 3 M KCl. Oocytes were clamped to a potential of -60 mV using a GeneClamp 500 amplifier (Axon Instruments). Current traces were recorded directly to disk. The oocytes are recorded while in (<500  $\mu\text{l}$ ) storage buffer without antibiotics and pyruvate. External  $\text{Ca}^{2+}$  and  $\text{Mg}^{2+}$  are added as experimentally required with buffer changes via total replacement.

#### II.2.11. *Statistical analysis*

Representative tracings of fluorescence intensities are given. Significance was determined by Tukey's analysis of variance or Student's *t*-test where appropriate. A probability of  $P < 0.05$  was taken to be statistically significant. All results are means  $\pm$  SE unless otherwise indicated.

### III. *Results*

In a preliminary study, with  $\text{Mg}^{2+}$ -depleted MDCT cells, we noted that 10 mM  $[\text{Ca}^{2+}]_i$  was without effect on hormone-stimulated  $\text{Mg}^{2+}$  refill, as determined with mag-fura-2, over 10-30 min of fluorescence determinations [49]. However, it was of interest in these studies that the addition of either  $[\text{Ca}^{2+}]_o$  or  $[\text{Mg}^{2+}]_o$  resulted in rapid and transient intracellular increase in  $\text{Ca}^{2+}$  concentration which prompted us to examine this cell line further for the expression of extracellular polyvalent cation-sensing receptors [44]. In the present studies, a functional polyvalent cation-sensitive receptor was shown, by two methods, to be expressed in MDCT cells [44]. First, the  $\text{Ca}^{2+}$ -SR sequence was obtained from RT-PCR amplified products of MDCT cell

mRNA, and Western analysis showed that the message was expressed in protein form. Second,  $\text{Ca}^{2+}$ -SR-stimulated intracellular  $\text{Ca}^{2+}$  concentration ( $[\text{Ca}^{2+}]_i$ ) release was determined by microfluorescence.

### III.1 *RT-PCR analysis of $\text{Ca}^{2+}$ -SR mRNA in MDCT cells.*

The primer set used here amplified a product from MDCT cell cDNA of 509-bp corresponding to a portion of the mRNA encoding the majority of the transmembrane spanning region of the  $\text{Ca}^{2+}$ -SR (Fig. 3). This was confirmed by subcloning and sequencing of the product (Fig. 4). As positive controls a similar PCR product was also obtained from AtT-20 and TT cell RNA - these cell lines have previously been reported to express the  $\text{Ca}^{2+}$ -SR [50,51,52]. As negative control, under the identical conditions of reverse transcription and amplification, no PCR product was obtained from RNA of COS-7, MC3T3-E1 or NIH3T3 cells, all previously reported to be negative for the  $\text{Ca}^{2+}$ -SR [53]. The nucleotide sequence of the MDCT RT-PCR product shared greater than 92% identity with the corresponding rat  $\text{Ca}^{2+}$ -SR sequence [13] (Fig. 4).

### III.2 *Western Analysis of the $\text{Ca}^{2+}$ -SR in MDCT cells.*

Western analysis of cell extracts from MDCT cells revealed a similar pattern of bands to that seen in parathyroid gland and kidney preparations (Fig. 5). The predominant species representing non-glycosylated and glycosylated forms ranged from 120-160 kDa with some additional higher molecular weight aggregates. The immunostaining of the bands was specifically abolished by pre-absorption of the antibody with peptide (data not shown). Extracts of COS-7 kidney cells, mouse MC3T3-E1 osteoblast-like cells and mouse NIH3T3 fibroblasts were negative for specific  $\text{Ca}^{2+}$ -SR staining (Fig. 5).

### III.3 *Intracellular $\text{Ca}^{2+}$ signalling in MDCT cells by $\text{Ca}^{2+}$ -SR activation.*

In parathyroid cells the  $\text{Ca}^{2+}$ -SR has been shown to be coupled to a  $\text{G}_q$ -protein which, upon activation, stimulates PLC activity leading to inositol 1,4,5- trisphosphate ( $\text{IP}_3$ ) generation and in turn intracellular  $\text{Ca}^{2+}$  release [54-59]. To determine if the  $\text{Ca}^{2+}$ -SR expressed in the MDCT cells is associated with similar intracellular signalling, we determined  $[\text{Ca}^{2+}]_i$  in response to extracellular polyvalent cations (Fig. 6).

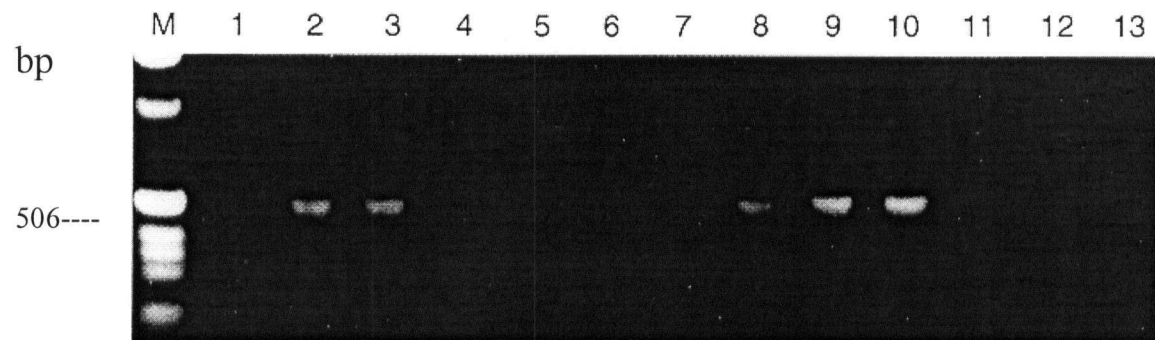


Fig. 3. RT-PCR analysis of  $\text{Ca}^{2+}$ -SR mRNA expression. Complementary DNA was synthesized from total RNA and used as template for PCR amplification. PCR products (4  $\mu\text{l}$ ) after either 24 (lanes 1-7) or 32 (lanes 8-13) cycles were electrophoresed on an ethidium-bromide-stained 1% agarose-TBE gel. Lane M, 1 kb ladder; lanes 1 and 8, MDCT; lanes 2 and 9, AtT-20; lanes 3 and 10, TT; lanes 4 and 11, COS-7; lanes 5 and 12, MC3T3-E1; lanes 6 and 13, NIH3T3; lane 7, -RT. After Southern blotting the PCR product was hybridized to a  $^{32}\text{P}$ -labelled  $\text{Ca}^{2+}$ -SR DNA probe (data not shown) [44].

<u>1</u>	<u>TTC</u>	<u>CGA</u>	<u>AAC</u>	<u>ACA</u>	<u>CCT</u>	<u>ATC</u>	<u>GTC</u>	<u>AAG</u>	<u>GCC</u>	<u>ACC</u>	<u>AAC</u>	<u>CGA</u>	<u>GAG</u>
1	phe	arg	asn	thr	pro	ile	val	lys	ala	thr	asn	arg	glu
<u>40</u>	<u>CTG</u>	<u>TCC</u>	<u>TAC</u>	<u>CTC</u>	<u>CTG</u>	<u>CTC</u>	<u>TTC</u>	<u>TCA</u>	<u>CTC</u>	<u>CTC</u>	<u>TGC</u>	<u>TGC</u>	<u>TTC</u>
14	leu	ser	tyr	leu	leu	leu	phe	ser	leu	leu	cyc	cys	phe
<u>79</u>	<u>TCC</u>	<u>AGC</u>	<u>TCC</u>	<u>CTG</u>	<u>TTC</u>	<u>TTC</u>	<u>ATT</u>	<u>GGG</u>	<u>GAG</u>	<u>CCC</u>	<u>CAG</u>	<u>GAC</u>	<u>TGG</u>
27	ser	ser	ser	leu	phe	phe	ile	gly	glu	pro	gln	gln	trp
<u>118</u>	<u>ACC</u>	<u>TGC</u>	<u>CGC</u>	<u>CTG</u>	<u>CGA</u>	<u>CAG</u>	<u>CCC</u>	<u>GCC</u>	<u>TTC</u>	<u>GGC</u>	<u>ATC</u>	<u>AGC</u>	<u>TTC</u>
40	thr	cys	arg	leu	arg	gln	pro	ala	phe	gly	ile	ser	phe
<u>157</u>	<u>GTG</u>	<u>CTT</u>	<u>TGT</u>	<u>ATC</u>	<u>TCG</u>	<u>TGC</u>	<u>ATC</u>	<u>TTG</u>	<u>GTG</u>	<u>AAG</u>	<u>ACC</u>	<u>AAT</u>	<u>CGA</u>
53	val	leu	cys	ile	ser	cys	ile	leu	val	lys	thr	asn	arg
<u>196</u>	<u>GTC</u>	<u>CTC</u>	<u>CTG</u>	<u>GTA</u>	<u>TTT</u>	<u>GAG</u>	<u>GCC</u>	<u>AAA</u>	<u>ATA</u>	<u>CCC</u>	<u>ACC</u>	<u>AGC</u>	<u>TTC</u>
66	val	leu	leu	val	phe	glu	ala	lys	ile	pro	thr	ser	phe
<u>235</u>	<u>CAC</u>	<u>CGG</u>	<u>AAG</u>	<u>TGG</u>	<u>TGG</u>	<u>GGA</u>	<u>CTC</u>	<u>AAC</u>	<u>CTG</u>	<u>CAG</u>	<u>TTC</u>	<u>CTG</u>	<u>CTG</u>
79	his	arg	lys	trp	trp	gly	leu	asn	leu	gln	phe	leu	leu
<u>274</u>	<u>GTT</u>	<u>TTC</u>	<u>CTC</u>	<u>TGC</u>	<u>ACC</u>	<u>TTC</u>	<u>ATG</u>	<u>CAG</u>	<u>ATT</u>	<u>GTC</u>	<u>ATC</u>	<u>TGC</u>	<u>ATC</u>
92	val	phe	leu	cys	thr	phe	met	gln	ile	val	ile	cys	ile
<u>313</u>	<u>ATC</u>	<u>TGG</u>	<u>CTC</u>	<u>TAC</u>	<u>ACG</u>	<u>GCA</u>	<u>CCC</u>	<u>CCC</u>	<u>TCC</u>	<u>AGC</u>	<u>TAC</u>	<u>CGC</u>	<u>AAC</u>
105	ile	trp	leu	tyr	thr	ala	pro	pro	ser	ser	tyr	arg	asn
<u>352</u>	<u>CAC</u>	<u>GAG</u>	<u>CTG</u>	<u>GAA</u>	<u>GAC</u>	<u>GAA</u>	<u>ATC</u>	<u>TTC</u>	<u>ATC</u>	<u>ACG</u>	<u>TGC</u>	<u>CAT</u>	<u>GAG</u>
118	his	glu	leu	glu	asp	glu	ile	phe	ile	thr	cys	his	glu
<u>391</u>	<u>GGC</u>	<u>TCA</u>	<u>CTC</u>	<u>ATG</u>	<u>GCG</u>	<u>CTC</u>	<u>GGC</u>	<u>TCC</u>	<u>CTG</u>	<u>ATC</u>	<u>GGC</u>	<u>TAC</u>	<u>ACC</u>
131	gly	ser	leu	met	ala	leu	gly	ser	leu	ile	gly	tyr	thr
<u>430</u>	<u>TGC</u>	<u>CTC</u>	<u>CTG</u>	<u>GCT</u>	<u>GCC</u>	<u>ATC</u>	<u>TGC</u>	<u>TTC</u>	<u>TTC</u>	<u>TTT</u>	<u>GCC</u>	<u>TTC</u>	<u>AAG</u>
144	cys	leu	leu	ala	ala	ile	cys	phe	phe	phe	ala	phe	lys
<u>469</u>	<u>TCT</u>	<u>CGG</u>	<u>AAG</u>	<u>CTG</u>	<u>CCA</u>	<u>GAG</u>	<u>AAC</u>	<u>TTC</u>	<u>AAC</u>	<u>GAA</u>	<u>GCC</u>	<u>AAG</u>	<u>TTC</u>
157	ser	arg	lys	leu	pro	gln	asn	phe	asn	glu	ala	lys	phe

Fig. 4. Nucleotide sequence of the MDCT cell RT-PCR product shown in Fig. 3. Primer sequences are underlined (with one nucleotide missing from each primer at the 5' and 3' ends of the actual PCR product). The sequence is greater than 92% homologous to the corresponding portion of the rat Ca<sup>2+</sup>-SR [44].

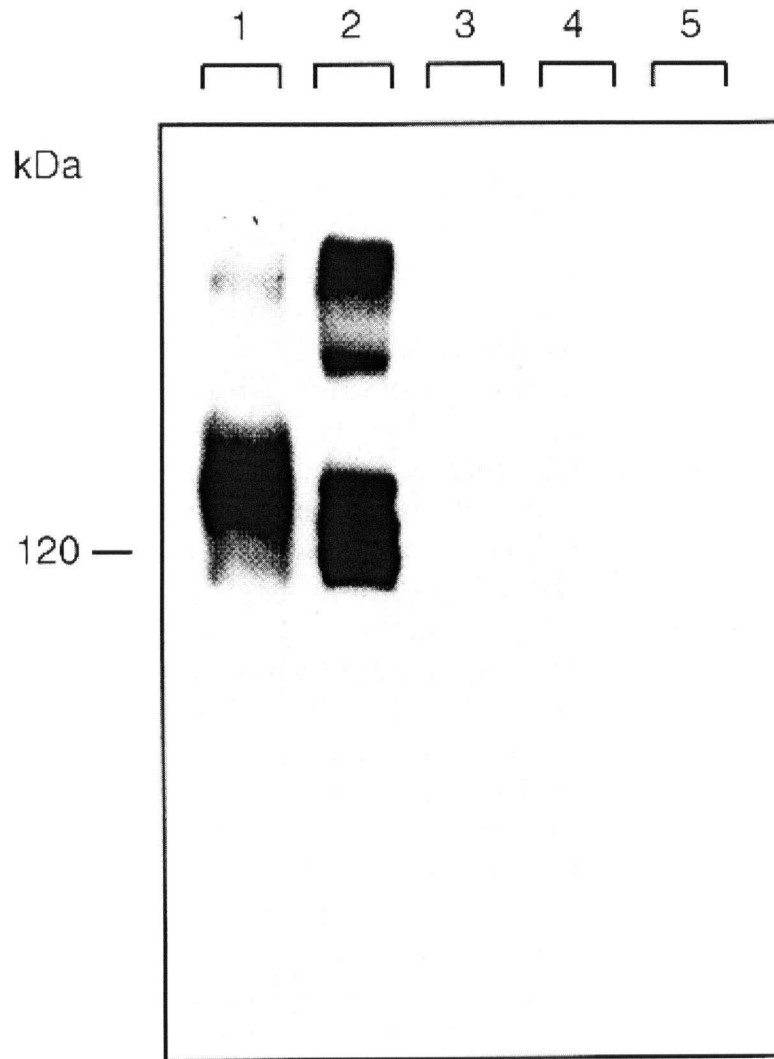


Fig. 5. Western analysis of the  $Ca^{2+}$ -SR. Cell or parathyroid gland extracts (10  $\mu$ g protein each) were subjected to SDS-PAGE on a 4-12% gradient gel. The blot was stained with  $Ca^{2+}$ -SR mouse monoclonal antibody (ADD [21]). Lane 1, MDCT cells; lane 2, rat parathyroid; lane 3, COS-7 cells; lane 4, MC3T3-E1; lane 5, NIH3T3 cells. The bands were demonstrated to be specific after staining the blot with the same antiserum pre-incubated with the peptide against which it was raised (data not shown) [44].

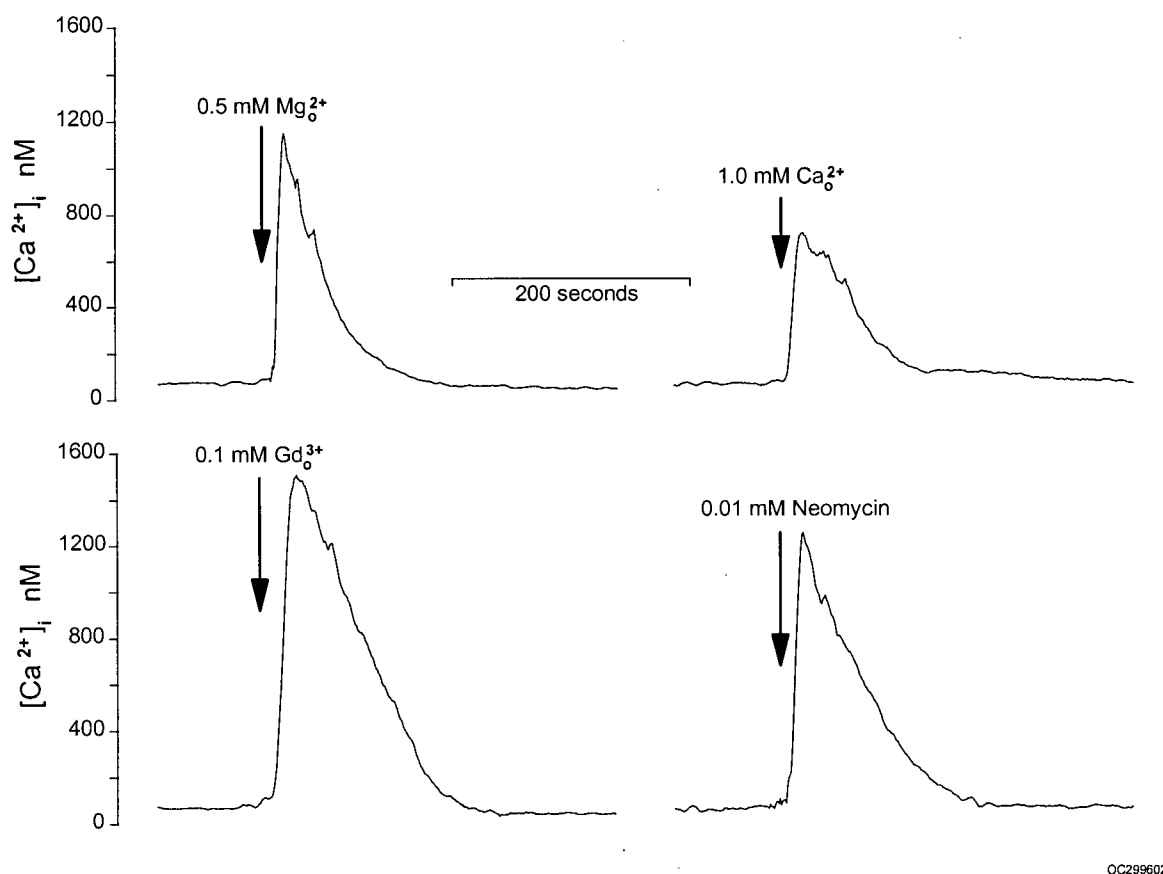


Fig. 6.

External polyvalent cations transiently increase cytosolic  $Ca^{2+}$  in MDCT cells. MDCT cells were cultured in DMEM/Ham's F-12 (1:1) with 10% fetal calf serum containing 0.6 mM magnesium and 1.5 mM calcium. The cells were loaded with fura-2 for 30 min in a buffer solution containing (in mM):  $MgCl_2$  0.5,  $CaCl_2$  1.0, NaCl 145, KCl 4.0,  $Ka_2HPO_4$  0.8,  $KH_2PO_4$  0.2, glucose 5, and HEPES-Tris 20, pH 7.4. In order to test the effect of  $[Mg^{2+}]_o$ , the buffer solution was changed to one containing the above but without  $MgCl_2$ . This bathing solution was replaced 1-2 min later with one containing 0.5 mM  $MgCl_2$ . To test  $[Ca^{2+}]_o$ , the cells were initially bathed with the above solutions containing no  $CaCl_2$ . This was replaced with one containing 1.0 mM  $CaCl_2$ . The complete buffer solution, containing 0.5 mM  $MgCl_2$  0.5, and 1.0 mM  $CaCl_2$ , was used to determine the effects of external 0.1 mM  $GdCl_3$  and 0.01 mM neomycin. Again, these were done through bath solution changes. Tracings are representative of 4-10 separate experiments [44].

MDCT cells were cultured in normal media containing 0.5 mM magnesium and 1.0 mM calcium. The cells were loaded with fura-2 for 30 min in buffer solutions containing 0.5 mM magnesium and 1.0 mM calcium; the extracellular fura-2/AM was removed with 2 x washes of nominally calcium-and magnesium-free buffer solutions and  $[Ca^{2+}]_i$  was quantified by fluorescence. The polyvalent cations (in mM):  $MgCl_2$  0.5,  $CaCl_2$  1.0,  $GdCl_3$  0.1, or neomycin 0.01, were added in buffer as indicated in Fig. 6. The cations were changed by complete replacement of bathing solutions.  $[Mg^{2+}]_o$  was tested in the presence of normal  $[Ca^{2+}]_o$  in the buffer and the effects of  $[Ca^{2+}]_o$  were determined in the presence of normal  $[Mg^{2+}]_o$ . Addition of external  $[Mg^{2+}]_o$  increased  $[Ca^{2+}]_i$  from basal levels of  $107 \pm 23$  nM to peak concentrations of  $1046 \pm 121$  nM,  $n = 6$ ,  $p < 0.05$  (Table 1).  $[Ca^{2+}]_o$  resulted in an increase in  $[Ca^{2+}]_i$  to  $732 \pm 92$  nM,  $Gd^{3+}$  to  $1637 \pm 161$  nM; and neomycin to  $1073 \pm 155$  nM from basal levels (Table 1).

**Table 1. Polyvalent cations stimulate cytosolic  $Ca^{2+}$  transients in MDCT cells.**

Extracellular Cation	Concentration mM	Response (pos/total)	Basal $[Ca^{2+}]_i$ / nM	$\Delta[Ca^{2+}]_i$ / nM
$Mg^{2+}$	0.5	(6/9)	$107 \pm 23(6)^n$	$1046 \pm 121^*(6)$
$Ca^{2+}$	1.0	(10/13)	$92 \pm 15(10)$	$732 \pm 92^*(10)$
$Gd^{3+}$	0.1	(5/8)	$93 \pm 13(5)$	$1637 \pm 161^*(5)$
Neomycin	0.01	(7/11)	$107 \pm 8(7)$	$1073 \pm 155^*(7)$

**Table 1 Legend:**

Normal MDCT cells were loaded with fura-2 and  $MgCl_2$ ,  $CaCl_2$ ,  $GdCl_3$  or neomycin added to buffer solutions at the indicated concentrations as given in legend to Fig. 3.  $\Delta[Ca^{2+}]_i$  was the maximal change in cytosolic  $Ca^{2+}$  from basal  $Ca^{2+}$  levels in those cells that responded. The cells which responded to the addition of the polyvalent cations is indicated as a fraction of the total cells studied (pos/total).  $( )^n$  is the number of separate observations and \* indicates significance,  $p < 0.05$  from basal  $[Ca^{2+}]_i$  [44]. Replacement of bathing solution

with isosmolar salt solutions, containing either NaCl or KCl, did not elicit cytosolic  $\text{Ca}^{2+}$  transients. Of 108 individual cells studied in this thesis and other reports, a total of 24 cells failed to respond to extracellular polyvalent cations. There were no differences in the number of non-responsive cells observed for each of the tested extracellular cations (Table 1). This appeared to be an all-or-none response as subsequent additions of very high concentrations of extracellular cations did not stimulate  $[\text{Ca}^{2+}]_i$  in those cells that initially did not respond. The reason for the non-responsiveness in some cells is not known. In all cases, the change in cytosolic  $\text{Ca}^{2+}$  in the positive cells was transient, returning to near basal levels within 1-2 min. The majority of the cytosolic  $\text{Ca}^{2+}$  transients were monophasic. Moreover, the responses were not dependent on the presence of extracellular  $\text{Ca}^{2+}$  indicating that the rise in  $[\text{Ca}^{2+}]_i$  was from intracellular sources. The profile of the  $\text{Ca}^{2+}$ -SR-mediated rise in cytosolic  $\text{Ca}^{2+}$  is different than the sustained rise in  $[\text{Ca}^{2+}]_i$  observed following the addition of PTH or calcitonin to MDCT cells [40,41,60]. There was no change in the mean cytosolic  $\text{Mg}^{2+}$  concentration,  $0.52 \pm 0.02$  mM,  $n = 5$ , during these manipulations as determined with the  $\text{Mg}^{2+}$ -sensitive fluorescent probe, mag-fura-2 (data not shown). These results support the notion that the MDCT cell line possesses a functional  $\text{Ca}^{2+}$ -SR which elicits a transient increase in cytosolic  $\text{Ca}^{2+}$  in response to extracellular polyvalent cations.

The relative potencies of extracellular cations in stimulating  $\text{Ca}^{2+}$ -SR-sensitive cytosolic  $\text{Ca}^{2+}$  signalling for many renal and extra-renal cells have been reported to be in the order of 3-5 mM for  $[\text{Ca}^{2+}]_o$  and about 5-20 mM for  $[\text{Mg}^{2+}]_o$  [4,12,13,56,58,59-61]. Figure 7 summarizes the changes in MDCT cytosolic  $\text{Ca}^{2+}$ , in response to  $[\text{Mg}^{2+}]_o$  and  $[\text{Ca}^{2+}]_o$ , in buffer solutions containing normal  $\text{MgCl}_2$ , 0.5 mM, and  $\text{CaCl}_2$ , 1.0 mM, concentrations. The addition of either 0.2 mM  $[\text{Mg}^{2+}]_o$  or 0.2 mM  $[\text{Ca}^{2+}]_o$  induced significant increases in cytosolic  $\text{Ca}^{2+}$  levels. Changing the bathing solution but not the  $[\text{Mg}^{2+}]_o$  concentration, 0.5 mM, had no effect on  $[\text{Ca}^{2+}]_i$  (Fig. 7, Panel A). Replacement of bathing solutions containing 0.7 mM  $\text{MgCl}_2$  (total) for normal buffer solutions (0.5 mM  $\text{MgCl}_2$ ) resulted in an increase in  $[\text{Ca}^{2+}]_i$  from basal levels of  $102 \pm 12$  to

$728 \pm 130$  nM,  $n = 4$ . Rapid replacement of normal buffer solutions with one containing 1.2 mM  $\text{CaCl}_2$  (total) resulted in an increase in  $[\text{Ca}^{2+}]_i$  to  $542 \pm 73$  nM,  $n = 4$  (Fig. 7, Panel B). Note, replacement of the normal bathing solution containing 1.0 mM  $[\text{Ca}^{2+}]_o$  did not elicit a response. Accordingly, the polyvalent cation-sensing mechanism in MDCT cells is sensitive to changes in both  $[\text{Mg}^{2+}]_o$  and  $[\text{Ca}^{2+}]_o$  within the physiological ranges of divalent cations. There may be other receptors in the MDCT cell which are sensitive to  $[\text{Mg}^{2+}]_o$  in the physiological range. The  $\text{Ca}^{2+}$ -SR has been proposed to be a  $\text{Mg}^{2+}$ -sensing receptor in addition to its role in  $\text{Ca}^{2+}$  metabolism [5,62]. There is some evidence of different binding sites for each polyvalent cation so that the receptor may respond in a selective manner to either  $[\text{Mg}^{2+}]_o$  and  $[\text{Ca}^{2+}]_o$  [62]. To test whether the MDCT  $\text{Ca}^{2+}$ -SR is responsive to  $[\text{Mg}^{2+}]_o$  independently of  $[\text{Ca}^{2+}]_o$ , we determined the response to  $\text{Mg}^{2+}_o$  in the presence of high concentrations of  $[\text{Ca}^{2+}]_o$  (Fig. 8). MDCT cells were bathed in buffer solution containing 5 mM  $\text{CaCl}_2$ , no magnesium and challenged with 0.2 mM  $\text{Mg}^{2+}_o$ . The addition of 0.2 mM  $[\text{Mg}^{2+}]_o$  stimulated a significant rise in  $[\text{Ca}^{2+}]_i$  in the presence of 5 mM  $[\text{Ca}^{2+}]_o$  (Fig. 8, Panel A). To determine the sensitivity of the  $\text{Ca}^{2+}$ -SR to  $[\text{Ca}^{2+}]_o$  in the presence of a background of high concentrations of  $\text{Mg}^{2+}_o$ , MDCT cells were immersed in a buffer solution containing 5.0 mM  $\text{MgCl}_2$ , zero calcium and 0.2 mM  $\text{CaCl}_2$  was added (Fig. 8, Panel B). The addition of 0.2 mM  $\text{CaCl}_2$  led to significant increases in  $[\text{Ca}^{2+}]_i$ . The polyvalent cation-sensitive mechanism present in MDCT cells is responsive to small changes in  $[\text{Mg}^{2+}]_o$  or  $[\text{Ca}^{2+}]_o$  in the presence of large background concentrations of extracellular calcium and magnesium, respectively. These results suggest that the  $\text{Ca}^{2+}$ -SR responds independently and equipotently to  $[\text{Ca}^{2+}]_o$  and  $[\text{Mg}^{2+}]_o$  or that there are separate receptors for the two cations. The term  $\text{Mg}^{2+}/\text{Ca}^{2+}$ -SR will, therefore, be used to indicate the response to polyvalent cations in MDCT cells.

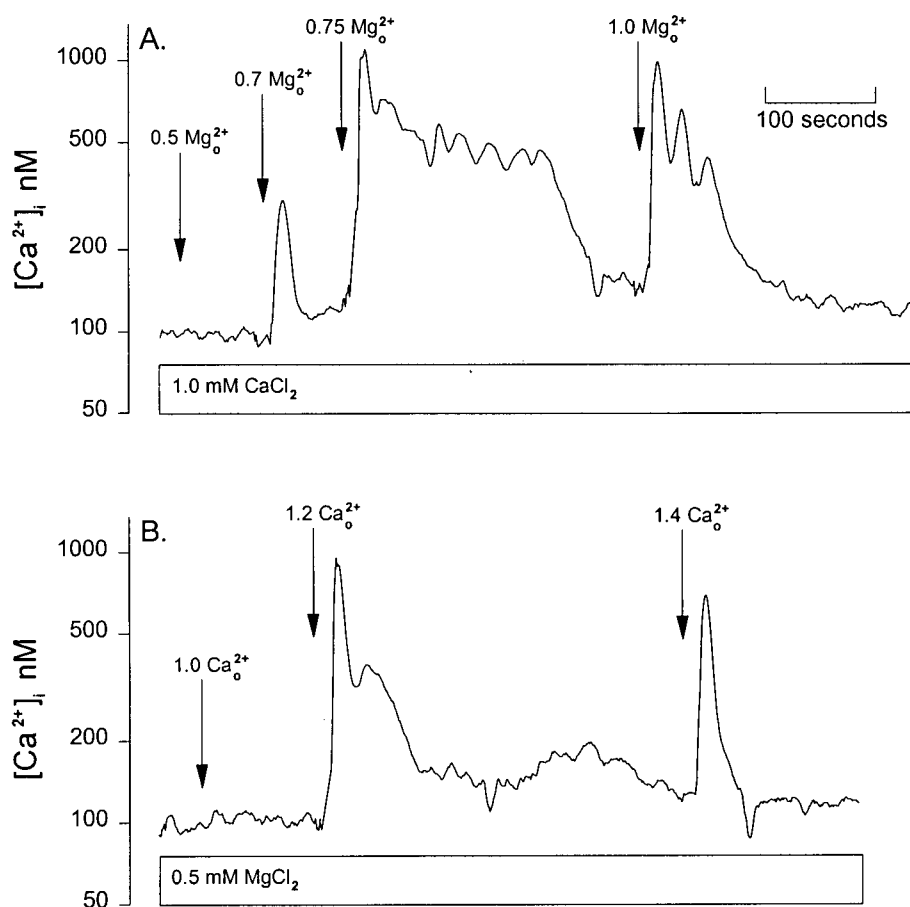
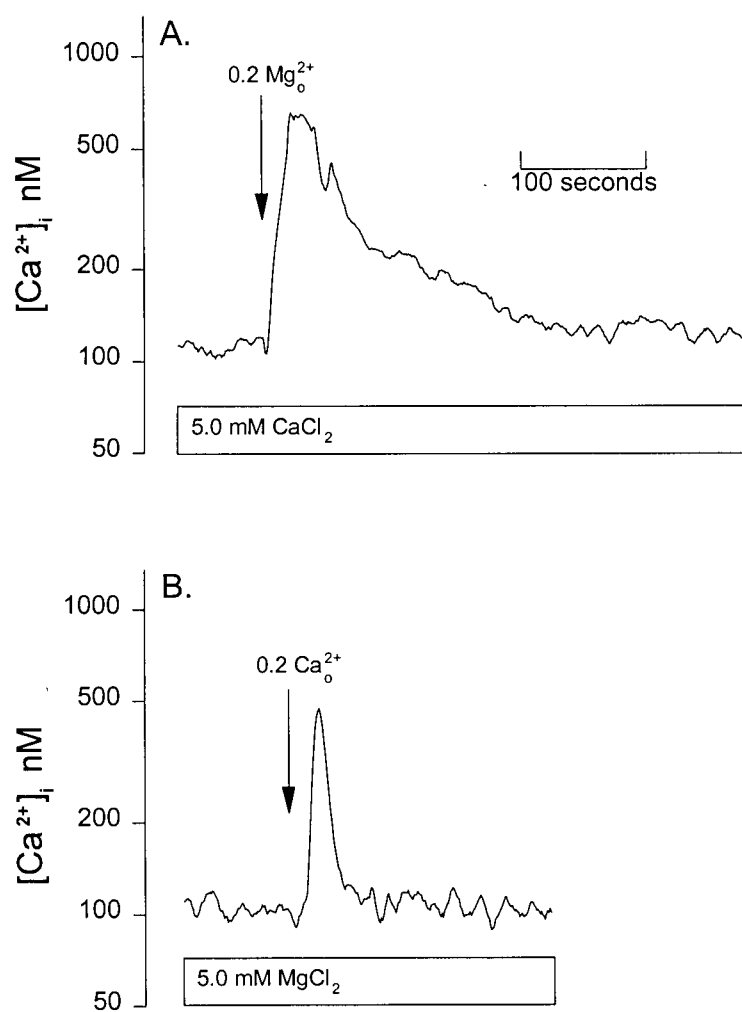


Fig. 7. The calcium sensing receptor of MDCT cells responds sensitively to  $[Mg^{2+}]$  and  $[Ca^{2+}]$ . MDCT cells were loaded with fura-2 according to the methods given in the legend to Fig. 6, but the loading and test buffer solutions contained (in mM):  $MgCl_2$  0.5,  $CaCl_2$  1.0, NaCl 145, KCl 4.0,  $Na_2HPO_4$  0.8,  $KH_2PO_4$  0.2, glucose 5, and HEPES-Tris 20 (pH 7.4).  $MgCl_2$  (A) or  $CaCl_2$  (B) were added by changing buffer solutions containing the concentrations shown. Tracings are representative of 4 to 5 separate experiments [44].



DE059602

Fig. 8. The  $Ca^{2+}$ -SR of MDCT cells is sensitive to small changes in  $[Mg^{2+}]_o$  and  $[Ca^{2+}]_o$  in the presence of elevated divalent cation concentrations. The MDCT cells were loaded with fura-2 as given in legend to Fig. 6. The bathing solution was changed to one containing either 5.0 mM  $CaCl_2$  (panel A) or 5.0 mM  $MgCl_2$  (panel B). About 5 min later, the MDCT cells were challenged with bathing solutions containing either 0.2 mM  $[Mg^{2+}]_o$  (panel A) or 0.2 mM  $[Ca^{2+}]_o$  (panel B), in the presence of 5.0 mM  $CaCl_2$  or 5.0 mM  $MgCl_2$ , respectively. Tracings are of one experiment but are representative of 4 separate experiments [44].

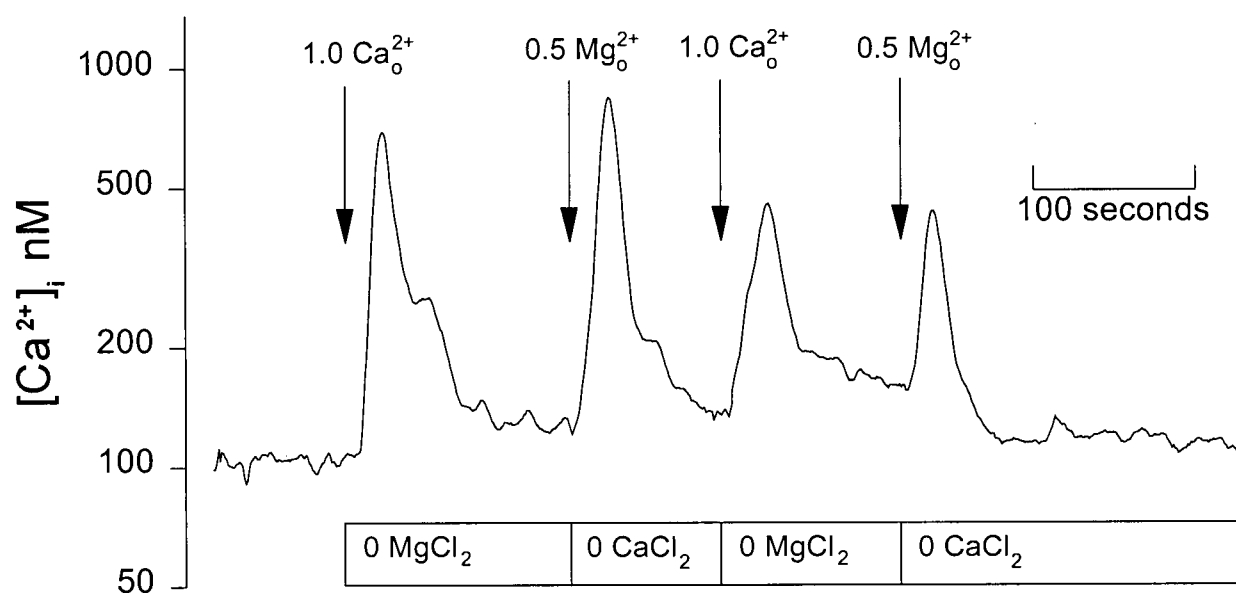


Fig. 9. Repetitive stimulation of MDCT-Mg<sup>2+</sup>/Ca<sup>2+</sup>-SR with [Mg<sup>2+</sup>]<sub>o</sub> and [Ca<sup>2+</sup>]<sub>o</sub>. MDCT cells were loaded with fura-2 in buffer solution (given in legend to Fig.4) containing no magnesium or calcium. Buffer solution containing [Mg<sup>2+</sup>]<sub>o</sub> 0.5 mM or [Ca<sup>2+</sup>]<sub>o</sub> 1.0 mM, were changed where indicated. The given [Mg<sup>2+</sup>]<sub>o</sub> and [Ca<sup>2+</sup>]<sub>o</sub> concentrations are final concentrations. Tracings are representative of 3 separate experiments [44].

Fig. 9 illustrates the effect of repetitive stimulations of the  $Mg^{2+}/Ca^{2+}$ -SR with sequential challenges of either  $MgCl_2$  or  $CaCl_2$ . Both  $[Mg^{2+}]_o$  and  $[Ca^{2+}]_o$  stimulated transient increases in cytosolic  $Ca^{2+}$  which diminished after a number of repetitive additions of divalent cation (Fig. 9). The diminution of  $Ca^{2+}$  signalling after many repetitive stimulations may reflect desensitization of the  $Mg^{2+}/Ca^{2+}$ -SR to  $[Mg^{2+}]_o$  and  $[Ca^{2+}]_o$  or depletion of intracellular  $Ca^{2+}$  stores as each cation challenge was applied. This phenomenon is distinct from the rapid desensitization observed in hormone-induced cytosolic  $Ca^{2+}$  transients observed in the thick ascending limb cell [63] or the sustained elevation seen in hormone-mediated increments in  $Ca^{2+}$  entry in distal convoluted tubule cells [39,61].

#### III.4 *$Mg^{2+}/Ca^{2+}$ -SR activation inhibits hormone-stimulated cAMP synthesis.*

Finally, we determined the effect of activation of  $Mg^{2+}/Ca^{2+}$ -SR on hormone-stimulated synthesis of cAMP. The MDCT cells possess parathyroid hormone (PTH), calcitonin, glucagon and arginine vasopressin (AVP) receptors which are coupled to adenylate cyclase [39]. PTH, calcitonin, glucagon at  $10^{-7}$  M, and AVP,  $10^{-8}$  M, increase cellular cAMP levels by about 3-fold. The potent polyvalent cation, neomycin, was used to activate the  $Mg^{2+}/Ca^{2+}$ -SR prior to the addition of hormones (Table 2). Pretreatment of the MDCT cells with neomycin inhibited hormone-stimulated cAMP accumulation. Next, we activated the  $Mg^{2+}/Ca^{2+}$ -SR with high levels of  $[Mg^{2+}]_o$  or  $[Ca^{2+}]_o$  (Table 2). Pretreatment of MDCT cells with 10 mM  $[Mg^{2+}]_o$  or  $[Ca^{2+}]_o$  inhibited hormone-mediated cAMP generation.

#### IV *Discussion:*

In this study, we show that the established MDCT cell line possesses a  $Mg^{2+}/Ca^{2+}$ -SR that responds to  $[Mg^{2+}]_o$  and  $[Ca^{2+}]_o$ , to transiently release  $Ca^{2+}_i$  from cytosolic stores. These cells possess components involved in calcium metabolism such as , hormone receptors, vitamin D receptors, vitamin D metabolite-induced 24 hydroxylase activity, P-450 metabolites, and the calbindin 28K calcium-binding protein that are important in vitamin D actions [39,64,65]. Accordingly, it is of interest that this cell line also has an

**Table 2. Activation of  $Mg^{2+}/Ca^{2+}$ -SR inhibits hormone-stimulated cAMP synthesis.**

	Control	PTH	Calcitonin	Glucagon	AVP
Control	19±1(11) <sup>n</sup>	56±2*(5)	60±0.1*(4)	105±5*(7)	71±2*(5)
Neomycin	22±2(3)	34±1**(3)	33±4**(3)	22±1**(7)	24±3**(4)
$Ca^{2+}_o$	23±2(3)	-	-	32±2**(3)	34±3**(3)
$Mg^{2+}_o$	24±3(3)	-	-	37±3(3)	27±3**(3)

**Table 2 Legend:**

Where indicated, neomycin, 50  $\mu$ M, extracellular  $Ca^{2+}_o$ , 10 mM, or extracellular  $Mg^{2+}_o$ , 10 mM, were added 5 min prior to the addition of parathyroid hormone (PTH),  $10^{-7}$  M, calcitonin,  $10^{-7}$  M, glucagon,  $10^{-7}$  M, or arginine vasopressin (AVP),  $10^{-8}$  M, and cAMP was measured 5 min later. Values are cAMP accumulation, pmol/mg protein • 5 min. ( )<sup>n</sup> is the number of separate observations. \* indicates significance,  $p < 0.01$ , from control values without hormone and \*\* indicates significance of neomycin or  $Ca^{2+}_o$  or  $Mg^{2+}_o$  values from those of the respective hormone treatments [44].

extracellular divalent cation-sensing receptor. Using RT-PCR and Southern blotting, we show that the MDCT cells possess transcripts for the  $Ca^{2+}$ -SR. The presence of the  $Ca^{2+}$ -SR protein in MDCT cells was documented by Western blot analysis using a specific  $Ca^{2+}$ -SR antiserum. Furthermore, monitoring of cytosolic  $[Ca^{2+}]$  showed that activation of the  $Mg^{2+}/Ca^{2+}$ -SR in MDCT cells elicits  $[Ca^{2+}]_i$  signals in response to increasing extracellular concentrations of polyvalent cations demonstrating that the receptor is functional. These studies with mouse distal convoluted cells are consonant with reports identifying  $Ca^{2+}$ -SR RNA

transcripts in the rat distal convoluted segment [11,13,17]. More recently, Riccardi *et al.* showed that the rat  $\text{Ca}^{2+}$ -SR is localized to the basolateral membrane of the distal convoluted tubule (15). The presence of a  $\text{Mg}^{2+}/\text{Ca}^{2+}$ -SR in the distal convoluted tubule may have important ramifications on cellular function within this segment.

## Chapter 2: Attempts to isolate a specific $Mg^{2+}$ -sensing Receptor

### I. Background

The results of Chapter 1, specifically the MDCT cell's ability to sense  $Mg^{2+}_o$  in the face of physiological levels of  $Ca^{2+}_o$ , as well as the body's ability to manage magnesium independently of calcium [74,76-78], strongly indicate the presence of an extracellular  $Mg^{2+}$ -SR. In order to see if  $Mg^{2+}$ -sensing occurs in other cell types, we determined the effect of extracellular  $Mg^{2+}$  versus  $Ca^{2+}$  on intracellular signalling in two different systems. A system, that specifically responds to magnesium, has been demonstrated in the oocyte of the prawn *Palaemon serratus* [79,80]. The presence of  $Mg^{2+}$  in sea water induces a  $Ca^{2+}$  wave within the cell similar to that seen with stimulation of the  $Ca^{2+}$ -SR [80]. A  $Ca^{2+}$  wave is also observed when Madin Darby Canine Kidney (MDCK) cells were exposed to 3 mM  $Mg^{2+}$  but not 5 mM  $Ca^{2+}$  (Fig 10). Given the results in these two systems it is clear there is an extracellular  $Mg^{2+}$  sensing mechanism that appears to be more responsive to extracellular  $Mg^{2+}$  than  $Ca^{2+}$ . Accordingly, we attempted to isolate a  $Mg^{2+}$ -sensing receptor from MDCK cells and *Palmaemon serratus* oocytes using a genetic screening.  $Ca^{2+}$ -SR's are most highly conserved, with respect to all known  $Ca^{2+}$ -SR's as well as to metabotropic glutamate receptors and pheromone receptors, in the transmembrane region [81-83]. Probes and primers used for this homology approach were therefore designed from this region.

*II Methods and Materials:* As described in Chapter 1.

*III Results:*

#### *III.1 Intracellular $Ca^{2+}$ signalling in MDCK, but not HEK cells, in response to $[Mg^{2+}]_o$*

MDCK and HEK cells were exposed to extracellular  $Ca^{2+}$  and  $Mg^{2+}$  as in chapter 1. When we challenged MDCK cells with 3 mM  $Mg^{2+}$  or 25  $\mu$ M neomycin, MDCK cells demonstrated a response similar

to MDCT cells (Fig. 10). However, 5 mM  $\text{Ca}^{2+}$  failed to induce an increase in intracellular  $\text{Ca}^{2+}$ . HEK cells, which do not express the  $\text{Ca}^{2+}$ -SR [25], are unresponsive to  $\text{Ca}^{2+}_o$  or  $\text{Mg}^{2+}_o$  up to 10 mM.

### III.2. *Expression of the $\text{Mg}^{2+}$ response in Xenopus oocytes injected with Palaemon mRNA.*

An expression protocol similar to that used by Brown *et al.* [4] was also attempted using *Palaemon* RNA. To test for functional expression of a  $\text{Mg}^{2+}$ -SR or  $\text{Ca}^{2+}$ -SR in *Xenopus* oocytes the ability of  $\text{Mg}^{2+}$  or  $\text{Ca}^{2+}$  to increase  $\text{Cl}^-$  currents was assessed. Water (50 nl), or 50 nl of shrimp mRNA ( $1\mu\text{g}/\mu\text{l}$ ), was injected into defolliculated *Xenopus* oocytes. Oocytes were then incubated for 2-3 days, exposed to 15 mM external  $\text{Mg}^{2+}$  or  $\text{Ca}^{2+}$ , and the chloride current measured as described. Currents of up to 80 nA were detected in response to  $\text{Mg}^{2+}$  (15 mM) in 50 % of mRNA injected oocytes (Fig. 11). In contrast extracellular  $\text{Ca}^{2+}$  (15 mM) did not cause changes in the  $\text{Cl}^-$  currents in any of the injected oocytes. Water injected oocytes were unresponsive to 15mM  $\text{Mg}^{2+}$  or  $\text{Ca}^{2+}$  (data not shown).

### III.3. *A $\text{Ca}^{2+}$ -SR cDNA, or related transcript, was not identified by screening a Palaemon serratus oocyte or MDCK cDNA library.*

The  $\text{Mg}^{2+}$ -sensing response of the *Palaemon serratus* oocyte was conveyed to the *Xenopus* oocyte with mRNA injection. Based on the hypothesis that an extracellular  $\text{Mg}^{2+}$ -SR gene is similar to a  $\text{Ca}^{2+}$ -SR gene, a homology-based screening approach was attempted. A cDNA library from the mouse kidney was obtained and cDNA libraries were made from the MDCT cell line, MDCK cell line, and *Palaemon* oocytes. These libraries were screened at low stringency using a probe comprising the majority of the transmembrane region of the  $\text{Ca}^{2+}$ -SR. This region has the most similarity among  $\text{Ca}^{2+}$ -SR's and their related genes [81]. Other than partial  $\text{Ca}^{2+}$ -SR clones from the MDCT, and mouse kidney, no related transcripts were identified.

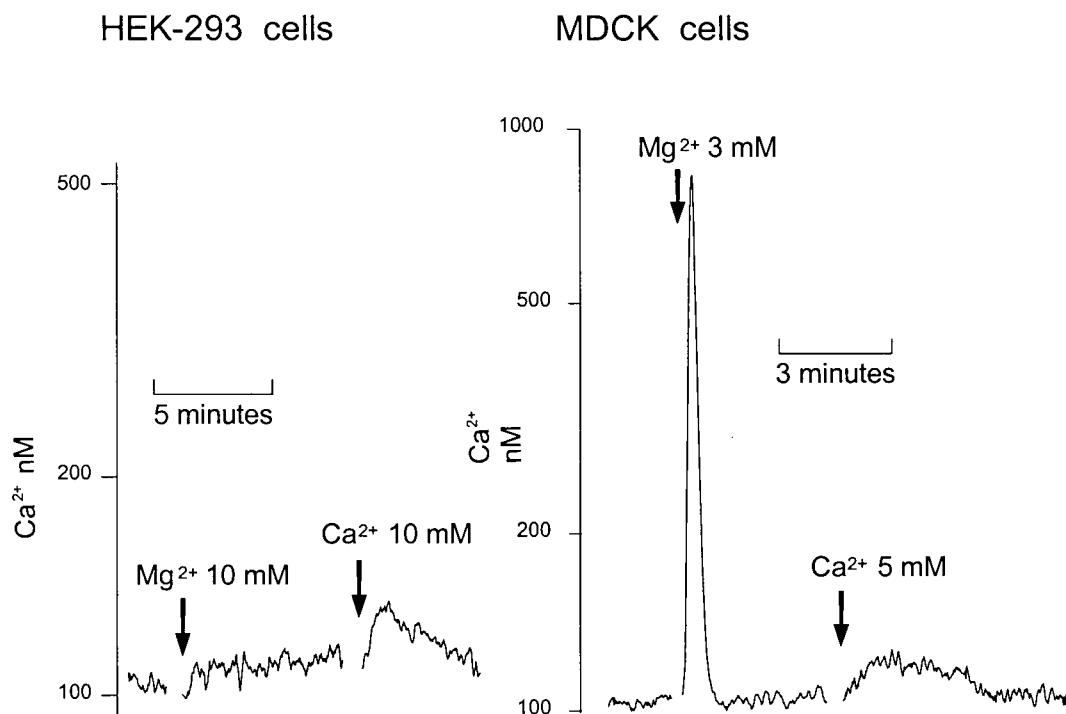
Multiple attempts to identify a related gene using PCR with primers designed from regions conserved from the  $\text{Ca}^{2+}$ -SR to the metabotropic glutamate receptor failed to identify any related gene. The  $\text{Ca}^{2+}$ -SR was not identified in MDCK cells using RT-PCR.

#### IV. Discussion

Preliminary evidence demonstrates that some cells may respond sensitively, to  $Mg^{2+}$ , relative to extracellular  $Ca^{2+}$ . Unfortunately, no mammalian receptors specific for magnesium control have been discovered. Reports of mammalian  $Ca^{2+}$ -SR homologues have been reported but none have proven to be specific for cations other than  $Ca^{2+}$  [81]. The putative  $Mg^{2+}$ -SR may be significantly different from the  $Ca^{2+}$ -SR making homology based screening an ineffective method for its isolation. A homologue has, however, been identified from the dogfish shark (*Squalus acanthias*) and reported in abstract form [84]. This protein shares 74% amino acid identity to the rat  $Ca^{2+}$ -SR and is 3.3 times more sensitive to  $Mg^{2+}$  than  $Ca^{2+}$  (half maximal activation of 7.5 mM for  $Mg^{2+}$ ) when expressed in HEK cells. Unfortunately no sequence data is available.

Initial data from *Xenopus* oocytes, injected with RNA isolated from *Palaemon* oocytes, was encouraging. Unfortunately, seasonal availability and limited supply of these oocytes made further experimentation impractical.

As we failed to identify a specific  $Mg^{2+}$ -SR, and the  $Ca^{2+}$ -SR clearly does respond to low concentrations of magnesium, we chose to use the MDCT cell for the rest of the experiments concerning characterization of the polyvalent-cation-sensing receptor. This does not preclude the possibility of separate  $Mg^{2+}$  sensing receptor(s) but it allows us to determine a response to a  $Mg^{2+}/Ca^{2+}$ -sensing system that we know is located within the MDCT cell line.



OC279701

Fig. 10. External polyvalent cations transiently increase cytosolic  $\text{Ca}^{2+}$  in MDCK but not HEK cells. Cells were cultured in DMEM/Ham's F-12 (1:1) with 10% fetal calf serum containing 0.6 mM magnesium and 1.5 mM calcium. The cells were loaded with fura-2 for 30 min in a buffer solution containing (in mM):  $\text{MgCl}_2$  0.5,  $\text{CaCl}_2$  1.0, NaCl 145, KCl 4.0,  $\text{K}_2\text{HPO}_4$  0.8,  $\text{KH}_2\text{PO}_4$  0.2, glucose 5, and HEPES-Tris 20, pH 7.4. In order to test the effect of  $[\text{Mg}^{2+}]_o$ , the buffer solution was changed to one without  $\text{MgCl}_2$ . This bathing solution was replaced 1-2 min later with one containing indicated  $\text{MgCl}_2$ . To test  $[\text{Ca}^{2+}]_o$ , the cells were initially bathed with the above solutions containing no  $\text{CaCl}_2$ . This was replaced with one containing indicated  $\text{CaCl}_2$ . Tracings are representative of 4-10 separate experiments.

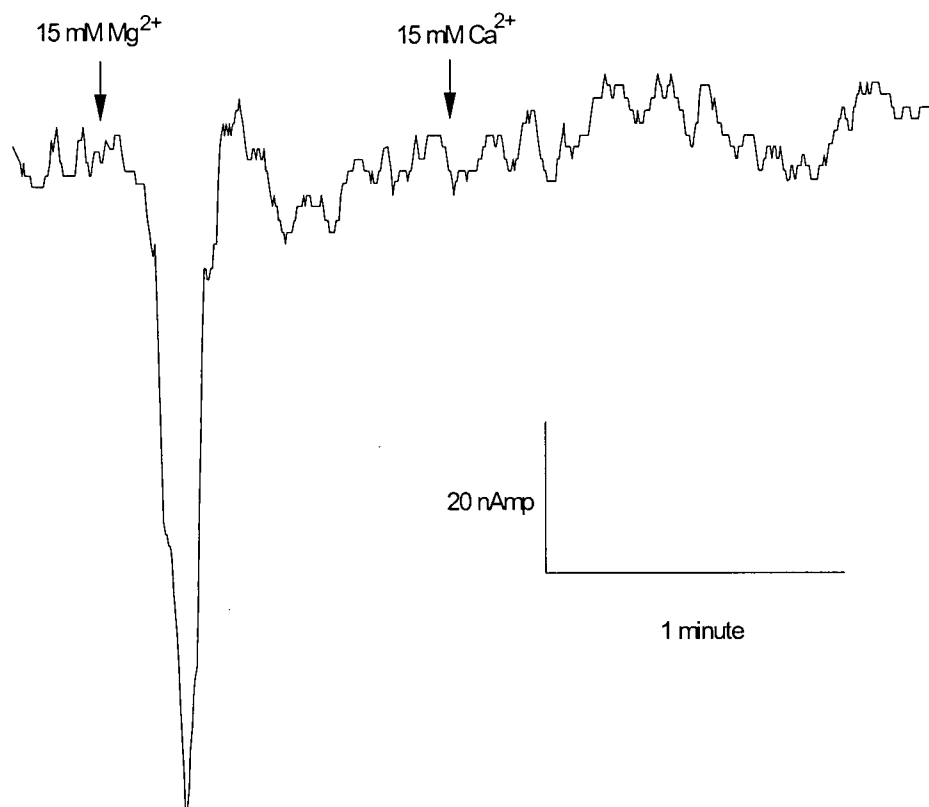


Fig 11. Extracellular  $\text{Mg}^{2+}$  (15 mM), but not  $\text{Ca}^{2+}$ , evokes increases in  $\text{Cl}^-$  currents in *Xenopus* oocytes injected with 50 ng prawn mRNA. Tracing is representative of those seen in three separate oocytes. There is no response evoked by water injected oocytes (data not shown).

### **Chapter III. Characterization of $Mg^{2+}$ Uptake Influenced by Peptide Hormones Acting Through G-Protein Linked Receptors.**

#### *I. Background.*

Magnesium reabsorption in the DCT is under the control of a number of hormones and altered by a number of influences. From the experiments of chapter 1, it was discovered that cAMP production, stimulated by hormones known to bind to G-protein linked receptors, was inhibited by high external magnesium [44]. It is interesting, therefore, to define the effect hormones have on this cell line with respect to magnesium uptake. As the dependence of magnesium absorption with magnesium delivery is maintained in the presence of these hormonal factors [85,86], these systems must be inter-related. In this chapter four, peptide hormones which act through G-protein linked receptors to generate cAM, are characterized with respect to magnesium uptake [87].

*Glucagon.* Glucagon is a potent renal magnesium conserving hormone [88]. Bailly and colleagues reported that the acute infusion of pharmacological concentrations of glucagon in rats with intact parathyroid glands leads to a rapid fall in fractional magnesium excretion from  $16 \pm 1\%$  to  $9 \pm 2\%$  [88]. The response to glucagon is even greater in hormone-deprived animals. Bailly *et al.* showed that fractional magnesium excretion markedly decreased by about 50% (from  $71.5 \pm 8.0$  to  $39.6 \pm 5.7$  nmoles/min) with glucagon administration in rats deficient in endogenous PTH, calcitonin, glucagon and antidiuretic hormone [89]. This was attributed to a doubling of absolute reabsorption within both the loop of Henle (increase from  $6.5 \pm 0.7$  to  $11.7 \pm 0.7$  nmoles/min) and the distal tubule (increase from  $0.85 \pm 0.1$  to  $1.75 \pm 0.3$  pmoles/min). Accordingly, glucagon acts within the loop and distal tubule of the rat.

*Arginine vasopressin.* The actions of arginine vasopressin (AVP) within the distal convoluted tubule are poorly understood [90]. AVP has been shown to be an effective magnesium-conserving hormone in anaesthetized and conscious hormone-deprived rats [91-93]. Micropuncture studies of these animals have shown that AVP acts principally within Henle's loop [92]. Elalouf and colleagues failed to discern any change in fractional magnesium absorption in the superficial distal tubule following physiological administration of AVP [92]. In these studies, Elalouf *et al.* reported that fractional calcium absorption significantly increased from  $42.0 \pm 5.8\%$  to  $62.8 \pm 7.1\%$ , whereas the change in fractional magnesium transport with AVP was not significant, although it increased from  $45.5 \pm 7.8\%$  to  $55.3 \pm 15.5\%$ . These changes may have been significant if a greater number of tubules had been sampled. Costanzo and Windhager did not observe any change in calcium absorption in the microperfused rat distal tubule with administration of AVP [94]. These animals had their thyroid and parathyroid removed (TPTXed), but were not hormone-deprived as were those used by Elalouf *et al.* [92]. In both studies, AVP enhanced sodium absorption in the distal tubule.

*Parathyroid hormone.* A number of hormones stimulate magnesium absorption within the distal tubule. The first to be described was parathyroid hormone (PTH). Infusion of PTH to TPTXed animals increased the reabsorption of magnesium and diminished urinary magnesium excretion [95]. Micropuncture studies showed that part of this hormonal action occurs within the distal tubule [89,96]. An increase in magnesium conservation was observed even in the face of enhanced magnesium delivery to this segment [97-100]. The largest changes were observed in TPTXed hamsters where the mean tubular fluid-to-ultrafilterable magnesium ( $TF/UF_{Mg}$ ) ratio at the distal sampling site fell from  $0.56 \pm 0.08$  to  $0.33 \pm 0.08$  following administration of PTH [101]. This was associated with a fall in fractional magnesium excretion from about 14% to 3%. De Rouffignac *et al.* and Bailly *et al.* have shown that PTH and other hormones stimulate magnesium absorption in the rat distal tubule [102]. They used Brattleboro rats with hereditary diabetes insipidus, that lack endogenous ADH, and they infused either glucose or somatostatin to inhibit glucagon

secretion. Furthermore, they TPTXed the animals to eliminate circulating PTH and calcitonin. Thus a "hormone-deprived" animal model was created to serve as a basis for evaluating the respective actions of each hormone [102]. Micropuncture studies were then performed to determine the effects of hormone administration; importantly, these studies were all performed with physiological hormone concentrations. Infusion of PTH<sub>1-34</sub> to hormone-deprived rats leads to diminished magnesium and calcium delivery to early and late distal tubule sampling sites. These studies clearly demonstrate that PTH enhances magnesium absorption within the distal tubule.

*Calcitonin.* Calcitonin infusions have clearly been shown to enhance renal magnesium conservation in the rat [103]. Poujeol *et al.* infused calcitonin to TPTXed rats and observed a fall in fractional magnesium excretion from  $4.1 \pm 0.4$  to  $1.0 \pm 0.3\%$  which they attributed to an increase in magnesium reabsorption in the loop of Henle [103]. However, subsequent studies with the hormone-deprived rat showed that calcitonin markedly stimulated fractional magnesium absorption in the superficial distal tubule as well as the loop [104]. These micropuncture studies indicate that calcitonin enhances magnesium conservation, in part, by actions within the distal tubule [104].

*II. Methods and Materials:* As previously described in chapter 1.

### *III. Results*

#### *III.1 Glucagon, arginine vasopressin, PTH, and calcitonin stimulate cAMP accumulation in Mg<sup>2+</sup>-depleted MDCT cells.*

In the present study, I determined the concentration-dependence of glucagon, AVP, PTH, (Fig.12) and calcitonin-stimulated cAMP generation in MDCT cells [87]. (PTH and calcitonin induce similar responses as glucagon and AVP in MDCT cells so these data will only be included in a summary figure (Fig.16 ).

These hormones elicited intracellular cAMP accumulation in a concentration-dependent fashion. Second, I determined whether these hormones elicit cAMP accumulation in the  $Mg^{2+}$ -depleted MDCT cells used here. Glucagon or AVP at submaximal ( $10^{-9}$  M) and maximal ( $10^{-7}$  M) concentrations increased cAMP by similar amounts in normal and  $Mg^{2+}$ -depleted MDCT cells (Table 3). The concentration-dependence of glucagon and AVP are far higher than the concentrations normally observed *in vivo*. Explanations for these discrepancies include absence of normal bathing plasma, diminished circulation of hormone or changes in membrane receptors due to cell culture conditions. Nevertheless, these responses indicate that hormone receptors are present in this cell line which activate intracellular signalling processes. These data confirm the observations of Friedman and Gesek et al. [108,109] that receptors for these hormones are present in the MDCT cells which upon stimulation release intracellular cAMP. Intracellular  $Mg^{2+}$  depletion did not alter hormone-responsive cAMP generation in these cells (Table 3). Finally, glucagon or AVP, PTH, and calcitonin did not induce rapid intracellular  $Ca^{2+}$  transients (data not given) indicating that cytosolic  $Ca^{2+}$  signalling is not a product of glucagon- or AVP-mediated pathways in MDCT cells [108,109].

### III.2 $Mg^{2+}$ uptake in MDCT cells.

In order to determine  $Mg^{2+}$  uptake, subconfluent MDCT monolayers were cultured in magnesium-free medium for 16 h. These cells possessed a significantly lower  $[Mg^{2+}]_i$ ,  $0.22 \pm 0.01$  mM than cells cultured in normal media,  $0.53 \pm 0.02$  mM. When the  $Mg^{2+}$ -depleted MDCT cells were placed in a bathing solution containing 1.5 mM  $MgCl_2$ , intracellular  $Mg^{2+}$  concentration increased with time and levelled off at a  $[Mg^{2+}]_i$  of  $0.52 \pm 0.06$  mM, ( $n = 9$ ) which was similar to basal levels observed in normal cells (Fig.13). The average rate of refill,  $d([Mg^{2+}]_i)/dt$ , measured as the change in  $[Mg^{2+}]_i$  with time, was  $164 \pm 5$  nM/s, ( $n = 6$ ) cells, as determined over the first 500 s following addition of 1.5 mM  $MgCl_2$ . [87]

**Table 3. Glucagon and AVP stimulate cAMP synthesis in magnesium-depleted MDCT cells**

cAMP accumulation		
pmol•mg•protein <sup>-1</sup> •5min <sup>-1</sup>		
	Normal Cells	Mg <sup>2+</sup> -depleted cells
Control	22± 2 (6)	21± 1 (5)
Glucagon, 10 <sup>-9</sup> M	60± 5* (4)	60± 3* (4)
Glucagon, 10 <sup>-7</sup> M	92± 5* (4)	89± 3* (4)
AVP, 3× 10 <sup>-9</sup> M	62± 4* (3)	61± 3* (4)
AVP, 3× 10 <sup>-7</sup> M	89± 5* (4)	81± 7* (4)

**Legend to Table 3**

Values are mean ± SE; number of experiments is in parentheses. Glucagon and arginine vasopressin (AVP) are added 5 min prior to the measurement of cAMP. \* $P < 0.01$ , significant vs. control values. There were no significant differences between normal and Mg<sup>2+</sup> depleted cells for each of the conditions tested. MDCT, mouse distal convoluted tubule [87].

**III.3 Glucagon stimulates Mg<sup>2+</sup> uptake in MDCT cells.**

Glucagon, 10<sup>-7</sup> M, added to the refill buffer solution increased the rate of Mg<sup>2+</sup> entry into Mg<sup>2+</sup>-depleted MDCT cells (Fig.13). Glucagon, 10<sup>-7</sup> M, increased the mean Mg<sup>2+</sup> entry rate from 164±5 to 196±11 nM/s, ( $n = 5$ ), which represented a stimulation of 20±6% above control values. In all cases where measured, [Mg<sup>2+</sup>]<sub>i</sub> returned to basal levels, 0.52±0.03 mM. The effect of glucagon on Mg<sup>2+</sup> uptake was concentration-dependent with maximal rate of stimulation at 10<sup>-6</sup> M, 273±6 nM/s, and half-maximal stimulation at a concentration about 10<sup>-7</sup> M (Fig.14). I have previously reported that dihydropyridines inhibit Mg<sup>2+</sup> uptake into Mg<sup>2+</sup>-depleted MDCT cells [61]. To determine whether glucagon-induced Mg<sup>2+</sup> entry is mediated through

a dihydropyridine-sensitive pathway, I examined the effect of the channel blocker, nifedipine, on the changes in  $[Mg^{2+}]_i$  following placement in the refill buffer solution containing 1.5 mM  $MgCl_2$ . The presence of  $10^{-5}$  M nifedipine inhibited glucagon-stimulated  $Mg^{2+}$  uptake,  $24 \pm 2$  nM/s, indicating that this pathway is sensitive to the channel blocker and supporting the notion that glucagon-stimulated uptake is the same as the entry pathway observed in control cells (Table 4).

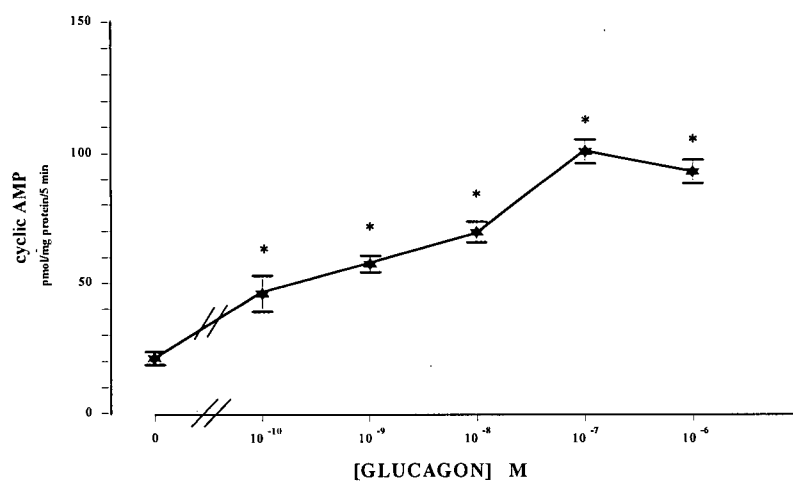
**Table 4 . Hormone-stimulated  $Mg^{2+}$  uptake in MDCT cells is dihydropyridine sensitive**

	Basal $[Mg^{2+}]_i$ , mM	$d([Mg^{2+}]_i)/dt$ , nM/s
Control	$0.22 \pm 0.02$ (6)	$164 \pm 5$ (6)
Control + Nifedipine	$0.22 \pm 0.02$ (4)	$42 \pm 21^*$ (4)
Glucagon	$0.22 \pm 0.01$ (4)	$196 \pm 11^*$ (4)
Glucagon + Nifedipine	$0.21 \pm 0.02$ (3)	$24 \pm 2^*$ (3)
AVP	$0.22 \pm 0.02$ (5)	$189 \pm 6^*$ (6)
AVP + Nifedipine	$0.21 \pm 0.02$ (3)	$75 \pm 9^*$ (3)

**Table 4 Legend:**

Values are mean  $\pm$  SE; number of experiments is in parentheses. Measurements were performed in presence of 1.5 mM  $MgCl_2$  with and without  $10^{-7}$  M Glucagon, or  $3 \times 10^{-7}$  M AVP according to the methods outlined in legend to Fig.13. Nifedipine,  $10^{-5}$  M, was added with the refill solution where indicated. \* $P < 0.05$ , significant vs. control values [87].

A



B

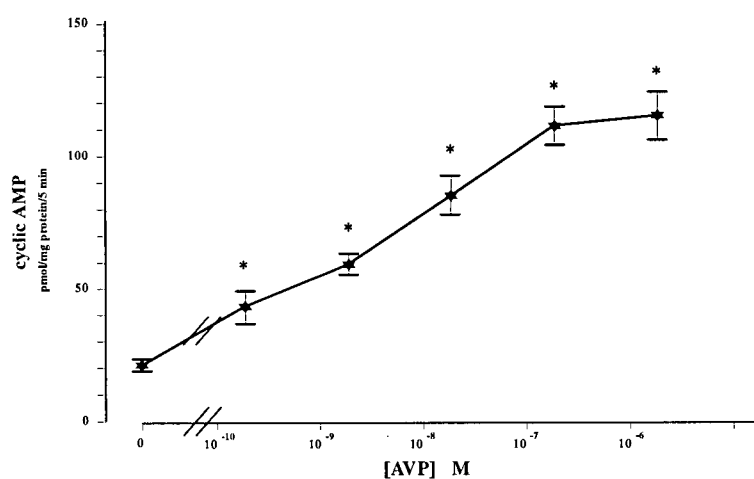


Fig.12. Glucagon and arginine vasopressin (AVP) stimulate cAMP accumulation in MDCT cells. Glucagon (panel A) or AVP (panel B) were added, at the concentrations indicated, 5 min prior to the measurement of cAMP. Values are means  $\pm$  SE for 3-9 observations, 2 separate preparations. \* indicates significance,  $p < 0.05$ , compared to control values [87].

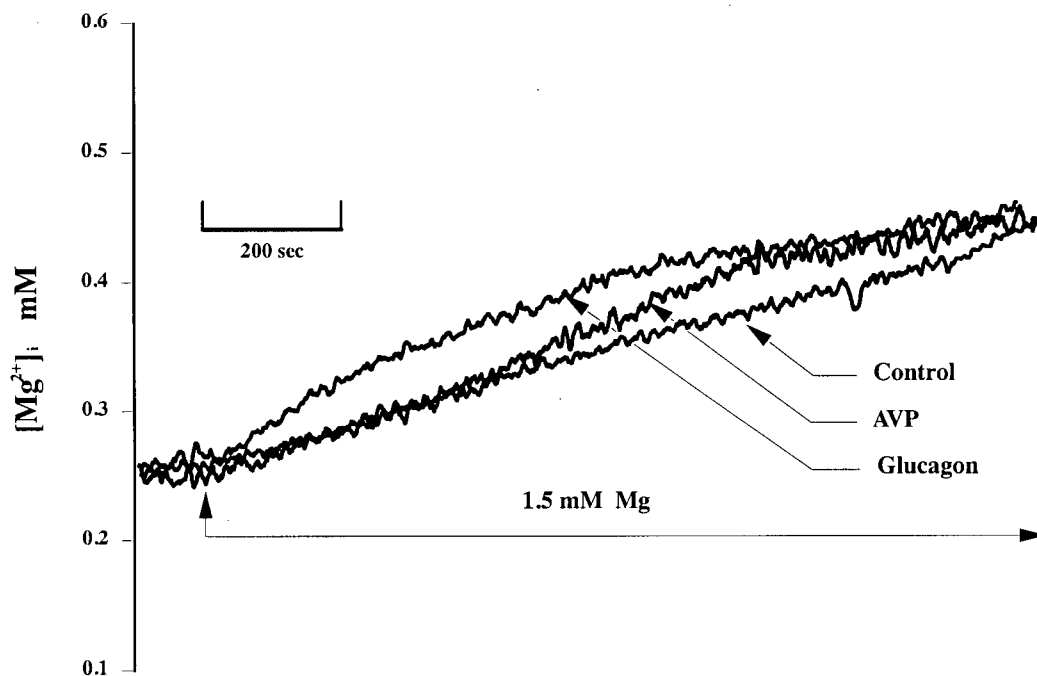


Fig. 13. Glucagon and arginine vasopressin (AVP) stimulate  $Mg^{2+}$  uptake in  $Mg^{2+}$ -depleted mouse distal convoluted tubule (MDCT) cells. Confluent MDCT cells were cultured in  $Mg^{2+}$ -free media ( $<0.01$  mM) for 16-20 hr. Fluorescence studies were performed in buffer solutions in absence of  $Mg^{2+}$ , and where indicated,  $MgCl_2$  (1.5 mM final concentration) was added to observe changes in intracellular  $Mg^{2+}$  concentration. The buffer solutions contained (in mM): 145 NaCl, 4.0 KCl, 0.8  $K_2HPO_4$ , 0.2  $KH_2PO_4$ , 1.0  $CaCl_2$ , 5.0 glucose, and 10 HEPES/Tris, pH 7.4, with and without 1.5 mM  $MgCl_2$ . Glucagon,  $10^{-7}$  M, or AVP,  $3 \times 10^{-7}$  M, were added to with this buffer solution. Fluorescence was measured at 1 data point/s with 25-point signal averaging, and the tracing was smoothed according to methods previously described [87].

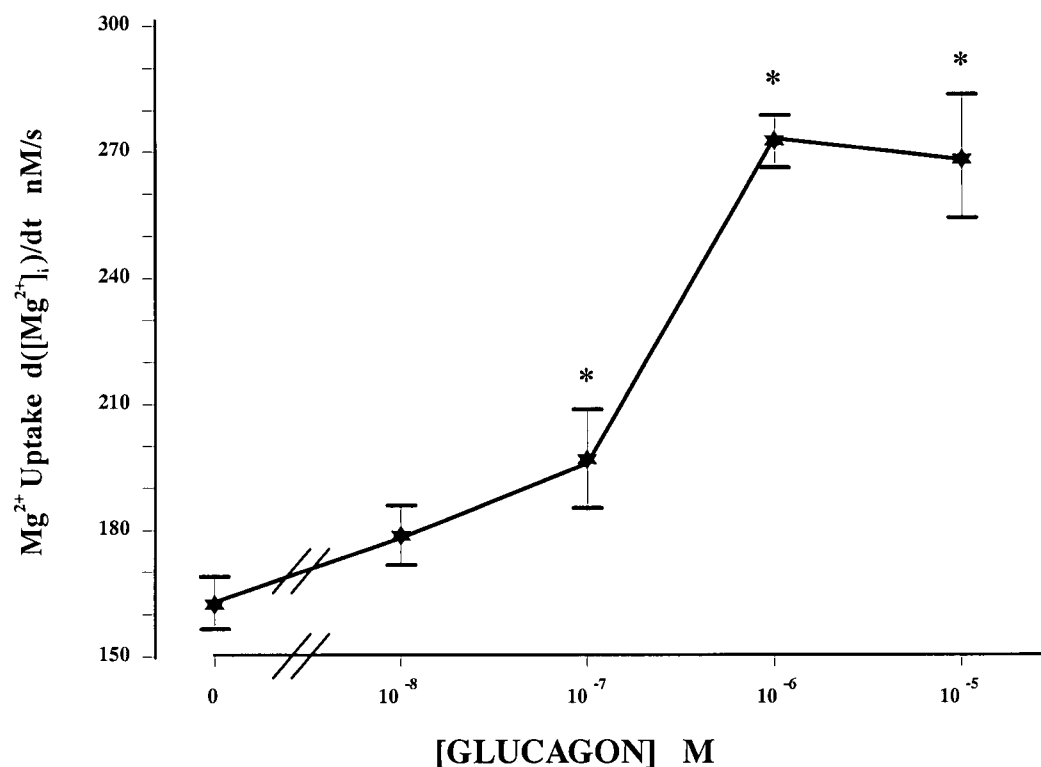


Fig. 14. Concentration-dependence of glucagon-stimulation of  $Mg^{2+}$  entry in MDCT cells. The rate of  $Mg^{2+}$  influx as determined by  $d([Mg^{2+}]_i)/dt$  was measured with the given glucagon concentrations using techniques performed according to that given in legend to Figure 1.  $d([Mg^{2+}]_i)/dt$  values were determined over the first 500 s of measurements. Values are means  $\pm$  SE for 3-6 cells [87].

### III.4 *AVP stimulates $Mg^{2+}$ uptake in MDCT cells.*

Fig. 13 illustrates the effect of AVP,  $3 \times 10^{-7}$  M, on  $Mg^{2+}$  uptake in  $Mg^{2+}$ -depleted MDCT cells. The mean uptake rate,  $d([Mg^{2+}])_i/dt$ , increased from control levels  $164 \pm 5$  nM/s to  $189 \pm 6$  nM/s,  $n = 6$ . Unlike the actions of glucagon, AVP responses were not immediate with the addition of the hormone to the refill solution. As shown, the response was observed only after 5-10 min after addition of the hormone to the superfusion solution. The reasons for this delay are not apparent at the present time. The following refill studies were uniformly performed 6 min after AVP was added to the MDCT cells. The refill rate,  $d([Mg^{2+}])_i/dt$ , was determined over a standard 500s time interval following the 6 min delay. AVP stimulates  $Mg^{2+}$  entry in a concentration-dependent manner (Fig. 15). The maximal effect was observed at about  $3 \times 10^{-6}$  M which resulted in an increase of  $d([Mg^{2+}])_i/dt$  to  $188 \pm 2$  nM/s. This change was significantly less than the response to maximal glucagon concentrations. AVP-stimulated  $Mg^{2+}$  uptake was inhibited by nifedipine indicating that the hormonal response is through activation of channels responsible for  $Mg^{2+}$  entry in MDCT cells (Table 4).

### III.5 *Calcitonin and PTH have effects on $Mg^{2+}$ uptake similar to glucagon and AVP.*

Under the same experimental conditions described in section III.3 and III.4, maximal concentrations of calcitonin [ $10^{-7}$  M] and PTH [ $10^{-7}$  M] stimulate  $Mg^{2+}$  uptake  $49 \pm 5\%$  and  $12 \pm 2\%$ , respectively, above control levels (Fig. 16).

### II.6 *Glucagon- and AVP-stimulated $Mg^{2+}$ entry does not require protein synthesis.*

Gesek and Friedman have reported that PTH-stimulated calcium uptake in MDCT cells is sensitive to cycloheximide (1  $\mu$ g/min for 30 min) whereas calcitonin actions are insensitive to protein synthesis inhibitors [41,108]. Accordingly, there may be diverse pathways involved with hormonal regulation of magnesium transport. Pretreatment of MDCT cells with cycloheximide, 1  $\mu$ g/ml for 30 min, did not alter glucagon or AVP stimulation of  $Mg^{2+}$  entry into MDCT cells (Table 5). It is apparent that *de novo* protein synthesis is not required for the acute actions of glucagon or AVP on magnesium uptake.

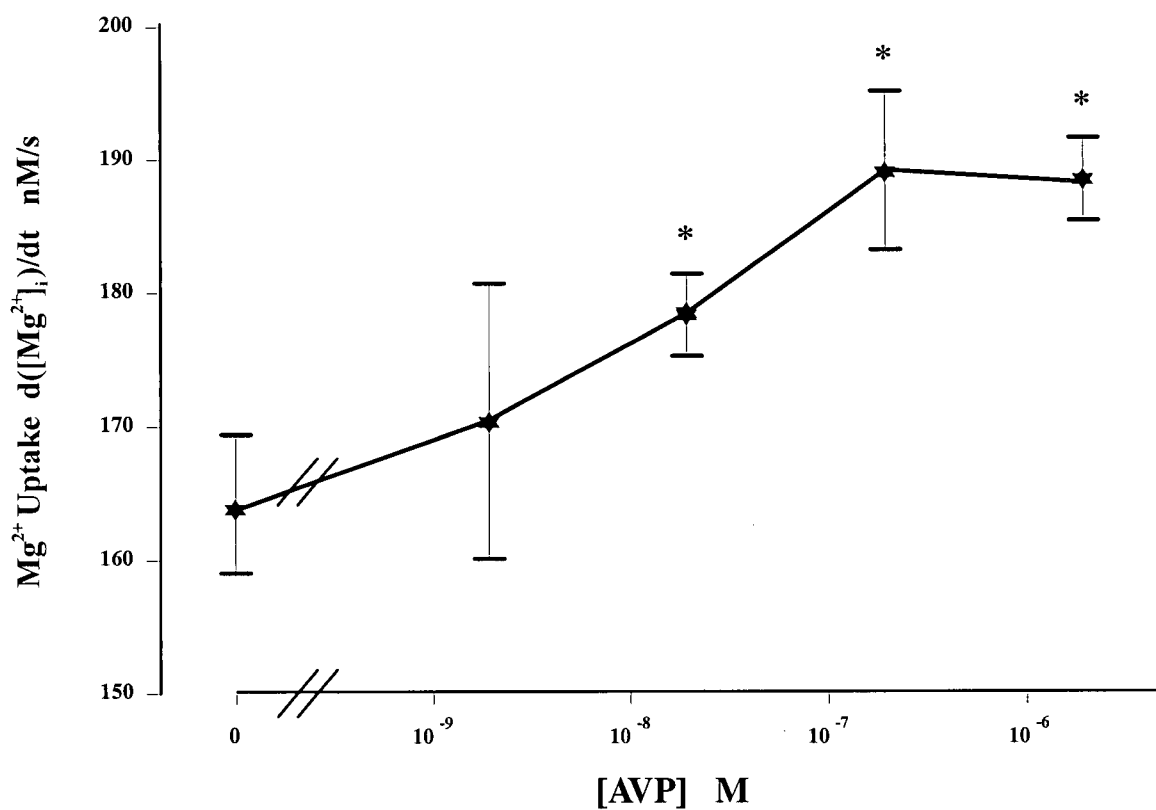


Fig. 15.

Concentration-dependence of AVP stimulation of  $\text{Mg}^{2+}$  uptake in MDCT cells. The rate of  $\text{Mg}^{2+}$  influx as determined by  $d([\text{Mg}^{2+}]_i)/dt$  was measured with the given AVP concentrations using techniques performed according to that given in legend to Figure \*. The entry rate,  $d([\text{Mg}^{2+}]_i)/dt$ , was determined over 500 s, 5 min after the addition of AVP. Values are means  $\pm$  SE for 3-6 cells [87].

**Table 5 . Role of protein synthesis on glucagon or AVP stimulated  $Mg^{2+}$  uptake in MDCT Cells**

	Control, nM/s	Cyloheximide, nM/s
Control	$164 \pm 5$ (6)	$163 \pm 6$ (3)
Glucagon	$196 \pm 11$ (4)	$197 \pm 11$ (3)
AVP	$189 \pm 6$ (6)	$192 \pm 2$ (4)

**Table 5 Legend**

Values are mean  $\pm$  SE; number of experiments is in parentheses.  $Mg^{2+}$  entry was determined in presence of  $10^{-7}$  M Glucagon, or  $3 \times 10^{-7}$  M AVP, with and without pretreatment with  $10^{-8}$  M cycloheximide. Protein synthesis inhibitor was applied 30 min prior to fluorescence studies. \*  $P < 0.05$ , significant for cycloheximide vs. control values for each of the respective hormone treatments [87].

**III.7 Exogenous cAMP stimulates  $Mg^{2+}$  uptake in MDCT cells.**

Next, I determined if activation of either protein kinase A or protein kinase C may have stimulated  $Mg^{2+}$  entry in  $Mg^{2+}$ -depleted MDCT cells. Friedman *et al.* and Hilal *et al.* have shown that activation of both pathways are necessary for PTH-mediated increases in calcium uptake in MDCT cells and distal tubule vesicles, respectively [109,111]. The activation of these kinases with added cAMP or phorbol esters were without effect alone but significantly stimulated calcium entry when administered together [110]. In the present studies, the addition of the long lasting cAMP analog 8-bromo cAMP,  $10^{-4}$  M, 6 min prior to the concentration determinations stimulated  $Mg^{2+}$  uptake by  $137 \pm 6\%$  above control values (Fig.17). There was an apparent latent period prior to the effects of 8-bromo cAMP of about 5-10 min, not unlike that observed for the responses of AVP. The addition of PMA, on the other hand, had no apparent effect on  $Mg^{2+}$

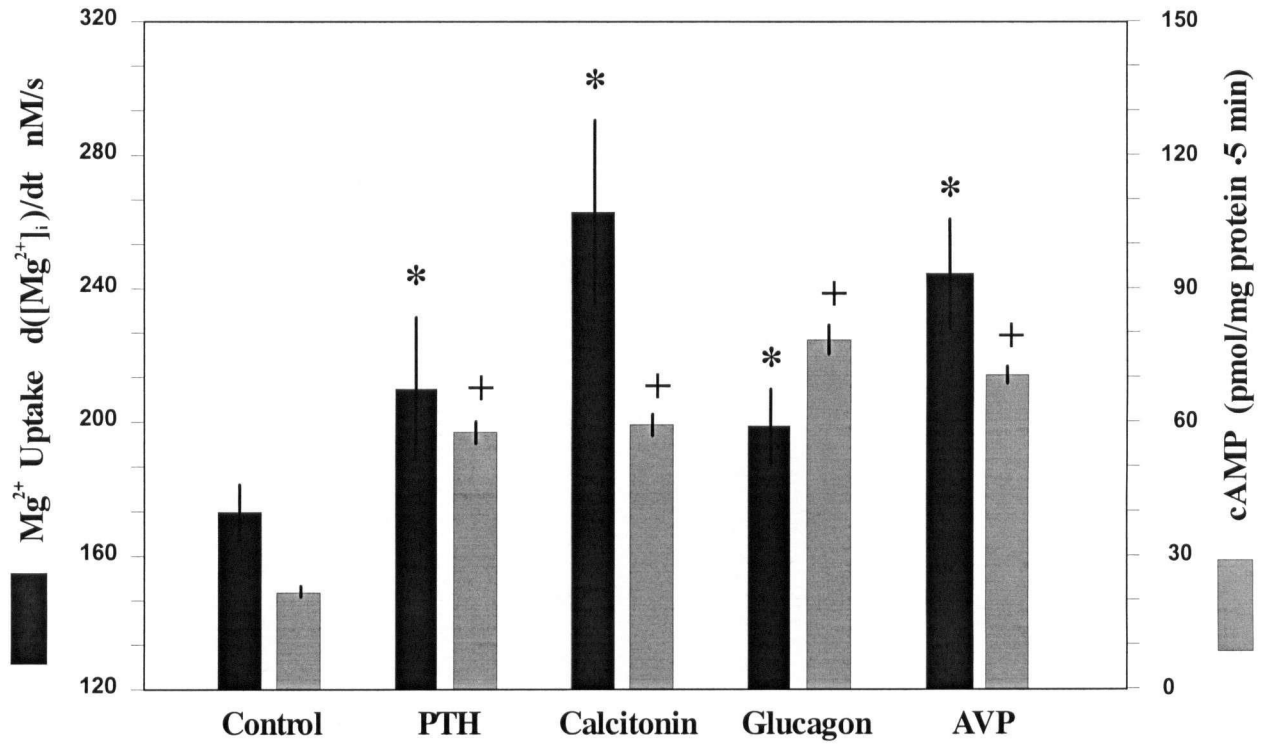


Fig 16. Summary of hormone induced stimulation of  $Mg^{2+}$  uptake and cAMP generation in MDCT cells. cAMP and  $Mg^{2+}$  uptake studies were performed as previously described. \* $P < 0.05$ , significant vs. control values for  $Mg^{2+}$  uptake. +  $P < 0.05$ , significant vs. control values for cAMP generation [87].

entry at any time (Fig.17). Moreover, cAMP,  $10^{-4}$  M, stimulated  $Mg^{2+}$  uptake in the presence of the PMA. I infer from these studies that hormone-stimulated  $Mg^{2+}$  uptake may involve intracellular cAMP accumulation.

### III.8 *The effect of PKA and PKC inhibition on hormone-stimulated $Mg^{2+}$ uptake.*

Finally, I determined the effect of protein kinase A and protein kinase C inhibition on hormone-stimulated  $Mg^{2+}$  uptake. Rp-cAMP, a protein kinase A inhibitor was applied 5 min prior to  $Mg^{2+}$  uptake measurements. Rp-cAMP abolished the effects of glucagon and AVP (Table 6) suggesting that activation of protein kinase A is involved with hormone actions. Ro31-8220, an inhibitor of protein kinase C, was without effect supporting the theory that this signalling pathway is not involved with hormone stimulation of  $Mg^{2+}$  uptake.

**Table 6. Glucagon and AVP act through PKA-mediated pathway**

	Control, nM/s	Glucagon, nM/s	AVP, nM/s
Control	$164 \pm 5$ (6)	$196 \pm 11^*$ (4)	$189 \pm 6^*$ (6)
Rp-cAMPS	$171 \pm 3$ (3)	$176 \pm 5$ (3)	$177 \pm 8$ (3)
Ro31-8220	$167 \pm 10$ (3)	$201 \pm 17^*$ (3)	$197 \pm 7^*$ (3)

#### **Table 6 Legend**

Values are mean  $\pm$  SE; number of experiments is in parentheses.  $Mg^{2+}$  entry was determined in presence of  $10^{-7}$  M Glucagon, or  $3 \times 10^{-7}$  M AVP, with and without a 5 min. pretreatment with either the PKA inhibitor, RpcAMPS ( $10^{-6}$  M) or the PKC inhibitor, Ro31-8220 ( $10^{-6}$  M). \* $P < 0.05$ , significantly different from control values [87].

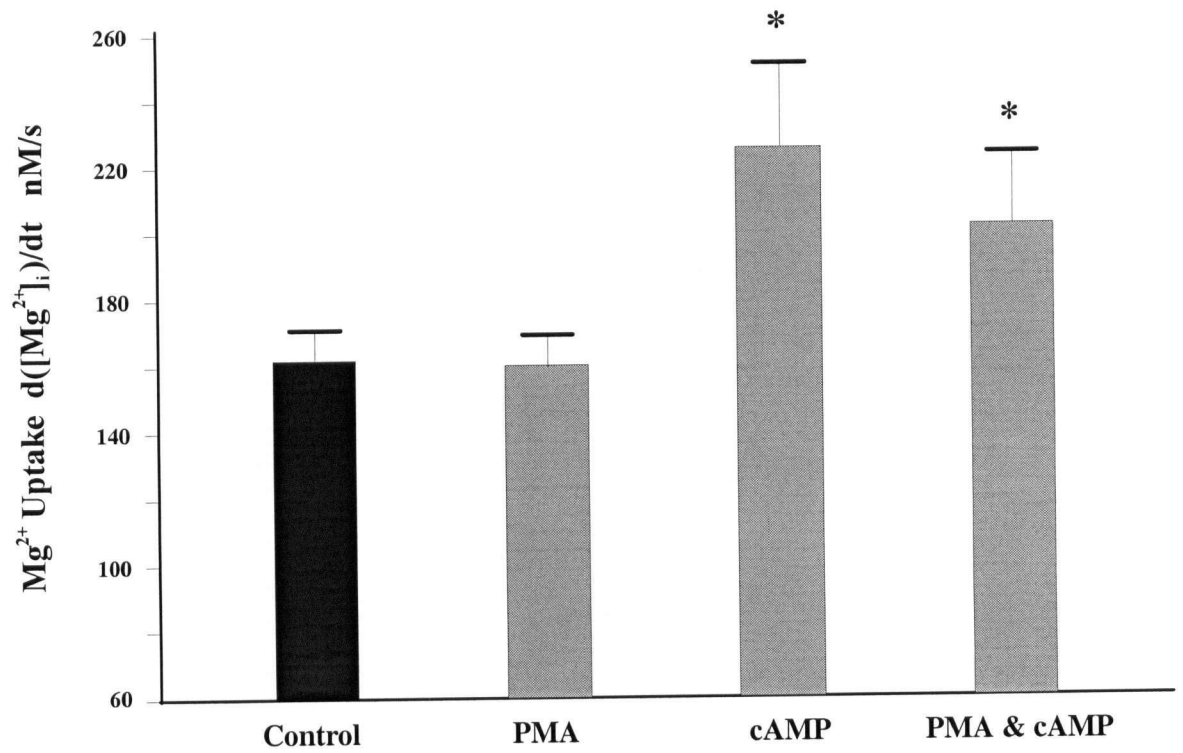


Fig. 17.

Exogenous cAMP stimulates Mg<sup>2+</sup> entry in MDCT cells. Either 8-bromo cAMP, 10<sup>-4</sup> M, or phorbol 12-myristate 14-acetate (PMA), 10<sup>-7</sup> M, were added 6 min prior to determination of d([Mg<sup>2+</sup>]<sub>i</sub>)/dt with the techniques illustrated in Fig. 1. Values are means ± SE for 3-6 cells and \* indicates significance, p<0.01, from control values [87].

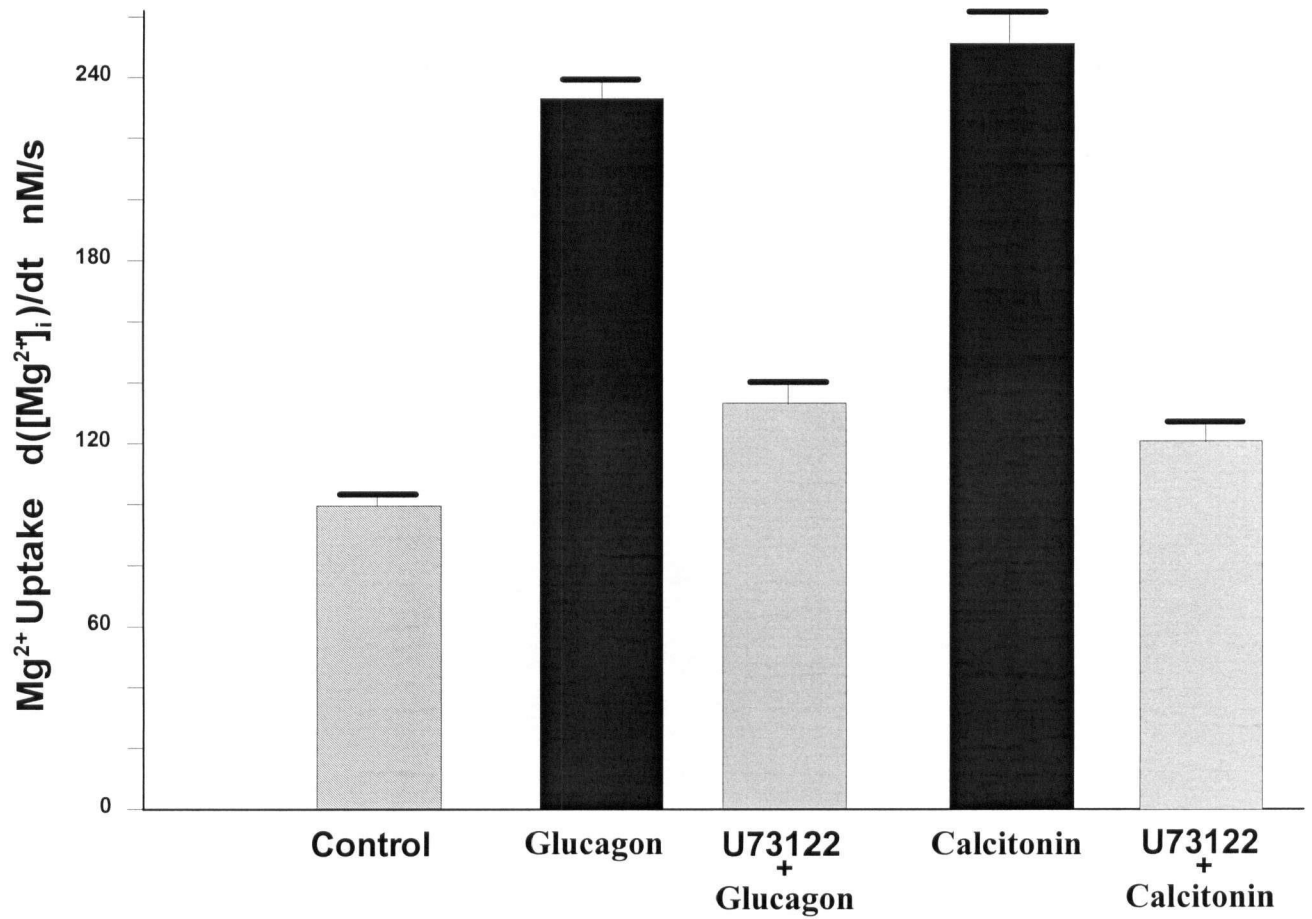


Fig 18.

The phospholipase inhibitor U73122 inhibits glucagon and calcitonin stimulated  $Mg^{2+}$  uptake. U73122 (15  $\mu$ M) was added 10 min prior to hormone addition. Techniques where as previously describe. Values are means  $\pm$  SE for 3-6 cells and \* indicates significance,  $p < 0.01$ , from control values [87].

### III.9 *Glucagon and calcitonin stimulated $Mg^{2+}$ uptake is inhibited with phospholipase-C inhibition.*

It is clear that cAMP production is related to hormonal stimulation and  $Mg^{2+}$  uptake. However, cAMP levels do not always correlate directly with the increase in uptake. Glucagon and calcitonin are both known to alter phosphoinositide metabolism [109] in addition to their effects on cAMP. To determine if phospholipase-C (PLC) was involved in increasing  $Mg^{2+}$  uptake, the PLC inhibitor, U-73122 ( $15\ \mu M$ ), was added 10 min prior to glucagon and calcitonin ( $10^{-7}\ M$ ) addition and uptake measurements. Glucagon- and calcitonin- stimulated magnesium uptake was inhibited with the phospholipase C inhibitor U-73122. In a separate experiment PTH stimulated  $Mg^{2+}$  uptake was also inhibited by U-73122 (data not shown).

## IV *Discussion*

Micropuncture studies clearly indicated that glucagon stimulates magnesium transport in the superficial distal tubule [88]. This segment is comprised of the distal convoluted tubule, connecting tubule and initial cortical collecting tubule. Prior to the present studies, information was not available concerning which distal segment was involved with hormone-stimulated distal tubular magnesium reabsorption. Of the segments comprising the distal tubule, evidence from the present studies clearly indicate that the convoluted portion is involved in glucagon-induced magnesium conservation. Indeed, it may be inferred that glucagon enhances active  $Mg^{2+}$  transport in the distal convoluted tubule. Cellular mechanisms of magnesium transport in the other distal segments, connecting tubule and initial collecting tubule, have not been studied.

AVP has been shown to be an effective magnesium-conserving hormone in anaesthetized and conscious hormone-deprived rats [90,91,111]. Micropuncture studies of these animals have shown that AVP actions occur principally within Henle's loop [92,111]. Using microperfusion studies, Wittner and Di Stefano demonstrated that AVP enhances magnesium absorption in mouse thick ascending limbs through changes in passive transport commensurate with increases in transepithelial voltage [112]. In the micropuncture studies

with hormone-deprived rats, Elalouf and colleagues failed to discern any change in fractional magnesium absorption in the superficial distal tubule following physiological administration of AVP [111]. In these studies, Elalouf *et al.* reported that the fractional calcium absorption increased significantly from  $42.0 \pm 5.8\%$  to  $62.8 \pm 7.1\%$  whereas AVP increased fractional magnesium transport from  $45.5 \pm 7.8\%$  to  $55.3 \pm 15.5\%$  but this change was not statistically significant [111]. Costanzo and Windhager did not observe any change in calcium absorption in the microperfused rat distal tubule with administration of AVP [93]. The animals used in this latter study were TPTXed but not hormone-deprived as were those used by Elalouf *et al.* [111]. In both studies, AVP enhanced sodium absorption in the distal tubule. In the present studies, AVP increased  $Mg^{2+}$  entry into an established distal convoluted tubule (MDCT) cell line suggesting that this hormone acts within this segment of the distal tubule and is involved with renal magnesium conservation. Magnesium transport in the distal convoluted tubule is probably transcellular and active in nature because of the high resistance and lumen negative transepithelial voltage of this segment [74]. Accordingly, AVP likely stimulates active  $Mg^{2+}$  transport in contrast to enhancing passive  $Mg^{2+}$  absorption in the thick ascending limb [112].

Interestingly, AVP stimulates  $Mg^{2+}$  entry 5-10 min following addition of the hormone. This pronounced latency period was not observed with glucagon stimulation of  $Mg^{2+}$  uptake. The reasons for these differences are not known. Friedman and Gesek observed similar differences in action of PTH and calcitonin stimulation of  $Ca^{2+}$  uptake in MDCT cells [41,60]. There was a latency period of 10-15 min prior to PTH-stimulation of  $Ca^{2+}$  entry compared to calcitonin actions which occurred immediately upon addition of the hormone [41,60]. Although the basis for this latency period is not known, it may have something to do with translational processes and protein synthesis because Friedman and Gesek showed that incubation of MDCT cells with cycloheximide for 15 min inhibited PTH-stimulated  $Ca^{2+}$  entry but had no effect on calcitonin actions [41,60]. Furthermore, treatment of the cells with  $1,25-(OH)_2 D_3$  shortened the latency period associated with PTH-stimulated increases of  $[Ca^{2+}]_i$  and  $Ca^{2+}$  entry but had no effect on  $Ca^{2+}$  entry by itself

[113]. These workers were unable to explain the origin of the latency period but concluded that it involved transcription because 5,6-dichloro-1- $\beta$ -D-ribofuranosyl benzimidazole blocked the stimulatory response of 1,25-(OH)<sub>2</sub> D<sub>3</sub> without inhibiting PTH actions [41]. Gesek and Friedman speculated that vitamin D may increase the number of PTH receptors expressed in the MDCT cells [113]. These investigators were unable to show hormone stimulated calcium entry with either AVP or glucagon [107]. In the present studies, pretreatment of MDCT cells with cycloheximide did not inhibit either AVP- or glucagon- stimulated Mg<sup>2+</sup> uptake nor did it affect the latent period associated with AVP. It is apparent from the above mentioned studies that peptide hormones act through different mechanisms to stimulate divalent cation transport in distal convoluted tubules. Further studies are needed to explain these diverse observations but the hormonal control of calcium and magnesium in the distal convoluted tubule may involve unique intracellular signalling pathways.

Recent studies by Gesek and Friedman indicate that PTH-mediated stimulation of calcium transport is through intermediary pathways involving activation of both protein kinase A and protein kinase C as cAMP or phorbol esters had no effect on Ca<sup>2+</sup> entry alone but together they enhanced uptake [109]. These studies are consistent with the observations of Hilalet *et al.* using isolated membrane vesicles from rabbit distal tubules [111]. Moreover, Lajeunesse *et al.* have shown that <sup>45</sup>Ca<sup>2+</sup> uptake in apical membrane vesicles harvested from rabbits pretreated with PTH is greater than those from control animals [114]. Accordingly, PTH may have additional effects on the apical membrane to cause an increase in Ca<sup>2+</sup> uptake. In the present studies, I show that addition of 8-bromo cAMP stimulates Mg<sup>2+</sup> uptake but PMA does not increase entry rates (Fig.17). I infer that activation of protein kinase A is involved in glucagon and/or AVP actions. However, it is not known how activation of protein kinase A stimulates Mg<sup>2+</sup> uptake nor what other pathways may be involved. On balance, the differences in time-frame of hormone action and the disparity of cAMP synthesis suggests that glucagon and AVP may operate through separate but interactive intracellular signalling pathways. More research is required to sort out these intracellular controlling mechanisms.

In summary, glucagon, AVP, calcitonin, and PTH stimulate  $Mg^{2+}$  uptake into MDCT cells, supporting the results of micropuncture reports that these hormones may act within the convoluted segment of the distal tubule [88,112,115,116,117]. The cellular mechanisms by which these hormones stimulate uptake are unclear; however, the involvement of signalling pathways influenced by phospholipase-C and protein kinase-A is clear. The notable difference in hormone responses include the time-frame of action suggesting different intracellular pathways are involved with stimulation of  $Mg^{2+}$  uptake. Further studies are required to determine the intracellular signalling pathway mediated by these hormones.

## Chapter IV. Inhibition of Hormone Stimulated $Mg^{2+}$

### Uptake with Activation of the Polyvalent Cation-Sensing Mechanism.

#### I. Background

In chapter 1 I show that activation of the polycation-sensitive mechanism with either extracellular  $Mg^{2+}$  or  $Ca^{2+}$  inhibited PTH-, calcitonin-, glucagon- and AVP-stimulated cAMP synthesis in MDCT cells [44]. In Chapter 3 I demonstrated the same hormones stimulate  $Mg^{2+}$  uptake. In the present study, I show that activation of  $Mg^{2+}/Ca^{2+}$ -sensing in MDCT cells inhibits hormone-stimulated  $Mg^{2+}$  entry in these cells [75].

*II Methods and Materials:* As previously described in chapter 1.

#### III Results

##### III.1 *Activation of the $Mg^{2+}/Ca^{2+}$ -sensing mechanism inhibits hormone-stimulated cAMP synthesis.*

Table 7 summarizes the effects of activation of the  $Mg^{2+}/Ca^{2+}$ -sensing mechanism on hormone-stimulated cAMP accumulation in normal MDCT cells. Glucagon,  $10^{-7}$  M, and AVP,  $10^{-8}$  M, increased cellular cAMP accumulation from control values of  $19 \pm 1$  to  $105 \pm 5$  and  $71 \pm 2$  pmol/mg protein  $\cdot$  5 min, respectively. Addition of neomycin, 50  $\mu$ M, 5 min prior to the cAMP determinations abolished hormone-stimulated cAMP synthesis (Table 7). Similarly, 10 mM  $[Mg^{2+}]_o$  or 10 mM  $[Ca^{2+}]_o$  completely abolished glucagon- and AVP-dependent cAMP accumulation.  $Gd^{3+}$ ,  $Ni^{2+}$ ,  $Ba^{2+}$ , and  $La^{3+}$  also inhibited glucagon-stimulated cAMP formation indicating that polyvalent cation-sensing in MDCT cells is similar to that observed in the parathyroid gland [4,8,54,75].

Next, I determined the concentration-dependence of extracellular  $Mg^{2+}$  or  $Ca^{2+}$  inhibition on glucagon-stimulated cAMP synthesis. Fig. 19 summarizes these results. The concentration of extracellular  $Mg^{2+}$  required for half-maximal inhibition was about 1.5 mM and glucagon-stimulated cAMP synthesis was

completely inhibited at about 2.5 mM  $\text{MgCl}_2$ . These studies were performed with normal  $\text{Ca}^{2+}$  concentration, 1.0 mM, in the bathing solution. Extracellular  $\text{Ca}^{2+}$  was less potent, as it maximally inhibited hormone-related cAMP synthesis at 5.0 mM with a half-maximal inhibition at about 3.0 mM. Accordingly, the  $\text{Mg}^{2+}/\text{Ca}^{2+}$ -sensing mechanism in MDCT cells is responsive within the physiological concentration range of these divalent cations and the potencies of extracellular  $\text{Mg}^{2+}$  and  $\text{Ca}^{2+}$  are almost equivalent. It is of interest that these results were obtained in the presence of normal extracellular concentrations of either 1.0 mM  $\text{Ca}^{2+}$ , or 0.5 mM  $\text{Mg}^{2+}$ , in the respective experiments.

### III.2 *Activation of $\text{Mg}^{2+}/\text{Ca}^{2+}$ -sensing diminishes hormone-stimulated $\text{Mg}^{2+}$ uptake into $\text{Mg}^{2+}$ -depleted MDCT cells.*

Using our MDCT cell model  $\text{Mg}^{2+}$ -depleted MDCT cells were placed in a bathing solution containing 1.5 mM  $\text{MgCl}_2$ . The  $[\text{Mg}^{2+}]_i$  increased with time and plateaued at  $0.52 \pm 0.06$  mM, ( $n = 9$ ) which was consistent with previous results [61]. The mean rate of refill,  $d([\text{Mg}^{2+}]_i)/dt$ , measured as the change in  $[\text{Mg}^{2+}]_i$  with time, was  $164 \pm 5$  nM/s, ( $n = 6$ ) experiments, as determined over the first 500 s following addition of magnesium (Fig. 20).

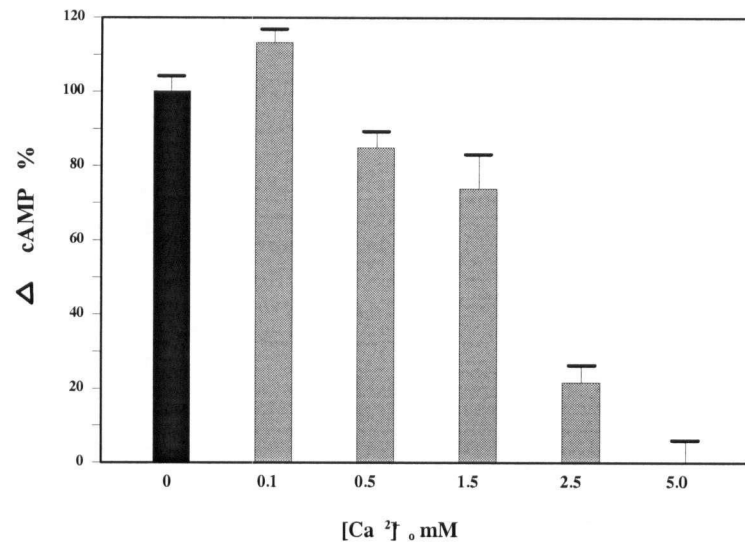
**Table 7.      Activation of  $Mg^{2+}/Ca^{2+}$ -sensing inhibits hormone-stimulated cAMP accumulation.**

	Hormone		
	Control (None)	Glucagon	AVP
cAMP accumulation (pmol/mg protein•5min)			
none	19±1 (11)	105±5 <sup>a</sup> (7)	71±2 <sup>a</sup> (5)
Neomycin	22±2 (3)	22±1 <sup>b</sup> (7)	24±3 <sup>b</sup> (4)
$Mg^{2+}_o$	24±3 (3)	37±3 <sup>ab</sup> (3)	27±3 <sup>b</sup> (3)
$Ca^{2+}_o$	23±2 (3)	32±2 <sup>ab</sup> (3)	34±3 <sup>ab</sup> (3)
$Gd^{3+}_o$	22±1 (5)	34±1 <sup>ab</sup> (5)	34±2 <sup>ab</sup> (5)
$Ni^{2+}_o$	25±1 (5)	41±3 <sup>ab</sup> (5)	34±2 <sup>ab</sup> (5)
$Ba^{2+}_o$	24±1 (5)	39±2 <sup>ab</sup> (5)	33±1 <sup>ab</sup> (5)
$La^{3+}_o$	24±0.3 (5)	32±1 <sup>ab</sup> (5)	27±1 <sup>ab</sup> (5)

**Table 7 Legend**

Where indicated, neomycin, 50  $\mu$ M, or extracellular  $Mg^{2+}_o$ , 10 mM,  $Ca^{2+}_o$ , 10 mM,  $Gd^{3+}_o$ , 0.5 mM,  $Ni^{2+}_o$ , 0.5 mM,  $Ba^{2+}_o$ , 0.5 mM or  $La^{3+}_o$ , 0.5 mM, were added 5 min prior to the addition of either glucagon,  $10^{-7}$  M, or arginine vasopressin,  $10^{-8}$  M, and cAMP was measured 5 min after addition of the respective hormones. <sup>a</sup> indicates significance,  $p < 0.01$ , of hormone-treated versus values without hormone treatment and <sup>b</sup> indicates significance,  $p < 0.01$ , of hormone-treated values in the presence of neomycin or  $Ca^{2+}_o$  or  $Mg^{2+}_o$  versus hormone-treated values in the absence of pretreatment with the polyvalent cations. ( ) is the number of observations [75].

A



B

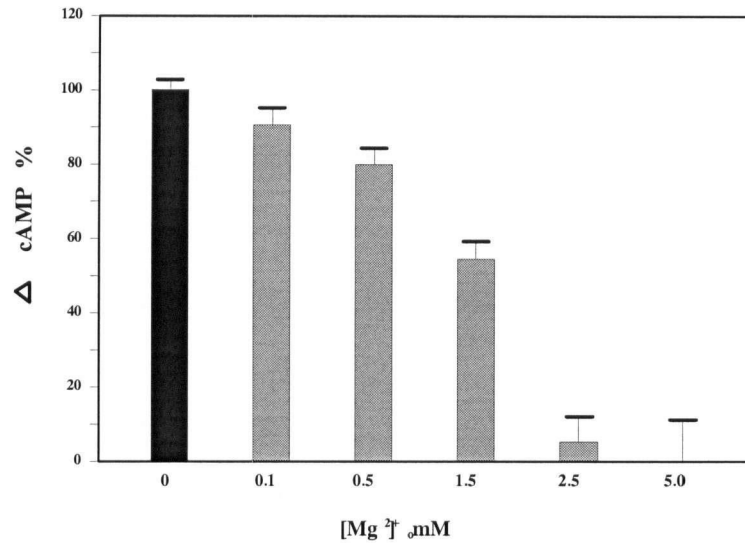


Fig. 19. Concentration-dependence of extracellular  $Mg^{2+}$  or  $Ca^{2+}$  inhibition of glucagon-stimulated cAMP. MDCT cells were cultured in DMEM/Ham's F-12 (1:1) with 0.2% BSA containing 0.6 mM magnesium and 1.5 mM calcium. At the time of experimentation, the cells were washed with a buffer solution containing (in mM):  $MgCl_2$  0.5,  $CaCl_2$  1.0, NaCl 145, KCl 4.0,  $K_2HPO_4$  0.8,  $KH_2PO_4$  0.2, glucose 5, and HEPES-Tris 20, pH 7.4. Panel A. To test  $[Ca^{2+}]_o$ , the cells were initially bathed with the above solutions containing no  $CaCl_2$ . This was replaced with one containing the indicated concentrations. Five minutes following the addition of either  $MgCl_2$  or  $CaCl_2$ , glucagon,  $10^{-7}$  M, was added and cAMP measured following a 5 min incubation period. Panel B. In order to test the effect of  $[Mg^{2+}]_o$ , the buffer solution was changed to identical to the above but without  $MgCl_2$ . This bathing solution was replaced 10 min later with one containing the indicated  $MgCl_2$  concentrations. Values are means  $\pm$  SE for 2-3 experiments consisting of 5 individual observations each and \* indicates significance,  $p < 0.01$ , from control values (set to 100%) [75].

Previously reported data that indicates the  $\text{Mg}^{2+}$  uptake is concentration-dependent and selective for  $\text{Mg}^{2+}$  [61]. I have further shown that glucagon and AVP stimulates  $\text{Mg}^{2+}$  entry into  $\text{Mg}^{2+}$ -depleted MDCT cells by 15-20% over basal entry rates [49]. Glucagon and AVP stimulate  $\text{Mg}^{2+}$  entry without changes in transmembrane voltage,  $-64.7 \pm 0.9$  mV, ( $n = 5$ )[49].

As neomycin stimulates the  $\text{Ca}^{2+}$ -SR neomycin was used to activate the  $\text{Mg}^{2+}/\text{Ca}^{2+}$ -SR [4,44]. Neomycin was added about 5 min prior to the addition of 1.5 mM  $\text{MgCl}_2$  for measurement of  $\text{Mg}^{2+}$  uptake. However, the addition of 50  $\mu\text{M}$  neomycin to the extracellular buffer solution had no effect on basal  $\text{Mg}^{2+}$  uptake, ( $155 \pm 5$  nM/s,  $n = 4$ ), into  $\text{Mg}^{2+}$ -depleted MDCT cells (Fig. 20). However, pretreatment of cells with neomycin inhibited glucagon-stimulated  $\text{Mg}^{2+}$  entry. The mean  $\text{Mg}^{2+}$  uptake rate of glucagon-treated cells was  $196 \pm 11$  nM/s, ( $n = 5$ ) and pretreatment with neomycin, 50  $\mu\text{M}$ , diminished uptake to  $162 \pm 3$  nM/s, ( $n = 3$ ) that was not different from control uptake rates (Fig. 21). Accordingly, activation of  $\text{Mg}^{2+}/\text{Ca}^{2+}$ -sensing mechanism with neomycin inhibits glucagon-stimulated  $\text{Mg}^{2+}$  entry. 50  $\mu\text{M}$  Neomycin, does not alter the membrane voltage either without or with glucagon, ( $-61.3 \pm 1.1$  mV vs.  $-62.0 \pm 2.3$  mV,  $n = 3$ ). Activation of the  $\text{Mg}^{2+}/\text{Ca}^{2+}$ -sensing mechanism also inhibits AVP- stimulated  $\text{Mg}^{2+}$  uptake (data not shown). Addition of neomycin 5 min prior to the application of AVP,  $3 \times 10^{-7}$  M, diminished  $\text{Mg}^{2+}$  uptake from  $189 \pm 6$  to  $163 \pm 4$  nM/s,  $n = 3$ . Next, I tested whether elevated extracellular  $\text{Ca}^{2+}$  may affect  $\text{Mg}^{2+}$  entry. I have previously shown that addition of 10 mM extracellular  $\text{Ca}^{2+}$  does not alter basal  $\text{Mg}^{2+}$  entry into  $\text{Mg}^{2+}$ -depleted MDCT cells [61]. Extracellular  $\text{Ca}^{2+}$  was added 5 min prior to measurement of  $\text{Mg}^{2+}$  uptake. As with neomycin  $[\text{Ca}^{2+}]_o$ , 5 mM, did not change basal  $\text{Mg}^{2+}$  uptake rates but inhibited glucagon-stimulated  $\text{Mg}^{2+}$  entry (Fig. 21). As with extracellular  $\text{Ca}^{2+}$ , large concentrations of extracellular  $\text{Mg}^{2+}$  inhibited glucagon-stimulated  $\text{Mg}^{2+}$  uptake into MDCT cells (Fig. 21). It should be kept in mind that  $\text{Mg}^{2+}$  uptake rate,  $d([\text{Mg}^{2+}]_i)/dt$ , appears to saturate at about 5 mM [61]. The basal  $[\text{Mg}^{2+}]_i$  refill rate was  $164 \pm 5$  nM/s in the presence of buffer containing no calcium and 5.0 mM  $\text{MgCl}_2$ . Glucagon failed to stimulate  $\text{Mg}^{2+}$  uptake,  $154 \pm 6$  nM/s,

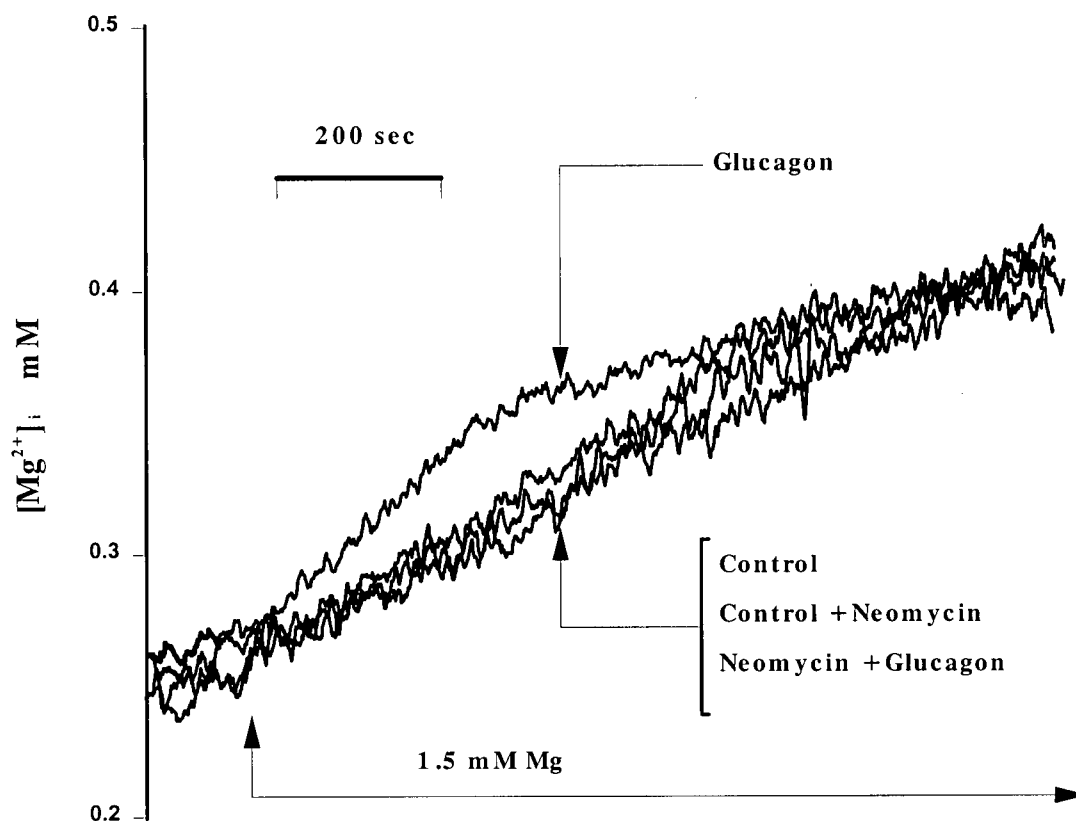


Fig. 20. Activation of the  $\text{Mg}^{2+}/\text{Ca}^{2+}$ -sensing mechanism diminishes hormone-stimulated  $\text{Mg}^{2+}$  uptake into MDCT cells. Intracellular magnesium concentration,  $[\text{Mg}^{2+}]_i$  was determined with mag-fura-2. Cells were cultured in media containing no magnesium (magnesium concentration  $<0.01$  mM) for 16 hr. The basal  $[\text{Mg}^{2+}]_i$  was determined and the cells were subsequently placed in buffer solution containing 1.5 mM  $\text{MgCl}_2$  at the time indicated. The buffer solutions contained (in mM): 145 NaCl, 4.0 KCl, 0.8  $\text{K}_2\text{HPO}_4$ , 0.2  $\text{KH}_2\text{PO}_4$ , 1.0  $\text{CaCl}_2$ , 5.0 glucose, and 10 HEPES/Tris, pH 7.4, with and without 1.5 mM  $\text{MgCl}_2$ . Where indicated 50  $\mu\text{M}$  neomycin was added 5 min prior to the addition of hormone and 1.5 mM  $\text{MgCl}_2$ . Fluorescence was measured at 1 data point/s with 25 signal-point averaging and smoothed according to methods previously reported (10). The Mg uptake,  $d([\text{Mg}^{2+}]_i)/dt$ , was 196 nM/s with glucagon and 165 nM/s in the presence of neomycin. These fluorescence tracings are representative of 9 cells [75].

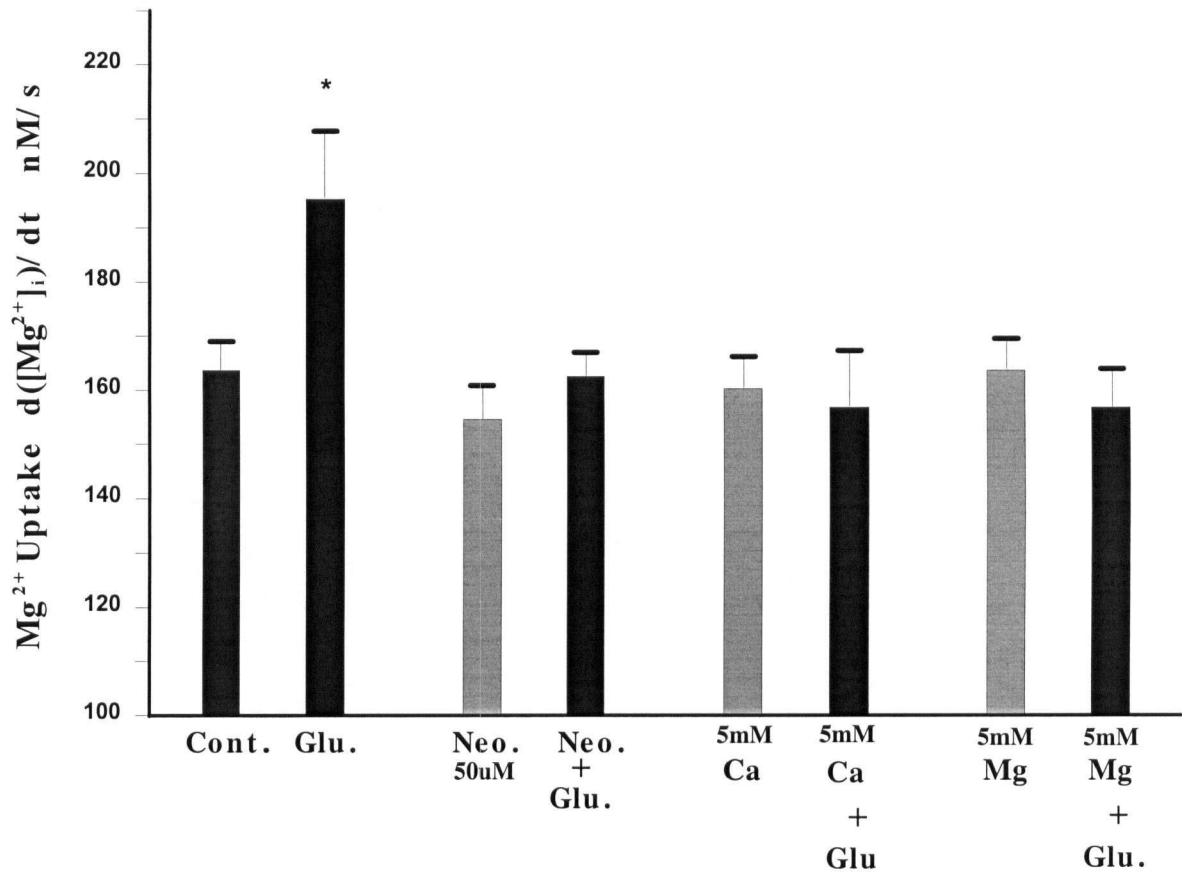


Fig. 21. Summary of the effects of  $\text{Mg}^{2+}/\text{Ca}^{2+}$ -sensing mechanism activation on hormone-stimulated  $\text{Mg}^{2+}$  uptake.  $\text{Mg}^{2+}$  uptake,  $(d[\text{Mg}^{2+}]_i)/dt$ , was determined with 1.5 mM extracellular  $\text{Mg}^{2+}$  in the absence and presence of neomycin, 50  $\mu\text{M}$ ,  $\text{Ca}^{2+}$ , 5.0 mM,  $\text{Mg}^{2+}$ , 5.0 mM, as indicated. Neomycin,  $\text{Ca}^{2+}$  or  $\text{Mg}^{2+}$  was added 5 min prior to the addition of glucagon,  $10^{-7}$  M, and  $\text{MgCl}_2$ , 1.5 mM. The studies were performed as given in legend to Fig. 2. The  $\text{Mg}^{2+}$  uptake rate was determined over 500 s following addition of glucagon. Values are mean  $\pm$  SE for 3-5 cells. \* indicates significance ( $p < 0.05$ ) from control values [75].

when determined in the presence of 5.0 mM  $\text{MgCl}_2$ . These results are consistent with the effects of the polyvalent cations on hormone-mediated cAMP accumulation (Table 7 and Fig. 19).

Next, I measured the glucagon-stimulated  $\text{Mg}^{2+}$  uptake rate, at concentrations below that which produces saturation of  $d([\text{Mg}^{2+}]_i)/dt$ . This was also observed in the presence of glucagon (Fig. 22). However, uptake rates below this value were increased so that the hormone-stimulated  $d([\text{Mg}^{2+}]_i)/dt$  was dependent on extracellular  $\text{Mg}^{2+}$  demonstrating greater fractional transport rates with the lower extracellular magnesium concentrations used to perform the uptake measurements (Fig. 22, insert).

Arthur has recently shown that activation of the calcium-sensing receptor of Madin-Darby canine kidney (MDCK) cells, another distal tubule cell line, with high extracellular calcium, inhibited basal transepithelial calcium transport after 30 min but not after 5 min [96]. I have tested whether the addition of neomycin, 50  $\mu\text{M}$ , for 30 min, might inhibit basal  $\text{Mg}^{2+}$  uptake in MDCT cells. The mean uptake rate,  $d([\text{Mg}^{2+}]_i)/dt$ , was  $153 \pm 10$ ,  $n = 6$  following a 30 min incubation with neomycin (Fig. 23). Accordingly, in MDCT cells, I have no evidence that activation of  $\text{Mg}^{2+}/\text{Ca}^{2+}$ -sensing inhibits basal  $\text{Mg}^{2+}$  uptake. Further studies are necessary to determine if this conclusion is valid for transepithelial  $\text{Mg}^{2+}$  transport.

### III.3 *Activation of $\text{Mg}^{2+}/\text{Ca}^{2+}$ -sensing does not affect cAMP stimulation of $\text{Mg}^{2+}$ uptake.*

From chapter 3 I have shown that the addition of exogenous 8-bromo cAMP stimulates  $\text{Mg}^{2+}$  entry into MDCT cells [49]. Furthermore, protein kinase A inhibition diminishes hormone-stimulated  $\text{Mg}^{2+}$  uptake [49]. Accordingly, glucagon and AVP act, in part, through a cAMP-dependent pathway.

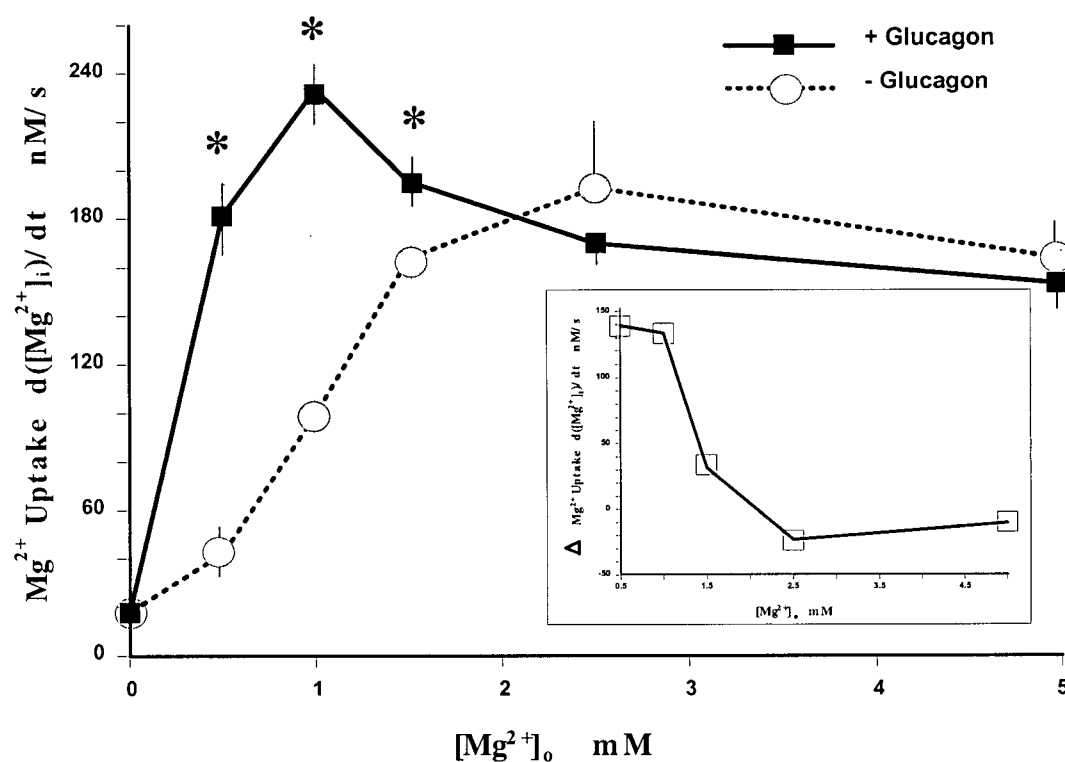


Fig. 22. Glucagon-stimulation of  $Mg^{2+}$  uptake is dependent on the concentration of extracellular  $Mg^{2+}$  used to determine  $d([Mg^{2+}]_i)/dt$ .  $Mg^{2+}$  uptake was measured with and without glucagon,  $10^{-7}$  M, in the presence of the extracellular  $MgCl_2$  concentrations as indicated. The insert shows the change of hormone-stimulated  $Mg^{2+}$  uptake as a function of extracellular  $Mg^{2+}$  concentration used to perform the refill studies. Values are means  $\pm$  SE for 3-6 observations and \* indicates significance,  $p < 0.05$ , from control values not treated with glucagon [75].

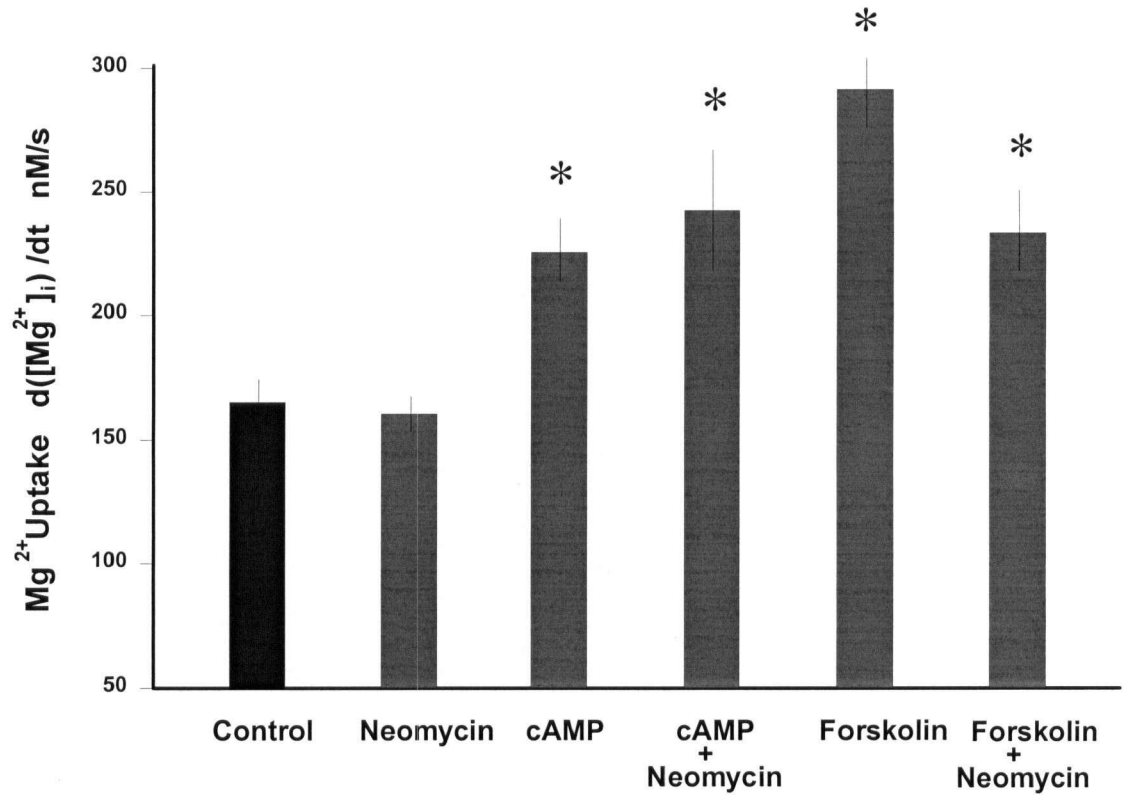


Fig. 23. Activation of  $\text{Mg}^{2+}/\text{Ca}^{2+}$  sensing does not alter cAMP-mediated  $\text{Mg}^{2+}$  uptake. Either forskolin,  $1\ \mu\text{M}$ , to generate endogenous cAMP synthesis or 8-bromo cAMP,  $10^{-4}\ \text{M}$ , was added 6 min prior to determination of  $d([\text{Mg}^{2+}]_i)/dt$  with microfluorescence according to the techniques illustrated in Fig. 3. Neomycin,  $50\ \mu\text{M}$ , was added 5 min prior to the addition of forskolin or 8-bromo cAMP. Values are means  $\pm$  SE for 3-6 cells and \* indicates significance,  $p < 0.01$ , from control values [75].

In order to determine if activation of the  $Mg^{2+}/Ca^{2+}$ -sensing mechanism affects cAMP-mediated processes, I pretreated cells with neomycin to activate the receptor then added 8-bromo cAMP and measured  $Mg^{2+}$  uptake rate. Fig. 23 summarizes these experiments. 8-bromo cAMP stimulated  $Mg^{2+}$  regardless of the presence of presence of neomycin. Forskolin stimulates intracellular cAMP production in the presence of activation of  $Mg^{2+}/Ca^{2+}$ -sensing [73,107]. Accordingly, I performed  $Mg^{2+}$  uptake studies in the presence of forskolin and neomycin to test whether forskolin alters transport despite activation of  $Mg^{2+}/Ca^{2+}$ -sensing. Again, forskolin stimulated  $Mg^{2+}$  uptake in the presence of activation of  $Mg^{2+}/Ca^{2+}$ -sensing by neomycin. These studies suggest that activation of the  $Mg^{2+}/Ca^{2+}$ -sensing mechanism inhibits hormone-stimulated  $Mg^{2+}$  uptake by inhibiting hormone-mediated cAMP generation.

III.4 *Activation of  $Mg^{2+}/Ca^{2+}$ -sensing does not inhibit amiloride-stimulated  $Mg^{2+}$  uptake.* I have shown that amiloride stimulates  $Mg^{2+}$  uptake rates by about 30-40% above basal levels in MDCT cells. Amiloride hyperpolarizes the plasma membrane by  $-28 \pm 8$  mV, thereby creating a more favourable electrical gradient for  $Mg^{2+}$  entry [61]. I pretreated MDCT cells with neomycin, then determined the effect of amiloride on  $Mg^{2+}$  uptake. Amiloride increased  $Mg^{2+}$  entry,  $221 \pm 12$  nM/s, in the presence of neomycin indicating that the activation of the  $Mg^{2+}/Ca^{2+}$ -sensing mechanism does not alter the cellular actions of this magnesium- conserving diuretic (Fig. 24). The increase in membrane voltage, from basal levels,  $-65.5 \pm 2.0$  mV, normally observed with amiloride,  $-75.3 \pm 1.8$  mV, was also not altered by neomycin,  $-74.7 \pm 1.2$  mV,  $n=5$ .

#### IV. Discussion

Activation of a  $Mg^{2+}/Ca^{2+}$ -sensing mechanism elicits cytosolic  $Ca^{2+}$  signals and diminishes hormone-mediated intracellular cAMP accumulation (as shown in Chapter 1 & 3) [44]. In the present

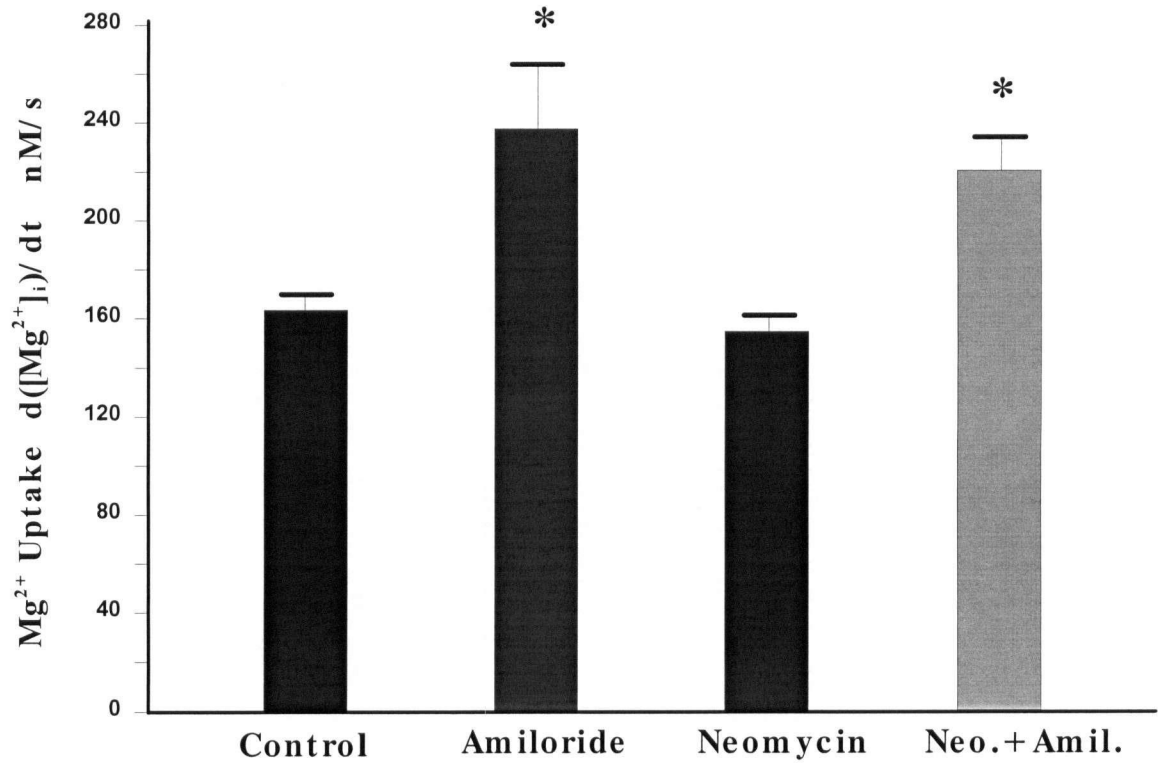


Fig. 24. Activation of  $Mg^{2+}/Ca^{2+}$  sensing does not alter amiloride-stimulated  $Mg^{2+}$  uptake.  $Mg^{2+}$  uptake,  $d([Mg^{2+}]_i)/dt$ , was performed in the presence of 1.5 mM  $MgCl_2$  and with or without 10  $\mu$ M amiloride. Neomycin, 50  $\mu$ M, was added where indicated 5 min prior to the addition of amiloride. Values are means  $\pm$  SE for 3-6 cells and \* indicates significance,  $p < 0.01$ , from control values [75].

study, I show that activation of this  $\text{Mg}^{2+}/\text{Ca}^{2+}$ -sensing mechanism also inhibits glucagon- and AVP-stimulated  $\text{Mg}^{2+}$  uptake into MDCT cells [75]. As this cell line possesses many of the transport properties of the intact distal convoluted tubule, I conclude that the  $\text{Mg}^{2+}/\text{Ca}^{2+}$ -sensing mechanism plays an important role in control of magnesium transport in this nephron segment.

## ***Chapter V. Mineralocorticoid Hormones Stimulate Hormone Mediated $Mg^{2+}$ uptake in MDCT cells.***

### ***I. Background***

Cells of the distal convoluted segment possess mineralocorticoid receptors [126-129]. Although there is some dispute concerning their functional purpose within this segment [130, 131], there is evidence that mineralocorticoid hormones enhance both  $Na^+$  conductance and  $NaCl$  co-transport in distal convoluted tubule cells [132, 133]. Accordingly, mineralocorticoid may alter  $Mg^{2+}$  entry by acting through changes in other ion transports [61]. Alternatively, mineralocorticoids may affect hormone-mediated control of  $Mg^{2+}$  transport within the distal tubule. Doucet *et al.* have shown that adrenalectomy reduced glucagon-stimulated adenylate cyclase activity in the thick ascending limb; this reduced cAMP response was prevented with aldosterone administration [134]. Other investigators have shown that vasopressin-sensitive adenylate cyclase is diminished in rat and rabbit collecting tubules harvested from adrenalectomized animals [135, 136, 137, 138]. Accordingly, mineralocorticoids could alter hormonal control of transport in the distal tubule through their actions on receptor-mediated signalling pathways.

Using the MDCT cell model I sought to determine the effect of the steroid hormones on  $Mg^{2+}$  transport and the interactions with hormone-stimulated  $Mg^{2+}$  uptake [139]. In the previous studies, it was shown that aldosterone potentiates glucagon- and AVP-stimulated intracellular cAMP accumulation and  $Mg^{2+}$  uptake in MDCT cells. The potentiation of hormone actions by mineralocorticoids may have significant effects on renal magnesium balance.

*II. Materials and Methods:* As previously described in chapter 1.

### III. Results

In the previous chapter I have showed that glucagon and AVP stimulate  $Mg^{2+}$  uptake into  $Mg^{2+}$ -depleted MDCT cells in a concentration-dependent fashion [87]. Maximal concentration of glucagon,  $10^{-6}$  M, and AVP,  $3 \times 10^{-7}$  M, enhanced mean  $Mg^{2+}$  uptake rates by  $273 \pm 6$  and  $189 \pm 6$  nM/s, respectively. Hormone-stimulated uptake was inhibited by nifedipine and was not affected by pretreatment with the protein synthesis inhibitor, cycloheximide. It was concluded that hormonal actions were likely through the activation of putative  $Mg^{2+}$  channels that is independent of *de novo* protein synthesis[87].

#### III.1 Aldosterone potentiates hormone-stimulated $Mg^{2+}$ uptake

The addition of  $10^{-7}$  M aldosterone, 20 min prior to the measurement of  $Mg^{2+}$  entry did not alter the rate of  $Mg^{2+}$  uptake ( $189 \pm 21$  nM/s,  $n = 3$ ) vs control. Incubation of MDCT cells with aldosterone,  $10^{-7}$  M, for 16 hr prior to determination of  $Mg^{2+}$  entry also had no effect on basal  $Mg^{2+}$  uptake, ( $172 \pm 8$  nM/s,  $n = 3$ ). However, pretreatment of MDCT cells with aldosterone potentiated both glucagon- and AVP-stimulated  $Mg^{2+}$  uptake rates (Fig. 25). Hormone-stimulated  $Mg^{2+}$ -refill was enhanced with aldosterone but aldosterone treatment had no effect on the final  $[Mg^{2+}]_i$  attained following refill; this first concentration was not different from control values, 0.52 mM. Furthermore, aldosterone potentiated glucagon and AVP at all hormone concentrations above  $10^{-9}$  M (Figs. 26 and 27). The glucagon concentration required to produce half-maximal stimulation of  $Mg^{2+}$  uptake in aldosterone-treated cells was about  $5 \times 10^{-7}$  M which was not different from control cells. Unlike glucagon, AVP stimulates  $Mg^{2+}$  uptake after a latent period of 5-10 min (Fig.25B). Pretreatment of cells with aldosterone appeared to shorten the duration of this latent period (Fig.25B). The AVP concentration for half-maximal stimulated  $Mg^{2+}$  uptake is not changed (Fig.27).

Fig. 28 shows that aldosterone potentiated hormone-stimulated  $Mg^{2+}$  uptake was sensitive to nifedipine, suggesting that  $Mg^{2+}$  entry was being affected.

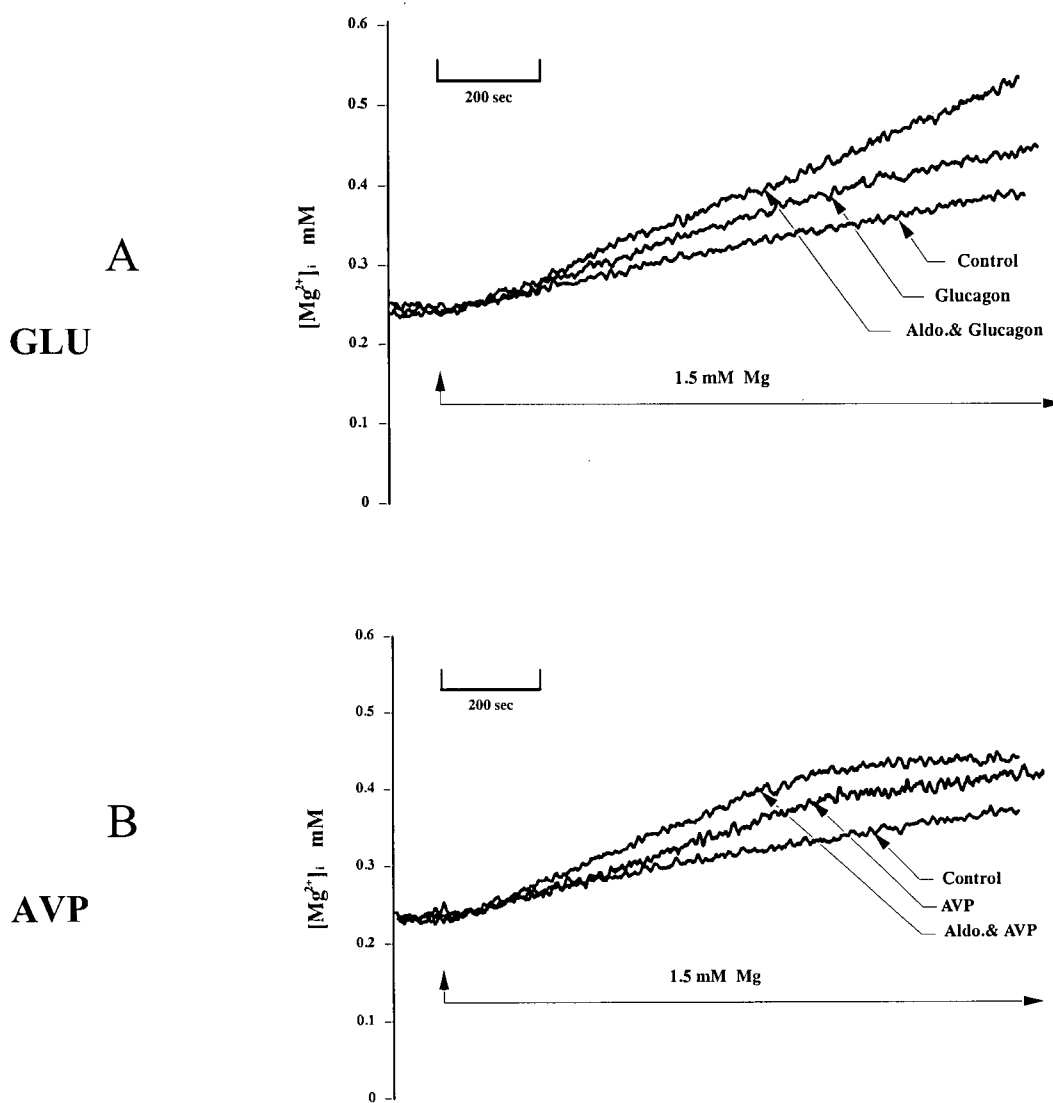


Fig. 25. Aldosterone potentiates glucagon- and AVP-stimulated  $\text{Mg}^{2+}$  uptake in  $\text{Mg}^{2+}$ -depleted mouse distal convoluted tubule (MDCT) cells. Confluent MDCT cells were cultured in  $\text{Mg}^{2+}$ -free media ( $<0.01$  mM) for 16-20 hr. Uptake studies were performed in buffer solutions in the absence of  $\text{Mg}^{2+}$ , and, as indicated,  $\text{MgCl}_2$  (1.5 mM final concentration) was added to observe changes in intracellular  $\text{Mg}^{2+}$  concentration. The buffer solutions contained (in mM): 145 NaCl, 4.0 KCl, 0.8  $\text{K}_2\text{HPO}_4$ , 0.2  $\text{KH}_2\text{PO}_4$ , 1.0  $\text{CaCl}_2$ , 5.0 glucose, and 10 HEPES/Tris, pH 7.4, with and without 1.5 mM  $\text{MgCl}_2$ . Panel A: glucagon,  $10^{-7}$  M, and panel B: AVP,  $3 \times 10^{-7}$  M, were added to this buffer solution where indicated. Were indicated the MDCT cells were treated with aldosterone,  $10^{-7}$  M, for 16 hr prior to analysis. Fluorescence was measured at 1 data point/s with 25-point signal averaging, and the tracing was smoothed as previously described [139].

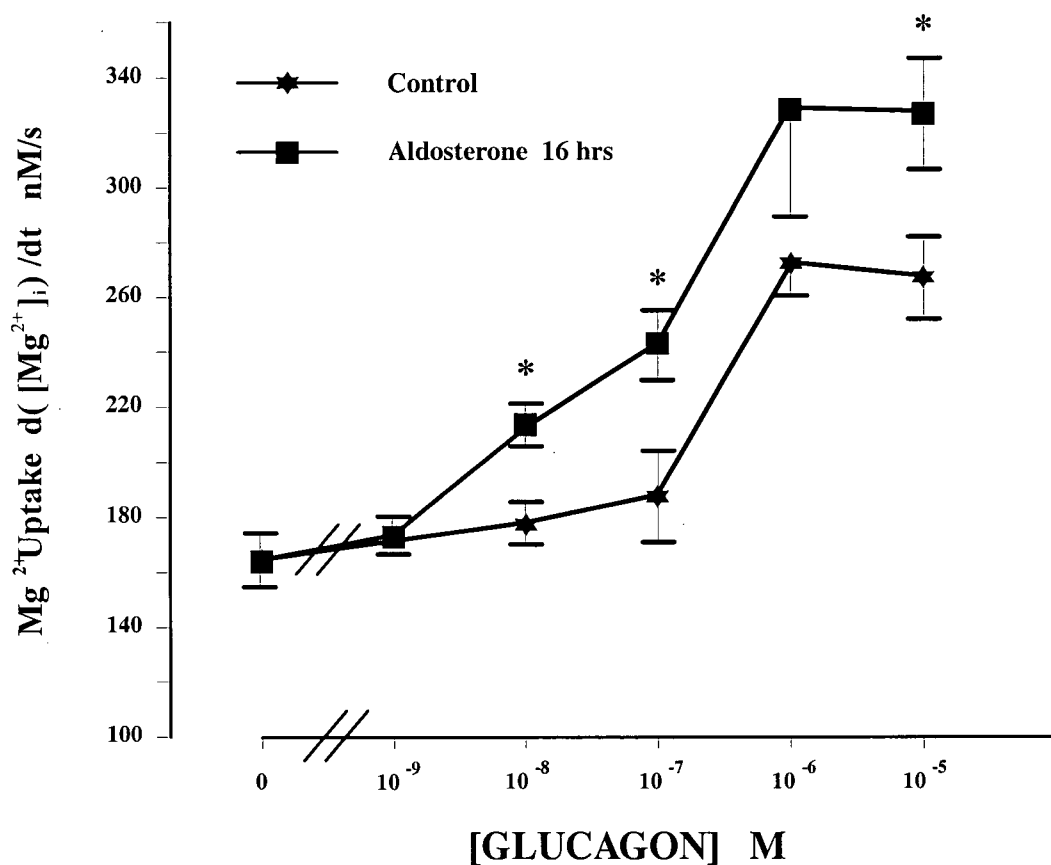


Fig. 26. Aldosterone potentiates glucagon-stimulated  $Mg^{2+}$  entry in MDCT cells. MDCT cells were incubated with and without aldosterone,  $10^{-7}$  M, for 16 hr prior to the determination of  $Mg^{2+}$  entry. The rate of  $Mg^{2+}$  uptake,  $d([Mg^{2+}]_i)/dt$ , was determined over the initial 500 s following addition of the hormone and  $MgCl_2$ . Glucagon was added at the concentrations indicated. Values without aldosterone are from ref. 4. Values are means  $\pm$  SE for 3-6 cells. \* indicates significance,  $p < 0.05$ , of  $Mg^{2+}$  uptake with glucagon vs aldosterone + glucagon [139].

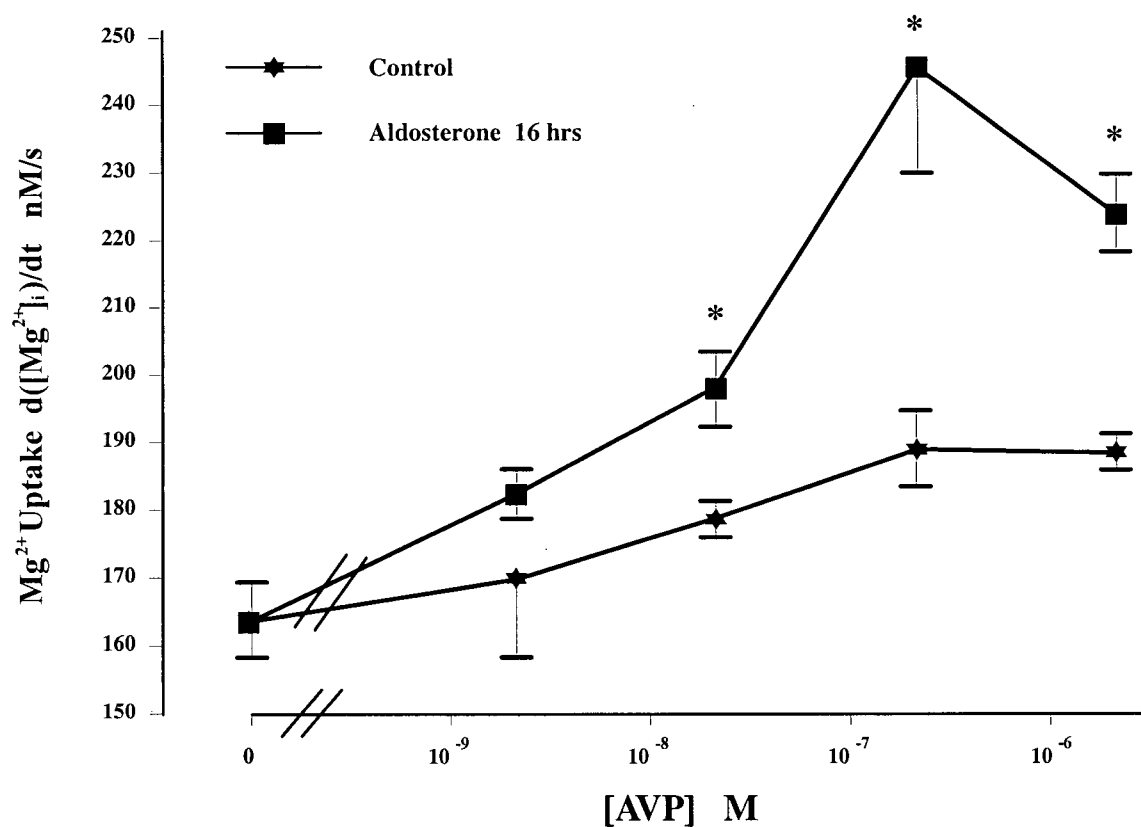


Fig. 27. Aldosterone potentiates AVP-stimulated  $\text{Mg}^{2+}$  uptake in MDCT cells. Magnesium uptake determinations were performed as given in legend to Fig. 1. AVP was added at the concentrations indicated. The cells were incubated with and without aldosterone,  $10^{-7}$  M, for 16-20 hr prior to uptake measurements.  $\text{Mg}^{2+}$  uptake rates were determined 6 min following addition of AVP. Tracings are representative of 4-6 cells [139].

### III.2 *Aldosterone potentiates hormone-stimulated cAMP accumulation in MDCT cells.*

Evidence has been given that mineralocorticoids may increase the coupling efficiency of hormone receptors through G-proteins to adenylate cyclase [134]. Accordingly, I determined hormone-stimulated cAMP synthesis in MDCT cells pretreated with aldosterone. Aldosterone did not have any effect on basal cAMP concentrations in control cells (Table 7). However, aldosterone potentiated cAMP accumulation in response to glucagon and AVP. Aldosterone also enhanced cAMP synthesis by parathyroid hormone (PTH) and calcitonin; accordingly, potentiation of hormone-mediated cAMP production by mineralocorticoids may be a general phenomenon (Table 7). These results indicate that mineralocorticoids increases receptor-mediated cAMP synthesis which may provide the basis for potentiation of  $Mg^{2+}$  uptake in MDCT cells.

Aldosterone potentiates glucagon-stimulated cAMP synthesis in a concentration-dependent manner (Fig. 29). Incubation of cells for 16 hr with various aldosterone concentrations potentiated maximal glucagon responses with a half-maximal aldosterone concentration at about  $10^{-8}$  M.

III.3 *Aldosterone potentiates hormone-stimulated  $Mg^{2+}$  uptake and cAMP generation through de novo protein synthesis.* As it has been well established that mineralocorticoids act, in part, through initiating protein production, I tested whether potentiation of hormone action may be through this process. In this study, the MDCT cells were depleted of  $Mg^{2+}$  for 16 hr prior to the addition of aldosterone, with or without cycloheximide. The cells were incubated for a further 3 hr and uptake measurements were performed in the presence of 1.5 mM  $MgCl_2$  to determine  $Mg^{2+}$  uptake.  $Mg^{2+}$  uptake was  $244 \pm 14$  nM/s (Table 9) in the presence of aldosterone plus glucagon. Addition of cycloheximide with aldosterone, 3 hr prior to uptake analysis resulted in the inhibition of aldosterone potentiation of glucagon-stimulated  $Mg^{2+}$  entry (Table 7 & 8). Cycloheximide did not have any effect on glucagon-stimulated  $Mg^{2+}$  entry in the absence of mineralocorticoids (Table 8). These observations indicate that aldosterone may potentiate hormone actions through mechanisms dependent on de novo protein synthesis.

Next, I determined the effect of cycloheximide on aldosterone potentiation of hormone-stimulated cAMP accumulation. Again, the cells were  $Mg^{2+}$ -depleted for 16 hr then treated with aldosterone,  $10^{-7}$  M, with and without cycloheximide. Three hours later hormone-responsive cAMP synthesis was determined by radioimmunoassay measurements. Glucagon,  $10^{-7}$  M, stimulated cAMP synthesis from  $19 \pm 1$  to  $105 \pm 5$  pmol/mg protein  $\cdot$  5 min (Table 8). Cycloheximide pretreatment did not alter cAMP generation. However, cycloheximide prevented the potentiation of aldosterone on glucagon induced cAMP synthesis (Table 9).

Table 8. **Aldosterone potentiates hormone-stimulation of cAMP synthesis (pmol/mg protein  $\cdot$  5 min) in MDCT cells.**

	Glucagon	AVP	PTH	Calcitonin
Control:				
19 $\pm$ 1	105 $\pm$ 5*	71 $\pm$ 2*	56 $\pm$ 2*	60 $\pm$ 0.1*
(5)	(4)	(5)	(5)	(4)
Aldosterone				
26 $\pm$ 4	251 $\pm$ 32**	139 $\pm$ 14**	153 $\pm$ 26**	286 $\pm$ 29**
(4)	(3)	(4)	(3)	(3)

**Table 8 Legend**

The hormones, glucagon,  $10^{-7}$  M, AVP,  $10^{-8}$  M, parathyroid hormone (PTH),  $10^{-7}$  M, and calcitonin  $10^{-7}$  M, were added 5 min prior to cAMP determinations. Where indicated aldosterone,  $10^{-7}$  M, was added to the culture media 16 hr prior to cAMP measurements (measured as pmol/mg protein  $\cdot$  5 min). Values are means  $\pm$  SE for (n) number of experiments. \*indicates significance,  $p < 0.01$ , vs. control values and \*\* indicates significance of hormone vs. aldosterone + hormone for each of the respective hormones [139].

**Table 9. Role of protein synthesis in glucagon-stimulated  $Mg^{2+}$  uptake and cAMP synthesis in MDCT cells.**

	$d([Mg^{2+}]_i)/dt$		cAMP synthesis	
	Control	Cycloheximide	Control	Cycloheximide
	nM/s	nM/s	pmol/mg protein • 5 min	
Control	164±5	163±6	19±1	26±7
(n)	(6)	(3)	(5)	(3)
Glucagon	196±11*	197±11*	105±5*	98±6*
(n)	(3)	(3)	(4)	(3)
Aldosterone + Glucagon	244±14*	195±18*(**)	251±32*	113±14*(☆☆)
(n)	(6)	(5)	(3)	(4)

**Table 9 Legend**

$Mg^{2+}$  entry,  $d([Mg^{2+}]_i)/dt$ , and cellular cAMP accumulation were determined with and without the presence of aldosterone,  $10^{-7}$  M for 3 hr and with the addition of glucagon,  $10^{-7}$  M, with and without pretreatment with cycloheximide, 1  $\mu$ g/ml, as indicated. The protein synthesis inhibitor was applied with the aldosterone 3 hr prior to uptake studies or measurement of cAMP accumulation. *n* is the number of observations and \* indicates significance,  $p < 0.05$ , of hormone vs control values. (☆☆) indicates significance,  $p < 0.05$ , of cycloheximide vs control values for each of the hormone treatments [139].

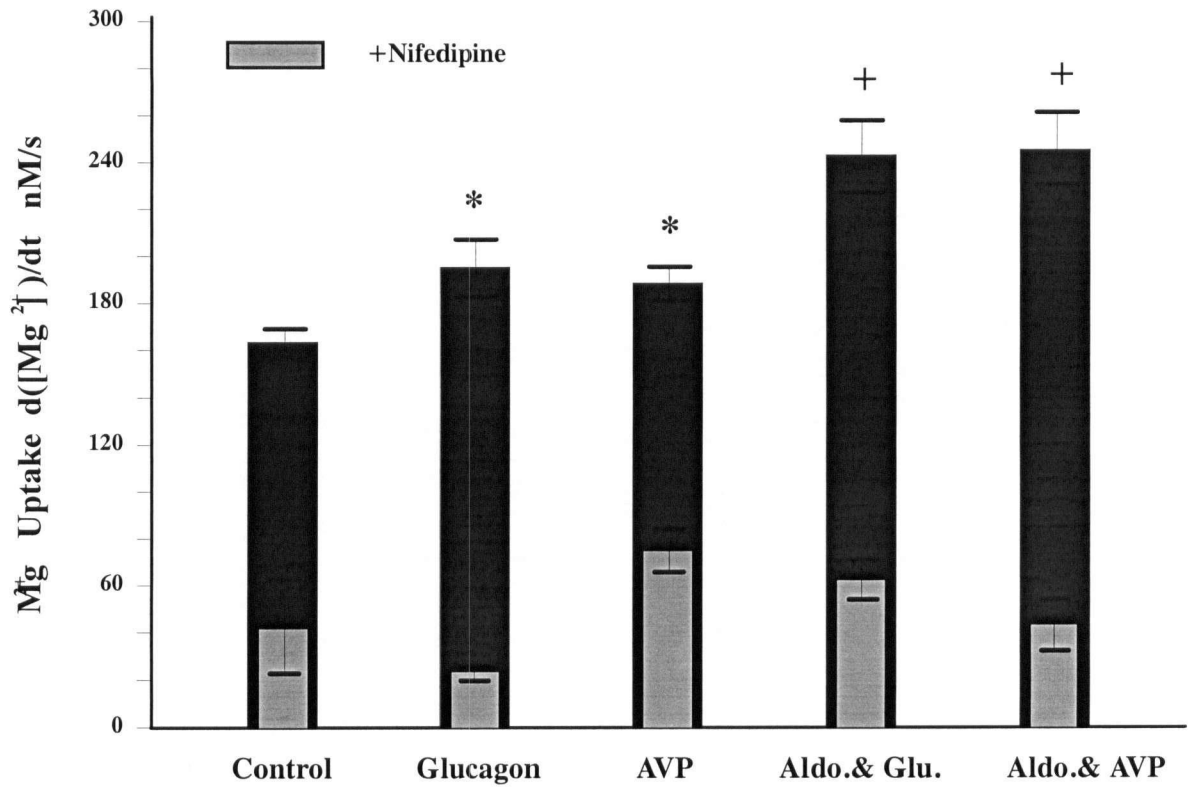


Fig. 28. Aldosterone potentiation of hormone-stimulated  $Mg^{2+}$  entry is through dihydropyridine-sensitive pathways. MDCT cells were treated with aldosterone,  $10^{-7}$  M, for 16 hr prior to determining hormone-responsive  $Mg^{2+}$  uptake. Nifedipine,  $10 \mu M$ , was added with the  $1.5$  mM  $MgCl_2$  refill solution. Values are means  $\pm$  3-6 cells. \* indicates significance from control values and + indicates significance of aldosterone plus hormone vs the respective glucagon or AVP values [139].

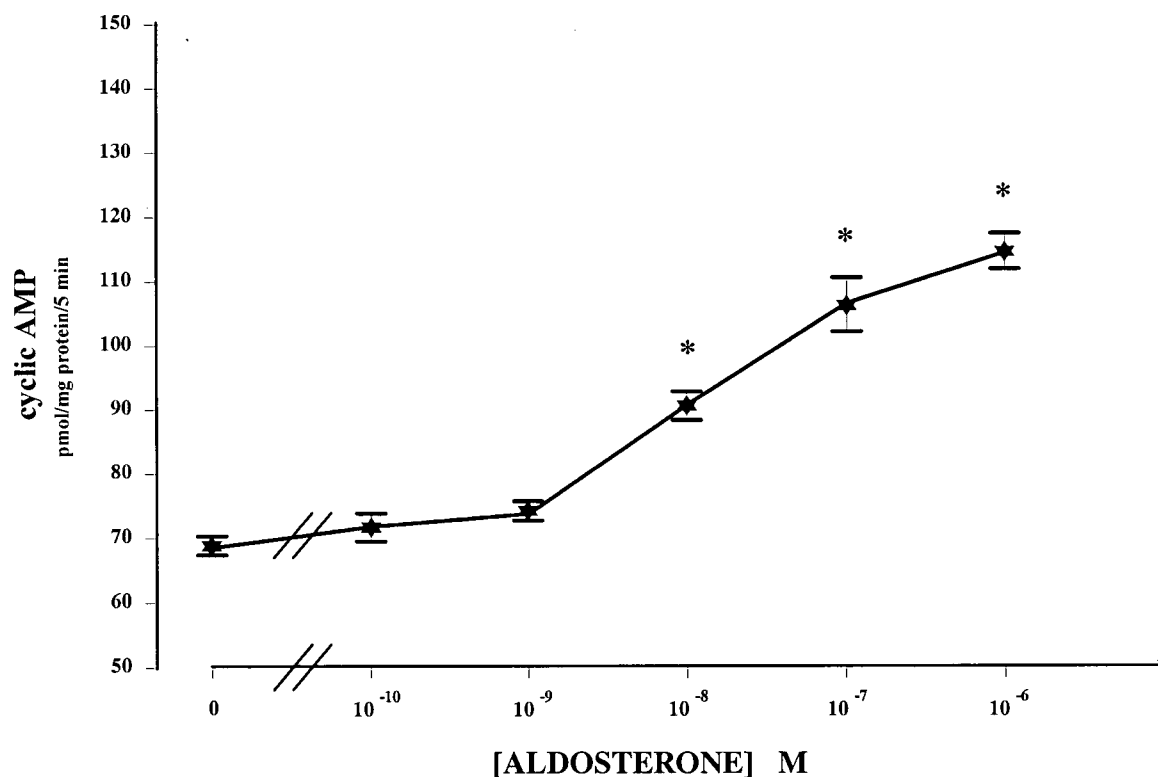


Fig. 29. Aldosterone potentiates glucagon-stimulated intracellular cAMP accumulation in a concentration-dependent manner. MDCT cells were incubated for 16 hr in magnesium-free buffer solution containing the indicated aldosterone concentrations. Glucagon,  $10^{-7}$  M, was added and cAMP was measured following 5 min in the presence of IBMX. Values are mean  $\pm$  SE for 3-5 observations. \* indicates significance,  $p < 0.05$ , from control values [139].

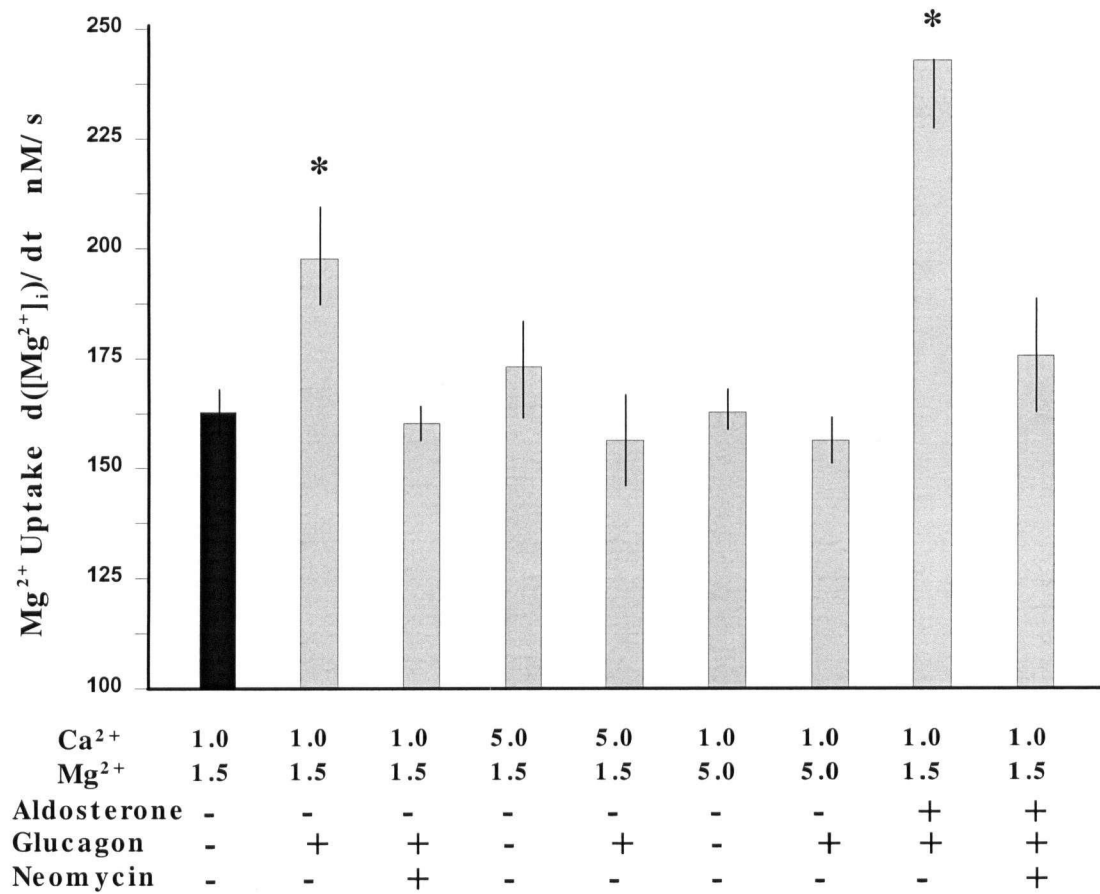


Fig. 30.  $\text{Mg}^{2+}$  entry,  $d([\text{Mg}^{2+}]_i)/dt$  was determined with and without the presence of aldosterone,  $10^{-7}$  M for 3 hr, and with or without the addition of glucagon ( $10^{-7}$  M) or neomycin ( $50\mu\text{M}$ ).  $\text{Ca}^{2+}$  and  $\text{Mg}^{2+}$  were altered as shown. Values are mean  $\pm$  SE for 3-5 observations. \* indicates significance,  $p < 0.05$ , from control values.

III.4      *Stimulation of the  $Mg^{2+}/Ca^{2+}$ -SR inhibits Aldosterone stimulated  $Mg^{2+}$  uptake.* Finally I tested if stimulation of the  $Mg^{2+}/Ca^{2+}$ -SR had any affect on  $Mg^{2+}$  uptake. Addition of  $50\mu M$  neomycin inhibited  $Mg^{2+}$  uptake stimulated with both  $10^{-7} M$  aldosterone and  $10^{-7} M$  glucagon (Fig.30).

#### IV. Discussion

In summary, these studies show that aldosterone potentiates glucagon- and AVP-stimulated  $Mg^{2+}$  uptake into MDCT cells. In additional studies not shown we have further demonstrated that aldosterone potentiates PTH- and calcitonin-stimulated  $Mg^{2+}$  uptake. Aldosterone's action is in part through potentiating hormone-stimulated cAMP formation. Important to the present study is the observation that activation of the  $Mg^{2+}/Ca^{2+}$  sensing receptor inhibits this aldosterone response.

## Chapter VI. 1,25-Dihydroxyvitamin D<sub>3</sub> stimulates Mg<sup>2+</sup> uptake into mouse distal convoluted tubule cells

### I. Background

Vitamin D metabolites have important effects on mineral metabolism by their actions on epithelial transport. Although it is clear that the hormonally-active vitamin D metabolite, 1 $\alpha$ ,25-dihydroxyvitamin D<sub>3</sub> [1,25(OH)<sub>2</sub>D<sub>3</sub>], increases calcium and magnesium absorption within the intestine, its actions within the kidney are more complex [78,107,142,143]. 1,25(OH)<sub>2</sub>D<sub>3</sub> increases calbindin-D<sub>28k</sub> in distal tubule cells including the convoluted and connecting tubule and collecting duct cells [144-147]. This calcium-binding protein is thought to be involved in epithelial calcium transport [148-156]. Bindelset *al* have shown that 1,25(OH)<sub>2</sub>D<sub>3</sub> stimulates transepithelial calcium absorption in primary rabbit connecting and cortical collecting tubule cells [157] whereas Friedman and Gesek have reported that it accelerates PTH-dependent calcium transport in immortalized mouse distal convoluted tubules (MDCT) cells [113]. Despite these cellular responses, the effects of 1,25(OH)<sub>2</sub>D<sub>3</sub> on overall renal calcium excretion are equivocal [156,158-160]. The actions of 1,25(OH)<sub>2</sub>D<sub>3</sub> on renal magnesium absorption are also controversial [161-169].

Although 1,25(OH)<sub>2</sub>D<sub>3</sub> seems to increase calcium absorption within the distal tubule, there is no evidence that it has any effect on distal magnesium transport [78,107,142,143]. To date, there are no experiments reporting the direct effects of vitamin D metabolites on cellular magnesium transport. In the present studies, I used our MDCT cell model to investigate the actions of 1,25(OH)<sub>2</sub>D<sub>3</sub> on Mg<sup>2+</sup> uptake rates. Friedman and Gesek have reported that, in MDCT cells, 1,25(OH)<sub>2</sub>D<sub>3</sub> accelerates PTH-dependent Ca<sup>2+</sup> uptake, suggesting that vitamin D receptors are present in this cell line [113]. Accordingly, these cells provide a useful model to determine the effects of vitamin D metabolites on magnesium handling in the distal convoluted tubule. The present studies demonstrate that 1,25(OH)<sub>2</sub>D<sub>3</sub> stimulates Mg<sup>2+</sup> uptake in MDCT cells,

independently of PTH, providing evidence that it also affects magnesium absorption in the intact distal tubule[139].

*II Methods: As previously described in Chapter one.*

### III. Results

III.1 *1,25(OH)<sub>2</sub>D<sub>3</sub> stimulates Mg<sup>2+</sup> entry in MDCT cells.* MDCT cells were treated with 10<sup>-7</sup> M 1,25(OH)<sub>2</sub>D<sub>3</sub> for 16 h prior to experimentation. During this time they were incubated in media without magnesium in order to deplete them of intracellular Mg<sup>2+</sup> [75]. The cells were then placed in 1.5 mM MgCl<sub>2</sub> and the [Mg<sup>2+</sup>]<sub>i</sub> monitored by fluorescence. Fig. 31 shows a typical experiment of MDCT cells pretreated with 1,25(OH)<sub>2</sub>D<sub>3</sub> compared to control cells. The rate of the entry in control cells, measured over the initial 500 s, was 164±5 nM/s, n=6 (Fig. 32,33). Pretreatment with 1,25(OH)<sub>2</sub>D<sub>3</sub> increased Mg<sup>2+</sup> uptake by 78±4 % to 210±11 nM/s, n=5 (Fig. 32,33). 1,25(OH)<sub>2</sub>D<sub>3</sub> increased Mg<sup>2+</sup> uptake in a concentration-dependent manner with half-maximal response, 185±3 nM/s, occurring at about 10<sup>-9</sup> M (Fig. 32).

Acute treatment of MDCT cells for 20 min with 1,25(OH)<sub>2</sub>D<sub>3</sub> had no effect on Mg<sup>2+</sup> uptake, 178±17 nM/s, n=3, which suggested that the action of the vitamin D<sub>3</sub> metabolite required transcription and translation [170]. I tested this by incubating MDCT cells with 50 μM cycloheximide and the 10<sup>-7</sup> M 1,25(OH)<sub>2</sub>D<sub>3</sub> for 16 h prior to uptake studies. 1,25(OH)<sub>2</sub>D<sub>3</sub> did not stimulate Mg<sup>2+</sup> uptake, (155±18 nM/s, n=4), in cycloheximide treated cells supporting my initial hypothesis response (Fig. 33). This data is in accord with the observations of Friedman and Gesek who reported a significant acceleration of PTH-stimulated calcium uptake in these cells at 3 hours and maximal stimulation at 5 hours with 1,25(OH)<sub>2</sub>D<sub>3</sub> [113].

I have shown that the hormone-induced intracellular second messenger, cAMP, increases Mg<sup>2+</sup> entry into MDCT cells [75]; accordingly, I measured cAMP concentrations in cells in the presence of

1,25(OH)<sub>2</sub>D<sub>3</sub>. There was no difference in cAMP levels in the 1,25(OH)<sub>2</sub>D<sub>3</sub>-treated cells compared to control (Fig. 33). Furthermore, treatment of cells with RpcAMPs, a protein kinase inhibitor, did not diminish 1,25(OH)<sub>2</sub>D<sub>3</sub>-stimulated Mg<sup>2+</sup> uptake, 210±15 nM/s, n=4, indicating that cAMP-mediated pathways are not involved with 1,25(OH)<sub>2</sub>D<sub>3</sub> activity (Table 10). These studies indicate that 1,25(OH)<sub>2</sub>D<sub>3</sub> mediates its effects independently of those involving protein kinase A.

*III.2 1,25(OH)<sub>2</sub>D<sub>3</sub> and PTH stimulate Mg<sup>2+</sup> uptake by separate pathways.* Our studies, as well as Gesek and Friedman's, have shown that PTH stimulates cAMP formation in MDCT cells [41,65,75 & Fig. 16, chapter 3]. Evidence has also been provided that PTH enhances magnesium reabsorption in the distal tubule of the rat, hamster, dog, and MDCT cells (PTH, 10<sup>-7</sup> M, increased Mg<sup>2+</sup> uptake from control levels of 164±5 to 209±21 nM/s) [41,85,88,93,94]. The PTH induced uptake and cAMP generation are similar to the glucagon and calcitonin uptake described in chapter 3 (Fig. 18) in that they are inhibited by the protein kinase A inhibitor Rp-cAMPS and phospholipase C inhibitor U73122 (data not shown). In order to compare the effects of the steroid action that does not involve protein kinase A or protein kinase C pathways, I used PTH as a prototypical hormone that requires cAMP, in part, to elicit its responses. In order to determine if 1,25(OH)<sub>2</sub>D<sub>3</sub> and PTH act through common mechanisms, I used maximal concentrations of 1,25(OH)<sub>2</sub>D<sub>3</sub>, 10<sup>-7</sup> M, and PTH, 10<sup>-7</sup> M, to test if they had additive responses.

1,25(OH)<sub>2</sub>D<sub>3</sub> + PTH increased cAMP formation to a similar extent as PTH alone (Fig. 34). However, Mg<sup>2+</sup> uptake with 1,25(OH)<sub>2</sub>D<sub>3</sub>, 251±16 nM/s, was greater than either with 1,25(OH)<sub>2</sub>D<sub>3</sub>, 210±11 nM/s, or PTH, 209±9 nM/s alone. Accordingly, the steroid metabolite, 1,25(OH)<sub>2</sub>D<sub>3</sub>, and the peptide hormone, PTH, seem to alter Mg<sup>2+</sup> entry rates by different intracellular pathways. Or, alternately, a single pathway can't be maximally stimulated by either 1,25(OH)<sub>2</sub>D<sub>3</sub> or PTH.

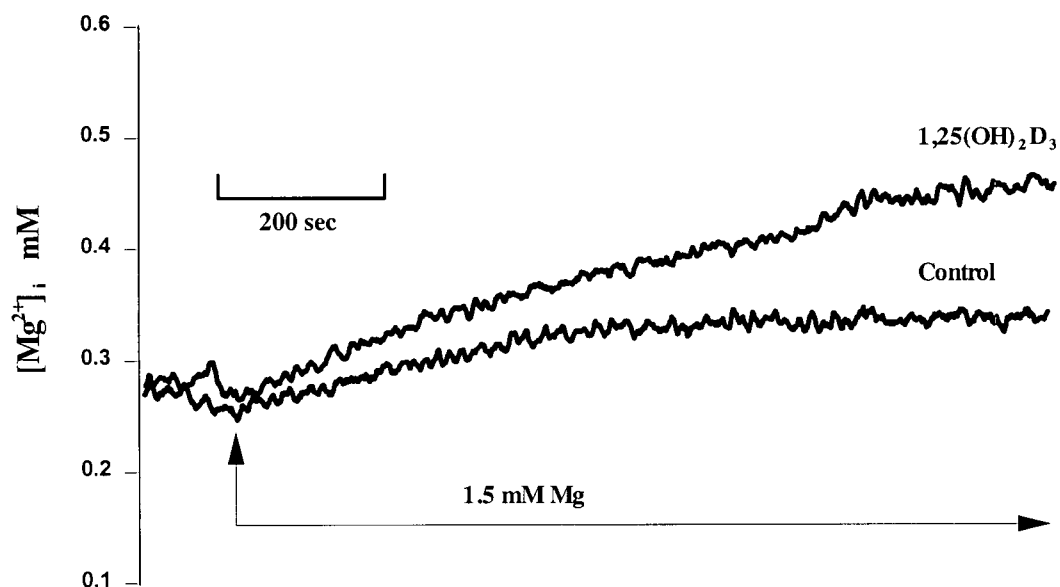


Fig. 31.  $1,25(OH)_2D_3$  stimulates  $Mg^{2+}$  uptake in  $Mg^{2+}$ -depleted mouse distal convoluted tubule (MDCT) cells. MDCT cells were cultured in  $Mg^{2+}$ -free media ( $<0.01$  mM) for 16 hr. Uptake studies were performed in buffer solutions in absence of external magnesium, and where indicated,  $MgCl_2$  (1.5 mM final concentration) was added to observe changes in intracellular  $Mg^{2+}$  concentration,  $[Mg^{2+}]_i$ . The buffer solutions contained (in mM): 145 NaCl, 4.0 KCl, 0.8  $K_2HPO_4$ , 0.2  $KH_2PO_4$ , 1.0  $CaCl_2$ , 5.0 glucose, and 10 HEPES/Tris, pH 7.4, with and without 1.5 mM  $MgCl_2$ . Where indicated,  $1,25(OH)_2D_3$ ,  $10^{-7}$  M, was added to this buffer solution from a stock solutions. Fluorescence was measured at 1 data point/s with 25-point signal averaging, and the tracing was smoothed according to methods previously described.

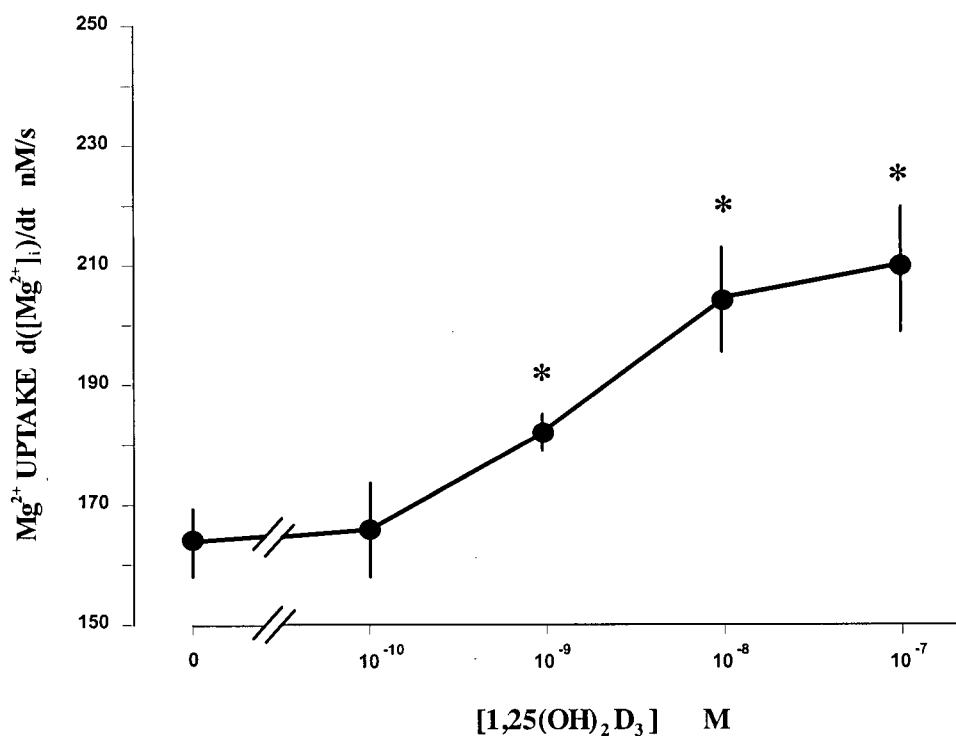


Fig. 32. Concentration-dependence of 1,25(OH)<sub>2</sub>D<sub>3</sub>-stimulation of Mg<sup>2+</sup> entry in MDCT cells. MDCT cells were treated with the given 1,25(OH)<sub>2</sub>D<sub>3</sub> concentrations for 16 h prior to fluorescence determinations. The rate of Mg<sup>2+</sup> influx as determined by d([Mg<sup>2+</sup>]<sub>i</sub>)/dt was measured with the given 1,25(OH)<sub>2</sub>D<sub>3</sub> concentrations using techniques performed according to that given in legend to Figure 34. d([Mg<sup>2+</sup>]<sub>i</sub>)/dt values were determined over the first 500 s of fluorescence measurements. Values are means ± SE for 3-6 cells and \* indicates significance,  $p < 0.05$ , from control values.

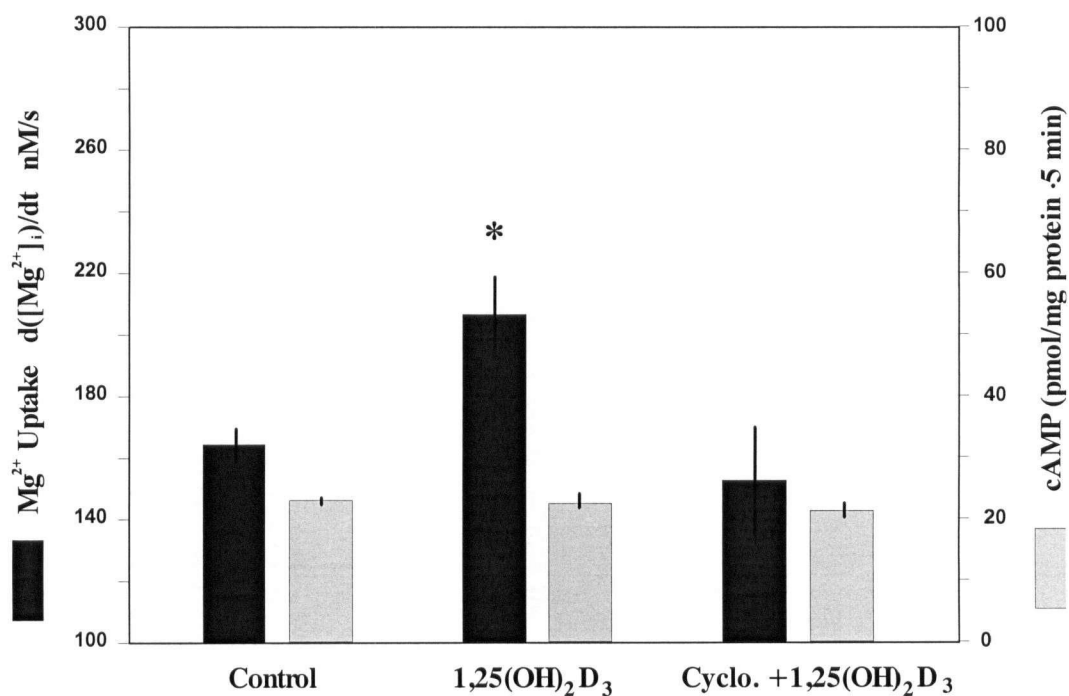


Fig. 33. Summary of  $1,25(\text{OH})_2\text{D}_3$ -stimulated  $\text{Mg}^{2+}$  uptake in MDCT cells. The MDCT cells were treated with  $1,25(\text{OH})_2\text{D}_3$ ,  $10^{-7}$  M, for 16 h prior to the determination of  $\text{Mg}^{2+}$  uptake or cAMP measurements.  $\text{Mg}^{2+}$  uptake was determined with microfluorescence according to methods given in legend to Fig. 34. In those cells indicated, cycloheximide,  $1\mu\text{g/ml}$ , was added with the  $1,25(\text{OH})_2\text{D}_3$  16 h prior to  $\text{Mg}^{2+}$  uptake and cAMP determinations. Values are mean  $\pm$ SE and \* indicates significance from control values.

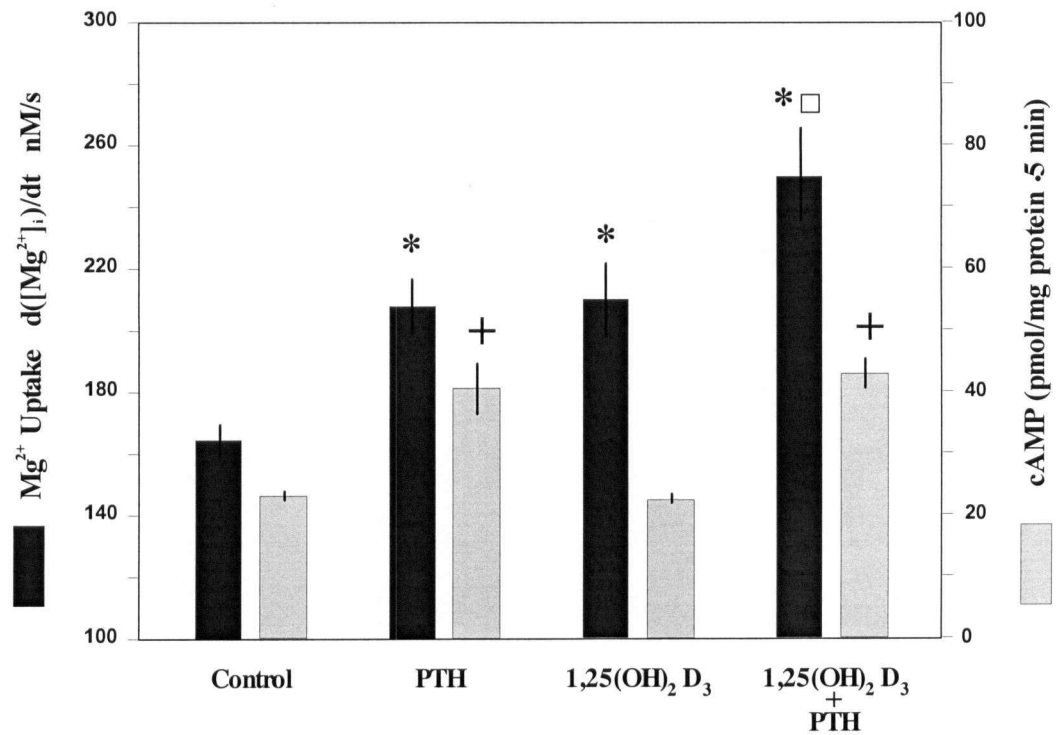


Fig. 34. PTH stimulates cAMP formation and  $\text{Mg}^{2+}$  entry into MDCT cells. PTH,  $10^{-7}$  M, and  $1,25(\text{OH})_2\text{D}_3$ ,  $10^{-7}$  M, were added where indicated. cAMP was measured by radioimmunoassay and  $d([\text{Mg}^{2+}]_i)/dt$  by fluorescence. Values are means  $\pm$  SE for 4-5 preparations. \* indicates significance,  $p < 0.01$ , of  $\text{Mg}^{2+}$  uptake rates and + indicates significance of cAMP concentrations following PTH or  $1,25(\text{OH})_2\text{D}_3$  + PTH compared to the control values. □ indicates significance,  $p < 0.01$ , of  $\text{Mg}^{2+}$  uptake of  $1,25(\text{OH})_2\text{D}_3$  versus  $1,25(\text{OH})_2\text{D}_3$  + PTH.

**Table 10. 1,25(OH)<sub>2</sub>D<sub>3</sub> does not stimulate Mg<sup>2+</sup> uptake through a protein kinase A pathway.**

	Control nM/s	1,25(OH) <sub>2</sub> D <sub>3</sub> nM/s
Control (n)	164±5 (6)	210±11* (4)
RpcAMPS (n)	171±3 (3)	196±5* (3)

**Table 10 Legend**

Mg<sup>2+</sup> entry was determined in the presence of 1,25(OH)<sub>2</sub>D<sub>3</sub>, 10<sup>-7</sup> M, with and without a 5 min pretreatment with the protein kinase A inhibitor RpcAMPS, 10<sup>-6</sup> M. The values are means ± SE with (n) observations and \* indicates significance, p<0.05, from control values.

**III.3 Stimulation of the Mg<sup>2+</sup>/Ca<sup>2+</sup>-SR does not inhibit 1,25(OH)<sub>2</sub>D<sub>3</sub> stimulated Mg<sup>2+</sup> uptake.**

Stimulation of the Mg<sup>2+</sup>/Ca<sup>2+</sup>-SR with addition of 50 μM neomycin did not change Mg<sup>2+</sup> uptake into 1,25(OH)<sub>2</sub>D<sub>3</sub>-treated cells (Fig. 35). This is in contrast to the actions of polyvalent cation-sensing hormones acting through G-protein linked receptors whereby both cAMP generation and Mg<sup>2+</sup> uptake are inhibited. Clearly, 1,25(OH)<sub>2</sub>D<sub>3</sub> alters Mg<sup>2+</sup> entry into MDCT cells by intracellular pathways that are distinctive to those of the peptide hormones, PTH, glucagon, calcitonin, and AVP.

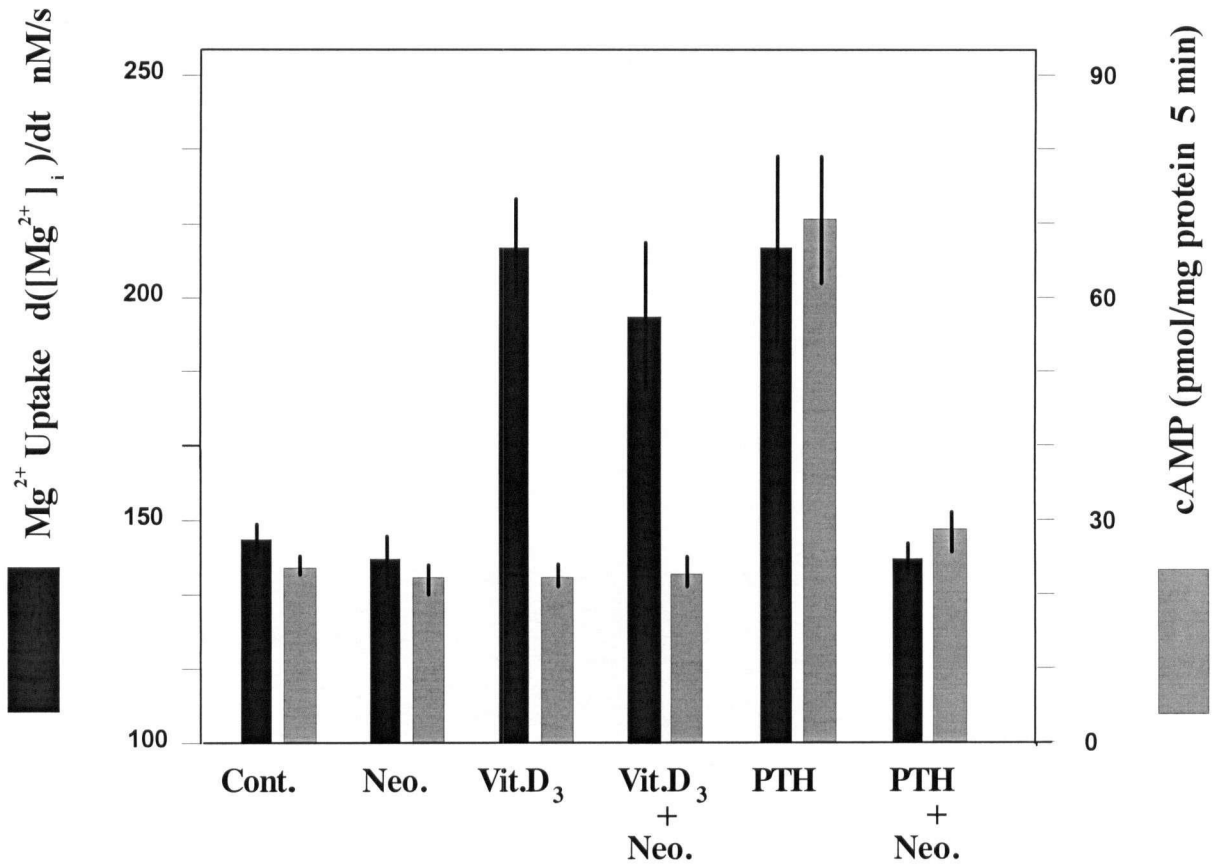


Fig. 35. Summary of the effects of activation of  $Mg^{2+}/Ca^{2+}$ -sensing on hormone-stimulated  $Mg^{2+}$  uptake.  $Mg^{2+}$  uptake,  $d[Mg^{2+}]_i/dt$ , was performed on  $Mg^{2+}$ -depleted cells treated with/without  $1,25(OH)_2D_3$  (note: Vit.D above =  $1,25(OH)_2D_3$ ), as indicated.  $Mg^{2+}$  uptake was determined with 1.5 mM extracellular  $Mg^{2+}$  in the absence and presence of neomycin, 50  $\mu$ M. Neomycin was added 5 min prior to the addition of PTH,  $10^{-7}$  M, and  $MgCl_2$ , 1.5 mM. The  $Mg^{2+}$  uptake rate was determined over 500 s following addition of PTH. Values are mean  $\pm$  SE for 3-5 cells. \* indicates significance ( $p < 0.05$ ) from control values.

Next, I determined the effects of chronic ( 16 h) elevation of extracellular  $\text{Ca}^{2+}$ , 5.0 mM, and neomycin, 50  $\mu\text{M}$ , on  $1,25(\text{OH})_2\text{D}_3$ -stimulated  $\text{Mg}^{2+}$  uptake.  $\text{Ca}^{2+}$  or neomycin were added with  $1,25(\text{OH})_2\text{D}_3$  16 h prior to uptake studies. In support of our earlier findings, high extracellular  $\text{Ca}^{2+}$  for 16 h did not alter basal  $\text{Mg}^{2+}$  uptake,  $165 \pm 7$  nM/s. The effect of 16 h high  $\text{Ca}^{2+}$  and neomycin on  $1,25(\text{OH})_2\text{D}_3$  -stimulated  $\text{Mg}^{2+}$  uptake was no different from acute treatment (as seen in Fig. 35).

#### IV. Discussion

The present studies show that activation of the  $\text{Mg}^{2+}/\text{Ca}^{2+}$ -sensing mechanism inhibits hormone stimulated  $\text{Mg}^{2+}$  uptake into MDCT cells.  $1,25(\text{OH})_2\text{D}_3$  stimulated uptake, in contrast, was not inhibited with stimulation of the  $\text{Mg}^{2+}/\text{Ca}^{2+}$ -sensing mechanism. These results further support my hypotheses that the  $\text{Mg}^{2+}/\text{Ca}^{2+}$ -SR has an important role in controlling magnesium absorption by acting in at least two nephron segments; the thick ascending limb and the distal convoluted tubule.

## GENERAL CONCLUSIONS

- 1: MDCT cells have proven to be a good model for studying distal convoluted tubule  $Mg^{2+}$  transport (Table 11).
- 2: The  $Ca^{2+}$ -SR is present in MDCT cells and there is evidence these cells have a mechanism which also responds selectively to extracellular  $Mg^{2+}$ .
- 3: Stimulation of the  $Mg^{2+}/Ca^{2+}$ -SR inhibits hormone stimulated  $Mg^{2+}$  uptake (Fig.36).

## GENERAL DISCUSSION

*Identification of extracellular polyvalent cation-sensing receptor in MDCT cells.* In this study, I show that the established MDCT cell line possesses a  $Ca^{2+}$ -SR that responds to  $[Mg^{2+}]_o$  and  $[Ca^{2+}]_o$ , to transiently release  $Ca^{2+}$  from cytosolic stores. This immortalized cell line is representative of the intact distal convoluted tubule as it possesses many of the properties characteristic of this segment including chlorothiazide-sensitive NaCl cotransport, amiloride-inhibitable  $Na^+$  conductance, and parathyroid hormone and calcitonin-stimulated calcium and magnesium transport [39,41,49,61]. Accordingly, it is of interest that this cell line also has an extracellular divalent cation-sensing receptor. Using RT-PCR and Southern blotting, I show that the MDCT cells possess transcripts for the  $Ca^{2+}$ -SR. The presence of the  $Ca^{2+}$ -SR protein in MDCT cells was documented by Western blot analysis using a specific  $Ca^{2+}$ -sensing receptor antiserum. Furthermore, determination of cytosolic  $Ca^{2+}$  with fluorescence showed that  $Ca^{2+}$ -SR in MDCT cells elicit

intracellular signals in response to increasing extracellular concentrations of polyvalent cations demonstrating that the receptor is functional. These studies with mouse distal convoluted cells are consonant with reports of  $\text{Ca}^{2+}$ -SR transcripts in the rat distal convoluted segment [11,13,17]. More recently, Riccardi et al. showed that the rat  $\text{Ca}^{2+}$ -SR is localized to the basolateral membrane of the distal convoluted tubule [11]. The presence of a  $\text{Ca}^{2+}$ -SR in the distal convoluted tubule may have important ramifications on cellular function within this segment.

The importance of the  $\text{Ca}^{2+}$ -SR in the control of  $[\text{Mg}^{2+}]_o$  and  $[\text{Ca}^{2+}]_o$  homeostasis is indicated by the fact that individuals with familial hypocalciuric hypercalcemia (FHH) manifest hypermagnesemia and hypercalcemia which is due, in part, to excessive renal reabsorption [26,66,67,68]. Additionally, mice that are heterozygous or homozygous with inactivating mutations of the  $\text{Ca}^{2+}$ -SR show significant increases in  $[\text{Mg}^{2+}]_o$  and  $[\text{Ca}^{2+}]_o$  relative to normal mice [26]. Attie et al performed clearance studies on hypoparathyroid patients and concluded that inappropriate renal calcium conservation is due to an inherent abnormality of the kidney [68]. Conversely, they suggested that inappropriate magnesium reabsorption might be due predominantly to elevated circulating PTH levels. Our functional studies addressed this issue (see below discussion).

In all studies to date,  $[\text{Ca}^{2+}]_o$  has been found to be a more potent stimulator of  $\text{Ca}^{2+}$ -SR-induced intracellular signalling than  $[\text{Mg}^{2+}]_o$ . The threshold value for  $[\text{Ca}^{2+}]_o$  has been reported to be of the order of 1-5 mM for renal cells whereas a similar cytosolic  $\text{Ca}^{2+}$  response requires the presence of 5-20 mM  $[\text{Mg}^{2+}]_o$  [39]. These relative potencies of  $[\text{Ca}^{2+}]_o$  and  $[\text{Mg}^{2+}]_o$  recapitulates their actions in bovine parathyroid cells and in *Xenopus* oocytes injected with cRNA of cloned  $\text{Ca}^{2+}$ -sensing receptor [4,56]. Thus, it was of interest that the polyvalent cation-sensitive mechanism of MDCT cells was apparently as sensitive to  $[\text{Mg}^{2+}]_o$  as it was to  $[\text{Ca}^{2+}]_o$ . This is particularly noteworthy as the  $[\text{Mg}^{2+}]_o$  studies were performed in the presence of normal or elevated  $[\text{Ca}^{2+}]_o$ . The functional consequences of changes in the amino acid sequence of the  $\text{Ca}^{2+}$ -SR has been investigated by expressing a variety of mutated receptors in HEK 293 cells [32]. Some of the

mutations diminish  $\text{Ca}^{2+}$ -SR signalling, others enhance the sensitivity to external  $[\text{Ca}^{2+}]_o$ , and still others are completely nonfunctional with no intracellular signalling as determined by changes in  $[\text{Ca}^{2+}]_i$  [28,29,33]. From these transfection studies of mutated  $\text{Ca}^{2+}$ -SRs, Bai et al. suggested that discrete but interrelated cation binding sites may exist in this receptor.  $\text{Ca}^{2+}$  binding to the  $\text{Ca}^{2+}$ -sensing receptor per se has yet to be examined [32]. These discrete sites remain to be identified but it is apparent from these studies that changes in the extracellular domain of the  $\text{Ca}^{2+}$ -SR may alter sensitivity to the various ligands [32]. The present studies with the endogenous polyvalent cation-sensitive mechanism of the MDCT cell show that the intracellular signalling is responsive to both  $[\text{Mg}^{2+}]_o$  and  $[\text{Ca}^{2+}]_o$  and that there appears to be little interaction between these cations. Accordingly, the  $\text{Ca}^{2+}$ -sensing receptor may function as a  $[\text{Mg}^{2+}]_o$  receptor ( $\text{Mg}^{2+}$ -sensing receptor) even in the presence of relatively high concentrations of  $[\text{Ca}^{2+}]_o$ . The sites involved in binding  $[\text{Mg}^{2+}]_o$  and  $[\text{Ca}^{2+}]_o$  and the cooperative association in intracellular signalling remain to be determined. Alternatively, the results of my studies may indicate the presence of separate receptors for  $[\text{Ca}^{2+}]_o$  and  $[\text{Mg}^{2+}]_o$  in MDCT cells.

*Evidence for a  $\text{Mg}^{2+}$ -sensing receptor.* The present studies suggest that a receptor for extracellular  $\text{Mg}^{2+}$  may exist in the MDCT cell line. There are two reports of the  $\text{Mg}^{2+}$ -SR in the literature. First, Goudeau and Goudeau have reported that the  $\text{Mg}^{2+}$ -SR is present in the shrimp oocyte [79,80]. This receptor is involved in developmental activation of the oocytes. In an effort to identify this receptor, I obtained shrimp oocytes and isolated poly (A<sup>+</sup>) RNA to inject into *Xenopus* oocytes for heterologous expression. The receptor was successfully expressed in *Xenopus* oocytes. Next, we attempted to clone the receptor by homology screening libraries prepared from the RNA of the oocytes. This was not successful. We concluded that the shrimp  $\text{Mg}^{2+}$ -SR is different from the  $\text{Ca}^{2+}$ -SR.

*Cellular mechanisms of the  $\text{Ca}^{2+}$ -SR.* Activation of the polyvalent cation-sensing mechanism in MDCT cells with neomycin inhibited PTH-, calcitonin-, glucagon- and AVP-stimulated cAMP release (Table

2). It has long been known that hypermagnesemia and hypercalcemia inhibit hormone-mediated cAMP accumulation in the proximal tubule, loop of Henle, and the collecting duct. Hypermagnesemia and hypercalcemia inhibit the PTH-mediated increase in cAMP in the proximal tubule and cortical thick ascending limb [69,70]. The elevation of  $[Ca^{2+}]_o$  also mitigates vasopressin-stimulated increases in cAMP production in the medullary thick ascending limb of Henle's loop [70,71] and PTH, calcitonin, vasopressin and glucagon-stimulated cAMP accumulation in the cortical thick ascending limb [70]. Jones et al. have shown that  $[Ca^{2+}]_o$  reduces the hydrosmotic response of cortical collecting ducts to AVP and cAMP [72]. Chen et al. have shown that polyvalent cations inhibit agonist-stimulated cAMP accumulation in bovine parathyroid cells [56]. This inhibition was totally prevented following preincubation of the cells with pertussis toxin which is known to ADP-ribosylate and uncouple the guanine nucleotide regulatory (G)-protein,  $G_i$ , from the cell surface receptors which are coupled to inhibition of adenylate cyclase [54]. Accordingly, the parathyroid gland *Casr* appears to be linked to adenylate cyclase via a  $G_i$  protein [54]. This also appears to be the case for MDCT cells. Glucagon-and AVP-stimulate magnesium and calcium transport in the rat distal tubule and magnesium entry into MDCT cells [43,87]. We postulate that activation of the polyvalent cation-sensing mechanism with high levels of  $[Ca^{2+}]_o$  or  $[Mg^{2+}]_o$  may inhibit glucagon-and AVP-stimulated magnesium and calcium transport. Further studies are needed to establish the functional roles of the polyvalent cation-sensing receptor(s) within the distal tubule.

In summary, a  $Ca^{2+}$ -SR is present in an immortalized mouse distal convoluted tubule (MDCT) cell line. This cell line has been extensively used to characterize magnesium and calcium transport in the distal convoluted segment of the nephron. The use of this cell line should allow insights into expression, control, and function of the  $Ca^{2+}$ -sensing receptor in distal convoluted tubule cells. This is particularly important as *in vivo* micropuncture and microperfusion approaches do not allow for study of cellular mechanisms of transport. *In vitro* microperfusions have not been performed in this portion of the tubule because of the

difficulty in isolating intact segments.

*Cellular mechanisms of peptide hormone actions and stimulation of  $Mg^{2+}$  uptake.* In order to determine the cellular actions of extracellular  $Ca^{2+}$ -SR on  $Mg^{2+}$  transport and the influences on hormonal controls, we characterised  $Mg^{2+}$  uptake in MDCT cells. In the present study, we show that PTH, calcitonin, glucagon, and AVP stimulate  $Mg^{2+}$  entry into MDCT cells in a concentration-dependent manner. Furthermore, these hormones appear to act through cAMP-, phospholipase C- and protein kinase C-dependent pathways. Although the details of these signalling pathways are not known this data provides some explanation in interpreting the cellular actions of the  $Ca^{2+}$ -SR in MDCT cells. By inference this information provides some detail as to what is occurring in the distal convoluted tubule.

The cellular mechanisms underlying the hormonal actions on distal magnesium absorption are largely unknown at the present time. Morel et al. have shown that PTH, calcitonin, and glucagon, stimulate receptor-mediated cAMP release in the DCT [173,174,106]. They also reported that AVP receptors may be present in the DCT but there were marked species differences in adenylate cyclase responsiveness [107]. There was little AVP-stimulated cAMP production in the DCT of the rabbit and human, intermediate response in the mouse, and greatest in the rat [106,174]. We have shown that PTH, calcitonin, glucagon, and AVP stimulates  $Mg^{2+}$  uptake into MDCT cells [49, unpublished observations]. Friedman and Gesek reported that these hormones also stimulate cellular cAMP accumulation [108,109]. We determined whether cAMP may influence  $Mg^{2+}$  entry into MDCT cells. The addition of the cAMP analogue, 8-bromo-cAMP, increased  $Mg^{2+}$  uptake whereas inhibition of protein kinase A with RpcAMPS prevented hormone-stimulated uptake [49]. Accordingly, receptor-mediated cAMP release and activation of protein kinase A plays a role in hormone-stimulated  $Mg^{2+}$  uptake in MDCT cells. However, it is apparent that other signaling pathways are present for hormone-mediated  $Mg^{2+}$  uptake in MDCT cells. Hormone-stimulated  $Mg^{2+}$  uptake rates do not correlate with the measured intracellular cAMP levels in MDCT cells [49]. Furthermore, phospholipase C inhibition, with

U-73122, but not protein kinase C inhibition with Ro31-8220, abolished PTH- and calcitonin-stimulated  $Mg^{2+}$  uptake. This was true for all of the hormones tested, PTH, calcitonin, glucagon, AVP [49, unpublished observations]. These hormones do not elicit receptor-mediated intracellular  $Ca^{2+}$  transients suggesting that  $Ca^{2+}$  signalling is not involved with the responses [39,108]. We have demonstrated, however, there is a requirement for some portion of the PLC pathway above the level of PKC. There may in fact be non-specific activity of the U-73122 or involvement of alternative phospholipases contributing to these observations. As the hormones used are not associated with  $Ca^{2+}$  transients the possibility arises that DAG, and its downstream metabolites, may be involved. Binding of the released  $G_{\beta\gamma}$  subunit, to an undetermined phospholipase, may also play a crucial role in this pathway. A variety of PLC isoforms have been identified in the distal nephron which lends some support to this theory [175]. It is well known that multiple receptors can converge on a single G protein and in many cases a single receptor can activate more than one G protein and thereby modulate multiple intracellular signals [176]. It is evident that cAMP-protein kinase A and phospholipase C pathways are necessary for hormone-stimulated  $Mg^{2+}$  entry into MDCT cells. The details of how peptide hormones act on  $Mg^{2+}$  transport in MDCT cells and intact distal tubules are unknown. However, these studies provide a background for understanding the actions of the  $Ca^{2+}$ -SR.

*The effect of the  $Ca^{2+}$ -SR on hormone-stimulated  $Mg^{2+}$  uptake.* In the present study, we show that activation of this  $Mg^{2+}/Ca^{2+}$ -sensing mechanism inhibits hormone-stimulated  $Mg^{2+}$  uptake into MDCT cells. The evidence provided here is that activation of  $Ca^{2+}$ -SR by extracellular polyvalent cations diminish hormone-stimulated  $Mg^{2+}$  uptake, in part, by inhibiting hormone-mediated cAMP formation. The effect of this receptor on phospholipase C and protein kinase C pathways is not known. As this cell line possesses many of the transport properties of the intact distal convoluted tubule, we conclude that the  $Mg^{2+}/Ca^{2+}$ -sensing mechanism plays an important role in control of magnesium transport in this nephron segment.

These conclusions are consonant with the results of earlier micropuncture studies. Le Grimellec and

colleagues used magnesium- or calcium-loaded rats having intact parathyroid glands. They performed free-flow micropuncture experiments to determine the effects of hypermagnesemia and hypercalcemia on distal tubular absorption [177,178]. They showed that magnesium delivery from the early distal tubule sampling site to the final urine relative to inulin delivery was markedly increased in hypermagnesemic and hypercalcemic rats. They interpreted this data to indicate "a drastic inhibition (by an unknown mechanism) of reabsorption taking place in the terminal segments of the nephron or a proportionately more important contribution of the deeply located nephrons to magnesium excretion than expected from their number" [177,178]. In support of these early micropuncture experiments, *in vivo* microperfusion studies indicated that the rate of magnesium absorption within the distal tubule was altered by extracellular magnesium and calcium [100]. Distal tubules were perfused from a proximal site and tubule fluid sampled from early and late sites of superficial distal tubules. Magnesium absorption within the superficial distal tubule of TPTXed rats was highly dependent on delivery of magnesium to this segment [98,99]. The fraction of delivered magnesium absorbed in distal tubules amounted to  $34 \pm 10\%$  in rats with normal plasma magnesium and calcium concentrations,  $0.78 \pm 0.04$  mM and  $2.24 \pm 0.04$  mM, respectively [100]. However, fractional magnesium absorption decreased significantly to  $6 \pm 3\%$  when the animals were made hypermagnesemic (plasma magnesium  $3.58 \pm 0.20$  mM) and to  $14 \pm 7\%$  in hypercalcemic rats (plasma calcium  $4.24 \pm 0.36$  mM) [78]. The animals used in these studies were TPTX but were intact with respect to other circulating hormones. The cellular basis for diminished fractional absorption in hypermagnesemia and hypercalcemia remained unexplained until a  $\text{Ca}^{2+}$ -SR was identified in the kidney and located to the distal tubule [11].

The  $\text{Ca}^{2+}$ -SR is localized along the length of the nephron from the proximal tubule to the collecting system with particular abundance in the basolateral membrane of the thick ascending limb and the apical membrane of the inner medullary collecting duct [11,17]. The functions of renal polyvalent cation-sensing receptor(s) are not fully understood. Hebert has recently summarized the salient features of increases in

extracellular  $\text{Ca}^{2+}$  and  $\text{Mg}^{2+}$  on loop and collecting duct function [123]. Hypercalcemia and hypermagnesemia inhibit  $\text{NaCl}$ , calcium, and magnesium absorption in the thick ascending limb [97] and water permeability in the medullary collecting duct [10]. Hebert and colleagues speculate that inhibition of salt reabsorption in the thick ascending limb and water transport in the medullary collecting duct together with diminished calcium absorption in the thick ascending limb would wash out the calcium cations minimizing the possibility of urinary stone formation [123]. The functional roles of the *Casr* within the proximal tubule and segments of the distal tubule have not been determined. The present studies show that activation of the  $\text{Mg}^{2+}/\text{Ca}^{2+}$ -sensing mechanism inhibits hormone-stimulated  $\text{Mg}^{2+}$  uptake into MDCT cells. These results suggest that this receptor might play an important role in controlling magnesium absorption acting in at least two nephron segments; the thick ascending limb and the distal convoluted tubule.

The mechanisms by which the  $\text{Mg}^{2+}/\text{Ca}^{2+}$ -sensing mechanism inhibits magnesium transport in the thick ascending limb and distal tubule are becoming clearer. In the cortical thick ascending limb, magnesium and calcium transport is passive, dependent on the transepithelial voltage and the permeability of the paracellular pathway [86]. Wang et al. have reported that neomycin inhibits apical  $\text{K}^+$  channels and possibly apical  $\text{Na}$ ,  $\text{K}$ ,  $\text{Cl}$  cotransport through signalling pathways involving cytochrome P-450 metabolites (7). Accordingly, activation of the  $\text{Ca}^{2+}$ -SR would lead to a decrease in transepithelial voltage and diminished passive calcium and magnesium transport in the thick ascending limb [78]. Unlike the thick ascending limb, magnesium transport within the distal tubule is active and transcellular in nature so that the receptor must affect active magnesium absorption. My results indicate that activation of the  $\text{Mg}^{2+}/\text{Ca}^{2+}$ -sensing mechanism inhibits hormone-stimulated  $\text{Mg}^{2+}$  uptake and hormone-mediated accumulation of cAMP in MDCT cells. As cAMP enhances  $\text{Mg}^{2+}$  entry into MDCT cells, I speculate that activation of the  $\text{Mg}^{2+}/\text{Ca}^{2+}$ -sensing mechanism may act, in part, through diminished hormone responsive cAMP release. We were unable to show any effects of neomycin activation of  $\text{Mg}^{2+}/\text{Ca}^{2+}$ -sensing on membrane voltage either with glucagon

or amiloride suggesting that these effects were independent of voltage. We infer from these studies that the  $Mg^{2+}/Ca^{2+}$ -sensing mechanism in the distal convoluted tubule plays an important role in renal magnesium conservation in addition to its effects within the loop of Henle.

It has long been known that hypermagnesemia and hypercalcemia inhibit hormone-mediated cAMP accumulation in the proximal tubule, loop of Henle, and the collecting duct. Hypermagnesemia and hypercalcemia inhibits the PTH-mediated increase in cAMP in the proximal tubule and cortical thick ascending limb [13,14]. The elevation of extracellular  $Ca^{2+}$  also mitigates vasopressin-stimulated increases in cAMP production in the medullary thick ascending limb of Henle's loop [123] and PTH-, calcitonin-, vasopressin- and glucagon-stimulated cAMP accumulation in the cortical thick ascending limb [123]. Finally, Sands et al. have shown that AVP-elicited water permeability in rat kidney terminal inner medullary collecting ducts is inhibited with elevated plasma calcium [10]. Accordingly, hypermagnesemia and hypercalcemia, probably through activation of the  $Mg^{2+}/Ca^{2+}$ -sensing mechanism, have significant effects on hormone-mediated cAMP generation along the length of the nephron. These actions are also apparent on hormone-stimulated cAMP accumulation in MDCT cells. We have previously shown that cAMP, in part, mediates hormone-stimulated  $Mg^{2+}$  uptake [87]. Accordingly, it is likely that functional responses within the distal convoluted tubule that are mediated by cAMP are also modulated by hypermagnesemia and hypercalciuria through  $Mg^{2+}/Ca^{2+}$  sensing.

*Examples of  $Ca^{2+}$ -SR controls on  $Mg^{2+}$  transport: steroid hormones.* Mineralocorticoid receptors are present in DCT cells which are thought to be involved in expression of NaCl cotransport,  $Na^+$  conductance, and sodium pump activity [132,133,134]. The effects of aldosterone on distal tubule magnesium absorption have not been studied with micropuncture techniques. Clearance studies have shown that chronic aldosterone administration results in renal magnesium-wasting but this has been explained by extracellular volume expansion leading to diminished NaCl and magnesium reabsorption within the loop [86]. We have

studied the effects of aldosterone on  $Mg^{2+}$  entry into MDCT cells [139]. Incubation of aldosterone, for 16 hr prior to determination of  $Mg^{2+}$  uptake failed to have any effect on basal magnesium transport. However, pretreatment of MDCT cells with aldosterone potentiated hormone-stimulated  $Mg^{2+}$  uptake. This was associated with potentiation of hormone-mediated cAMP release in aldosterone-treated MDCT cells. Cycloheximide, an inhibitor of protein synthesis, abolished the potentiation of aldosterone on glucagon- and AVP-stimulated cAMP release and  $Mg^{2+}$  uptake [139]. Accordingly, aldosterone may enhance hormone-stimulated  $Mg^{2+}$  entry by increasing cAMP and its responses. This notion is supported by the observations of others [136]. Rajerison et al. demonstrated that adrenalectomy reduced AVP-stimulated adenylate cyclase activity in membrane fractions prepared from rat kidney medulla [137]. Doucet et al. have shown that glucagon- and AVP-responsive cAMP generation is diminished in thick ascending limb and collecting tubule segments harvested from adrenalectomized rats compared to animals treated with physiological doses of aldosterone [134,135]. These investigators postulate that aldosterone induces a protein(s) which stimulates hormone-sensitive adenylate cyclase activity. Studies with kidney membrane fractions and isolated segments in the absence of aldosterone demonstrated an impairment of coupling between hormone receptors and adenylate cyclase catalytic units was responsible for diminished cAMP generation [134]. Steroid hormones have significant effects on expression and posttranslational targeting of heterotrimeric G-proteins so that associated channels are covalently modified [131,140]. The mechanism(s) through which steroids control  $G_s$  proteins (synthesis and/or degradation vs. activity of each unit) associated with  $Mg^{2+}$  uptake in MDCT cells is not known. The role of mineralocorticoids in the physiological maintenance of renal magnesium handling also requires further research.

Vitamin  $D_3$  metabolites have important effects on mineral metabolism by  $1,25(OH)_2D_3$  actions on epithelial transport [142,143]. The distal tubule, including the convoluted segment, also possesses  $1,25(OH)_2D_3$  receptors [144,145,146,147]. We have demonstrated that  $1,25(OH)_2D_3$  increases  $Mg^{2+}$  entry rates in MDCT

cells. The response is concentration-dependent, involves transcriptional processes involving de novo protein synthesis and does not appear to be related to cAMP-mediated stimulation of  $\text{Mg}^{2+}$  uptake. These studies suggest that vitamin D<sub>3</sub> may modulate magnesium transport in the distal tubule. Important to the present study is that activation of the extracellular  $\text{Ca}^{2+}$ -SR does not inhibit 1,25(OH)<sub>2</sub>D<sub>3</sub>-stimulated  $\text{Mg}^{2+}$  transport. Accordingly, there are some hormonal controls of  $\text{Mg}^{2+}$  transport that are not modulated by extracellular cation-sensing, i.e. hypermagnesemia and hypercalcemia.

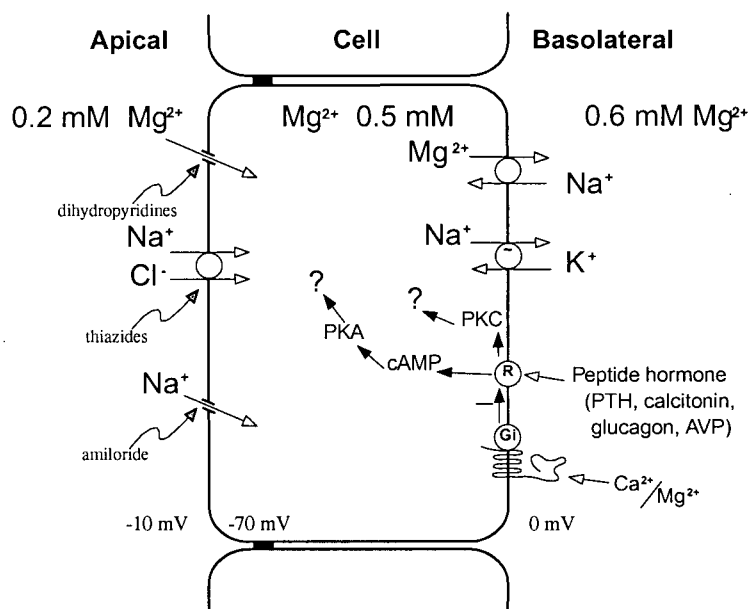
*Summary.* In summary, a  $\text{Mg}^{2+}/\text{Ca}^{2+}$ -sensing mechanism is present in MDCT cells which upon activation inhibits hormone-mediated cAMP accumulation and peptide hormone-stimulated  $\text{Mg}^{2+}$  uptake in  $\text{Mg}^{2+}$ -depleted cells. It is not known if these responses or others are present in normal distal tubule cells. Also, the pathways by which the  $\text{Mg}^{2+}/\text{Ca}^{2+}$ -sensing mechanism alter these activities are yet to be fully elucidated. However, the functional responses observed in the present studies are in keeping with earlier microperfusion studies demonstrating that hypermagnesemia and hypercalcemia diminish magnesium absorption within the distal tubule [98,100]. These studies show that the  $\text{Mg}^{2+}/\text{Ca}^{2+}$ -sensing mechanism is important in the regulation of renal magnesium transport at both the level of the distal convoluted tubule as well as the loop of Henle. It is envisioned that either hypermagnesemia or hypercalcemia could inhibit divalent cation absorption in the loop and hormone-mediated absorption in the distal convoluted tubule. The latter response would be appropriate to mitigate excessive magnesium and perhaps calcium reabsorption in the face of increased delivery to this segment.

Table 11. Controls of Magnesium Reabsorption in Intact Distal Tubule Compared to MDCT Cells

		<b>Intact DT</b>	<b>MDCT</b>
Peptide hormones:	Parathyroid Hormone	Increase (*)	Increase (*)
	Calcitonin	Increase (*)	Increase (*)
	Glucagon	Increase (*)	Increase (*)
	Arginine Vasopressin	Increase (*)	Increase (*)
Prostaglandins:	PGE <sub>2</sub>	?	Increase (*)
Mineralocorticoids:	Aldosterone	?	Increase (*)
Vitamin D:	1,25(OH) <sub>2</sub> D <sub>3</sub>	?	Increase (*)
Magnesium restriction		Increase (*)	Increase (*)
Metabolic acidosis		Decrease (*)	Decrease (*)
Metabolic alkalosis		Increase (*)	Increase (*)
Hypermagnesemia		Decrease (*)	Decrease (*)
Hypercalemia		Decrease (*)	Decrease (*)
Phosphate-depletion		Decrease (*)	Decrease (*)
Potassium-depletion		?	Decrease (*)
Diuretics:	Furosemide	No effect (*)	No effect (*)
	Amiloride	?	Increase (*)
	Chlorothiazide	Increase (*)	Increase (*)

Data derived from intact distal tubule was obtained from micropuncture and microperfusion studies. ? indicates not known; u.p. unpublished results.

## Model of Magnesium Transport in DCT



971218b

Figure 36. Schematic representation of the  $\text{Mg}^{2+}/\text{Ca}^{2+}$ -SR in the distal convoluted tubule and its inhibitory effect on hormone stimulated  $\text{Mg}^{2+}$  uptake.

## FUTURE RESEARCH

The focus of future and current research with this cell line includes identification of a specific  $Mg^{2+}$ -SR. As I could not isolate a  $Mg^{2+}$ -SR by homology (with a  $Ca^{2+}$ -SR) through homology screening of libraries it would suggest that the receptor may be quite different. Accordingly, future, experimentation should use an expression based approach. It will be important to use tissue with higher abundance of the  $Mg^{2+}$ -SR and low abundance of the  $Ca^{2+}$ -SR as determined by physiological means. Mg Finally, determining the genetic controls on expression of the  $Ca^{2+}$ -SR, and how this may also be influenced by hormone and external cationic stimulation, should be established.

### Bibliography:

- 1     Watson, S., Arkinstall, S.(1994) Superfamily of seven transmembrane proteins. In "The G-protein linked receptor facts book" (S. Watson, S. Arkinstall eds.), pp.2-6. Academic Press, Harcourt Brace and Company, San Diego, CA.
  
- 2     Hall, JM., Caulfield, MP., Watson SP., Guard, S.: Receptor subtypes or species homologues: relevance to drug discovery: Trends in Pharmacological Sciences.14(10):376-83, 1993.
  
- 3     Jackson, TR.: Structure and function of G protein coupled receptors: Pharmacology & Therapeutics. 50(3):425-42, 1991
  
- 4     Brown, EM., Gamba, G., Riccardi, D., Lombardi, M., Butters, R., Kifor, O., Sun, A., Hediger, MA., Lytton, J., Hebert, SC.: Cloning and characterization of an extracellular  $\text{Ca}^{2+}$ -sensing receptor from bovine parathyroid. Nature 366:575-580, 1993
  
- 5     Brown, EM., Vassilev, PM., and Hebert, SC.: Calcium ions as extracellular messengers. Cell 83: 676-682, 1995
  
- 6     Kifor, O. Diaz, R., Butters, R., Brown, E.: The  $\text{Ca}^{2+}$  sensing receptor (CaR) activates Phospholipases C, A2, and D in bovine parathyroid and CaR-transfected, human embryotic kidney (HEK293) cells. J. of Bone Research 12(5):715-725, 1997
  
- 7     Wang, W-H., La, M., and Hebert, SC.: Cytochrome P-450 metabolites mediate extracellular  $\text{Ca}^{2+}$ -induced inhibition of apical  $\text{K}^{+}$  channels in the TAL. Am. J. Physiol.(271 Cell Physiol). 40: C103-C111, 1996.
  
- 8     Mathias, RS., and Brown EM. :Divalent cations modulate PTH-dependent 3', 5'-cyclic adenosine monophosphate production in renal proximal tubular cells. Endocrinology 128: 3005-3012, 1991.
  
- 9     Chou, Y-HW., Brown, EM., Levi, T., Crowe, G., Atkinson, AB., Arnqvist, HJ., Toss, G. :The gene responsible for familial hypocalciuric hypercalcemia maps to chromosone 3q in four unrelated families. Nature Genetics 1:295-299.1993

- 10 Sands, JM., Naruse, M., Baum, M., Hebert, SC., Brown, EM., and Harris, HW. :Apical extracellular calcium/polyvalent cation-sensing receptor regulates vasopressin-elicited water permeability in rat kidney inner medullary collecting duct. *J. Clin. Invest.* 99: 1399-1405, 1997.
- 11 Riccardi D., Lee W-S., Lee K, Segre G.V., Brown EM., Hebert, SC. :Localization of the extracellular  $\text{Ca}^{2+}$ -sensing receptor and PTH/PTHrP receptor in rat kidney. *Am. J. Physiol.* 271:F951-F956, 1996
- 12 Paulais M., Baudouin-Legros M., Teulon J.: Functional evidence for a  $\text{Ca}^{2+}$ /polyvalent cation sensor in the mouse thick ascending limb. *Am. J. Physiol.* 271:F1052-F1060, 1996
- 13 Riccardi, D., Park, J., Lee, W-S., Gamba, G., Brown, EM., Hebert, SC.: Cloning and functional expression of a rat kidney extracellular calcium/polyvalent cation-sensing receptor. *Proc. Natl. Acad. Sci. U.S.A.* 92:131-135, 1995
- 14 Aida, K., Koishi, S., Tawata, M., Onaya, T. : Molecular cloning of a putative  $\text{Ca}^{2+}$ -sensing receptor cDNA from human kidney. *Biochem. Biophys. Res. Comm.* 214:524-529, 1995
- 15 Riccardi, D., Hall, AE., Chattopadhyay, N., Xu, NJZ., Brown, EM. and Hebert, SC.: Localization of  $\text{Ca}^{2+}$  /polyvalent cation-sensing receptor protein in rat kidney. *Am. J. Physiol.* 244 (Renal Physiol. 43): F611-F622, 1998.
- 16 Cattopadhyay, N., Baum, M., Bai, M., Riccardi, D., Hebert, H., Harris, W., Brown, E. : Ontogeny of the extracellular calcium-sensing receptor in rat kidney. *Am. J. Physiol.* 244 (Renal Fluid Electrolyte Physiol. 40): F736-F743, 1996.
- 17 Yang, TX., Hassan, S., Huang, YNG., Smart, AM., Briggs, JP., and Schnerman, JB. : Expression of PTHrP, PTH/PTHrP receptor and  $\text{Ca}^{2+}$ -sensing receptor RNAs along the rat nephron. *Am. J. Physiol.* 41 (Renal Physiol.): F751-F758, 1997.
- 18 Ruat, M., Snowman, AM., Hester, LD., Snyder, SH.: Cloned and expressed rat  $\text{Ca}^{2+}$ -sensing receptor: differential cooperative responses to calcium and magnesium. *J. Biol. Chem.* 271:5972-5975, 1996
- 19 Bai, M., Trivedi, S., Lane, C., Yang, Y., Quinn, S., Brown, E. :Protein kinase C phosphorylation at position 888 in the  $\text{Ca}^{2+}$ sensing receptor (CaR) inhibits coupling to  $\text{Ca}^{2+}$  store release. *J. of Biol. Chem.* 273(33): 21267-21275. 1998

- 20 Takaichi, K., Uchida, I., and Kurokawa, K.: High  $\text{Ca}^{2+}$  inhibited AVP-dependent cAMP production in thick ascending limb of Henle. *Am. J. Physiol.* 250 (*Renal Fluid Electrolyte Physiol.* 19): h-F776, 1986.
- 21 Celeste, M., Ferreira, De J., Bailly, C.: Extracellular  $\text{Ca}^{2+}$  decreases chloride reabsorption in rat CTAL by inhibiting the cAMP pathway. *Am. J. Physiol.*, 275 (*Renal Physiology* 40): F198-F203, 1998
- 22 Desfleurs, E., Wittner, A., Simeone, S., Pajaud, S., Moine, G., Rajerison, R., Di Stefano, A.: Calcium-Sensing Receptor : Regulation of electrolyte transport in the thick ascending limb. *Kidney and Blood Pressure Research* 822, 1-12. 1998
- 23 Chabardes, D., Firsov, D., Aarab, I., Clabecq, A., Bellanger, A-C., Siaume-Perez, Elalouf, J-M.: Localization of mRNAs encoding  $\text{Ca}^{2+}$ -inhibitable adenylyl cyclases along the renal tubule. *J. of Biol. Chem.*, 271(32) 19264-19271. 1996
- 24 Stow JL., Almeida, JB. :Distribution and role of heterotrimeric G-proteins in the secretory pathway of polarized epithelial cells. *J. of Cell Science* 17,33-39. 1993.
- 25 Pearce S., Bai, M. Quinn, S., Kifor, O., Brown, E., Thakker, R. Functional characterization of calcium-sensing receptor mutations expressed in human embryonic kidney cells. *J. Clin. Invest.* 98(8): 1860-1866, 1996.
- 26 Ho, C., Conner, DA., Pollack, MR., Ladd, DJ., Kifor, O., Warren, HB., Brown, EM., Seidman, JG., Seidman, CE. : A mouse model of human familial hypocalciuric hypercalcemia and neonatal severe hyperparathyroidism. *Nature Genetics* 11: 389-394, 1995
- 27 Aida, K. Koishi, S., Inoue, M. Nakazato, M., Tawata, M., Onaya, T. : Familial hypocalciuric hypercalcemia associated with mutation in the human  $\text{Ca}^{2+}$ -sensing receptor gene. *J. of Clin. Endocrinology and Metabolism.* 80(9): 2594-2598, 1995
- 28 Bai, M., Janicic, N., Trivedi, S., Quinn, S.J., Cole, DEC., Brown, EM., Hendy, GN. :Markedly reduced activity of mutant calcium-sensing receptor with an inserted alu element from a kindred with familial hypocalciuric hypercalcemia and neonatal severe hyperparathyroidism. *J. Clin. Invest.* 99:1917-1925, 1997

- 29 Heath, III., Odelberg, S., Jackson, CF., Teh, BT., Hayward, N., Larsson, C., Buist, NRM., Krapcho, KJ., Hung, BC., Capuano, I., Garrett, JE., Leppert, MF. : Clustered inactivating mutations and benign polymorphisms of the calcium receptor gene in familial benign hypocalciuric hypercalcemia suggest receptor functional domains. *J. Clin. Endocrinol. Metab.* 81:1312-1317, 1996
- 30 Chou, Y., Pollak, M., Brandi, G., Toss, H., Arnqvist A., Atkinson, S. Papapoulos, S., Marx, S.E., Brown, E., Seidman, J., Seidman, C. : Mutations in the human  $\text{Ca}^{2+}$ -sensing receptor gene that cause familial hypocalciuric hypercalcemia. *Am. J. of Human Genetics.* 56:1075-1079. 1995
- 31 Pearce, S.H. Bai, M., Quinn, S.J., Kifor, O. Brown, EM. Thakker, RV. :Functional characterization of calcium-sensing receptor mutations expressed in human embryonic kidney cells. *J Clin. Invest.* 98(8):1860-6, 1996.
- 32 Bai, M., Quinn, S., Trivedi, S., Kifor, O., Pearce, SHS., Pollak, MR., Krapcho, K., Hebert, SC., Brown, EM. :Expression and characterization of inactivating and activating mutations in the human  $\text{Ca}^{2+}$ -sensing receptor. *J. Biol. Chem.* 271:19537-19545, 1996
- 33 Pollak, MR., Brown, EM., Estep, HL., McLaine, PN., Kifor, O., Park, J., Hebert, SC., Seidman, CE., Seidman, JG. : Autosomal dominant hypocalcemia caused by a  $\text{Ca}^{2+}$ -sensing receptor gene mutation. *Nature Genetics* 8:303-307, 1994
- 34 Brown, E.: Mutations in the calcium-sensing receptor and their clinical implications. *Hormone Research* 48: 199-208. 1997
- 35 Pearce, S.H., Brown, EM. :Calcium-sensing receptor mutations: insights into a structurally and functionally novel receptor. *J. of Clin. Endocrinology & Metabolism.* 81(4):1309-11, 1996
- 36 Quamme, GA.: Magnesium homeostasis and renal magnesium handling. *Mineral & Electrolyte Metabolism.* 19(4-5):218-25, 1993.
- 37 Costanza, L. and Windhager, E.: Renal regulation of calcium: In *The Kidney: Physiology and Pathophysiology* edited by D.W. Seldin and G. Giebisch. New York: Raven, p.2375-2393, 1992
- 38 Kriz, W., and Bankir, L. : A standard nomenclature for structures of the kidney. *Am. J. Physiol.* 254 (Renal Fluid Electrolyte Physiol.23): F1-F8, 1988
- 39 Friedman, PA., Gesek, FA.: Cellular calcium transport in renal epithelia: measurement, mechanisms, and regulation. *Physiological Reviews* 75:429-471, 1995

- 40 Friedman, P.A., Gesek, F.A. : Sodium entry mechanisms in distal convoluted tubule cells. *Am. J. Physiol.* 268:F89-F98, 1995
- 41 Gesek, F.A., and Friedman, P.A. On the mechanism of parathyroid hormone stimulation of calcium uptake by mouse distal convoluted tubule cells. *J. Clin. Invest.* 90: 749-758, 1992.
- 42 Pizzonia, JH., Gesek, F.A., Kennedy, SM., Coutermarsh BA., Bacskai, BJ., Friedman, P.A.: Immunomagnetic separation, primary culture and characterization of cortical thick ascending limb plus distal convoluted tubule cells from mouse kidney. *In Vitro Cell. & Dev. Biol.* 27A: 409-416, 1991.
- 43 Friedman, P.A. and Gesek, F.A.: Mechanism of calcium transport stimulated by chlorothiazide in mouse distal convoluted tubule cells. *J. Clin. Invest.* 90: 429-438, 1992.
- 44 Bapty, BW., Dai, L-J., Ritchie, G., Jirik, F., Canaff, L., Hendy, GN., Quamme, GA.: Extracellular  $Mg^{2+}$ - and  $Ca^{2+}$ -sensing in mouse distal convoluted tubule cells. *Kidney Int.*, 53: 583-592, 1998.
- 45 Fan, G., Goldsmith, P.K., Collins, R., Dunn, C.K., Krapcho, K.J., Rogers, K.K., Spiegel, AM.: N-linked glycosylation of the human  $Ca^{2+}$  receptor is essential for its expression at the cell surface. *Endocrinology* 138:1916-1922, 1997
- 46 Grynkiewicz, G., Poenie, M., Tsien, R.Y.: A new generation of  $Ca^{2+}$  indicators with greatly improved fluorescence properties. *J. of Biol. Chem.* 260(6):3440-50, 1985.
- 47 Malgaroli, A., Milani, D., Meldolesi, J., Pozzan, T.: Fura-2 measurement of cytosolic free  $Ca^{2+}$  in monolayers and suspensions of various types of animal cell. *J. of Cell Biology.* 105(5):2145-55, 1987
- 48 Dai, L.J., Quamme, GA.: Cyclic nucleotides alter intracellular free  $Mg^{2+}$  in renal epithelial cells. *Am. J. Physiol.*, 262,F1100, 1992.
- 49 Dai, L-J., Bapty, BW., Ritchie, G., and Quamme, GA.: Glucagon and arginine vasopressin stimulates  $Mg^{2+}$  uptake in mouse distal convoluted tubule cells. *Am. J. Physiol.* 274 (Renal Physiol. 43): F328-F335, 1998.

- 50 Emanuel, RL., Adler, GK., Kifor, O., Quinn, SJ., Fuller, F., Krapcho, K., Brown, EM. : Calcium-sensing receptor expression and regulation by extracellular calcium in the AtT-20 pituitary cell line. *Molecular Endocrinology* 10:555-565, 1996
- 51 Garrett, JE., Tamir, H., Kifor, O., Simin, RT., Rodgers, KV., Mithal, A., Gagel, RF., Brown, EM. : Calcitonin-secretory cells of the thyroid express an extracellular calcium receptor gene. *Endocrinology* 136:5202-5211, 1995
- 52 Freichel, M., Zink-Lorenz, A., Holloschi, A., Hafner, M., Flockerzi, V., Raue, F. : Expression of a calcium-sensing receptor in a human medullary thyroid carcinoma cell line and its contribution to calcitonin secretion. *Endocrinology* 137:3842-3848, 1996
- 53 Quarles, LD., Hartle, JE., Siddhanti, SR., Guo, R., Hinson, TK. : A distinct cation-sensing mechanism in MC3T3-E1 osteoblasts functionally related to the calcium receptor. *J. Bone Miner. Res.* 12:393-402, 1997
- 54 Brown, EM., Fuleihan, GEH., Chen, C., Kifor, O.R. : A comparison of the effects of divalent and trivalent cations on parathyroid hormone release, 3', 5'-cyclic-adenosine monophosphate accumulation, and the levels of inositol phosphates in bovine parathyroid cells. *Endocrinology* 127: 1064-1071, 1990.
- 55 Brown, EM., Enyedi D., Leboff M., Rotberg J., Preston J., Chen C. : High extracellular  $\text{Ca}^{2+}$  and  $\text{Mg}^{2+}$  stimulate accumulation of inositol phosphates in bovine parathyroid cells. *FEBS Lett.* 218:113-118, 1987
- 56 Chen, C.J., Anast, CS., Posillico, JT., and Brown, EM.: Effects of extracellular calcium and magnesium on cytosolic calcium concentration in fura-2-loaded bovine parathyroid cells. *J. Bone Mineral Res.* 2: 319-327, 1987.
- 57 Hawkins, D., Enyed, IP., Brown, EM.: The effects of high extracellular  $\text{Ca}^{2+}$  and  $\text{Mg}^{2+}$  concentrations on the levels of inositol 1,3,4,5 tetrakisphosphate in bovine parathyroid cells. *Endocrinology* 124:838-844, 1989
- 58 Nemeth, EF., Scarpa, A: Rapid mobilization of cellular  $\text{Ca}^{2+}$  in bovine parathyroid cells by external divalent cations. Evidence for a cell surface calcium receptor. *J. Biol. Chem.* 262: 5188-5196, 1987

- 59 Shoback, DM., Thatcher, JG., Brown, EM. : Interaction of extracellular calcium and magnesium in the regulation of cytosolic calcium and PTH release in dispersed bovine parathyroid cells. *Mol. Cellular Endocrinol.* 38:179-181, 1984
- 60 Gesek, F.A., and Friedman, PA.: Calcitonin stimulates calcium transport in distal convoluted tubule cells. *Am. J. Physiol.* 264 (Renal Fluid Electrolyte Physiol.33): F744-F751, 1993.
- 61 Dai, L-J., Raymond, L., Friedman, PA., Quamme, GA.: Cellular mechanisms of amiloride stimulation of  $Mg^{2+}$  uptake in mouse distal convoluted tubule cells. *Am. J. Physiol.* 272 (Renal Physiol. 41): F249-F256, 1997.
- 62 Ruat, M., Snowman, AM., Hester, LD., Snyder, SH. : Cloned and expressed rat  $Ca^{2+}$ -sensing receptor: differential cooperative responses to calcium and magnesium. *J. Biol. Chem.* 271:5972-5975, 1996
- 63 Dai, L-J., Quamme, GA.: Hormone-mediated  $Ca^{2+}$  transients in isolated renal cortical thick ascending limb cells. *Pflügers Archiv.* 427:1-8, 1994
- 64 Clemens, TL., Mcglade, SA., Garrett, KP., Craviso, GL., Hendy, GN. : Extracellular calcium modulates vitamin D-dependent calbindin-D28K gene expression in chick kidney cells. *Endocrinology* 124:1582-1584., 1989
- 65 Sneddon, WB., Gesek, FA., Friedman, PA. :  $1,25-(OH)_2$  vitamin  $D_3$  up-regulates the expression of the parathyroid hormone receptor in distal convoluted tubule cells. *J. Am. Soc. Nephrol.* 4:729, 1993 (Abstract)
- 66 Marx, SJ., Spiegel, A.M., Brown, EM., Koehler, JO., Gardner, DG., Brennan, MF., Aurbach, GD.: Divalent cation metabolism: familial hypocalciuric hypercalcemia versus typical primary hyperparathyroidism. *Am.J. Med.* 65:235-242, 1978
- 67 Marx, SJ., Attie, MF., Levine, MA., Spiegel, A.M., Downs, RW Jr., Lasker, RD. : The hypocalciuric or benign variant of familial hypercalcemia: clinical and biochemical features in fifteen kindreds. *Medicine (Baltimore)* 60:235-242, 1981
- 68 Attie, MF., Gill, Jr J., Stock, JL., Spiegel, AM., Downs, AM. Jr., Levine, MA., Marx, SJ. : Urinary calcium excretion in familial hypocalciuric hypercalcemia. Persistence of relative hypocalciuria after induction of hypoparathyroidism. *J. Clin. Invest.* 72:667-676, 1983

- 69 Slatopolsky, E., Mercado, A., Morrison, A., Yates, J., Klahr, S. : Inhibiting effects of hypermagnesiuria on the renal action of parathyroid hormone. *J. Clin. Invest.* 58: 1273-1279., 1976
- 70 Takaichi, K., Kurokawa, K. : High  $\text{Ca}^{2+}$ -inhibits peptide hormone-dependent cAMP production specifically in thick ascending limbs of Henle. *Miner. Electrolyte Metab.* 12:342-346, 1986
- 71 Takaichi, K., Kurokawa, K. : Inhibitory guanosine triphosphate-binding protein-mediated regulation of vasopressin action in isolated single medullary tubules of mouse kidney. *J. Clin. Invest.* 82:1437-1444, 1988
- 72 Jones, SM., Frindt, TG., Windhager, EE. : Effect of peritubular  $[\text{Ca}]$  or ionomycin on hydrosmotic response of CCD to ADH or cAMP. *Am. J. Physiol.* 254:F240-F253, 1988
- 73 Chen, C.J., Barnett, J.V., D.A. Congo, and Brown, EM.: Divalent cations suppress 3',5'-adenosine monophosphate accumulation by suppressing a pertussis toxin-sensitive guanine nucleotide-binding protein in cultured bovine parathyroid cells. *Endocrinology* 124: 233-239, 1989.
- 74 Quamme GA. : Magnesium: Cellular and renal exchanges. In: *The Kidney: Physiology and Pathophysiology* edited by D.W. Seldin and G. Giebisch. New York: Raven, p.2339-2356, 1992
- 75 Bapty, BW., Dai, L-J., Ritchie, G., Canaff, L., Hendy, GN., Quamme, GA.: Activation of  $\text{Mg}^{2+}/\text{Ca}^{2+}$ -sensing inhibits hormone-stimulated  $\text{Mg}^{2+}$  uptake in mouse distal convoluted tubule cells. *Am. J. Physiol. (Renal Physiology.* 44): F353-360, 1998.
- 76 Shafik, I., Quamme, G.: Early adaptation of renal magnesium reabsorption in response to magnesium restriction. *Am. J. Physiol.* 257:F974-F977, 1989.
- 77 Carney, SL., Wong, NLM., Quamme, GA., Dirks JH. : Effect of magnesium deficiency on renal magnesium and calcium transport in the rat. *J. Clin. Invest.* 65: 180-188, 1980.
- 78 Quamme, GA. Renal magnesium handling: New insights in understanding old problems. *Kidney Int.* 52: 1180-1195, 1997.
- 79 Goudeau, M., and Goudeau, H. External  $\text{Mg}^{2+}$  triggers oscillations and subsequent sustained level of intracellular free  $\text{Ca}^{2+}$ , correlated with changes in membrane conductance in the oocyte of the prawn *Palaemon serratus*. *Developmental Biology* 177: 178-189, 1996.

- 80 Goudeau, M., and Goudeau, H.: Depletion of intracellular  $\text{Ca}^{2+}$  stores, mediated by  $\text{Mg}^{2+}$ -stimulated  $\text{IP}_3$  liberation or thapsigargin, induces a capacitative  $\text{Ca}^{2+}$  influx in prawn oocytes. *Developmental Biology*, 193, 225-238. 1998
- 81 Hinson, TK., Damodaran, J., Chen, J., Zhang, X., Qumsiyeh, MB., Seldin, MF., Quarles, LD.: Identification of putative transmembrane receptor sequences homologous to the calcium sensing G-protein coupled receptor. *Genomics* 45, 279-289, 1997.
- 82 Naito, T., Saito, Y., Yamamoto, J., Nozaki, Y., Tomura, K. Hazama, M., Nakaanishi, S., Brenner, S.: Putative pheromone receptors related to the  $\text{Ca}^{2+}$ -sensing receptor in Fugu. *Proc. Nat. Acad. Sc. USA* 95, 5178-5181, 1998
- 83 Ryba, NJP., Tirindelli, R.: A new multigene family of putative pheromone receptors. *Neuron* 19, 371-379, 1997.
- 84 Nearing, J., Bai, M., Albanese, T., Abe, T., Hebert, SC., Brown, EM., and Harris, HW.: Cloning and expression of a homologue of the calcium ( $\text{Ca}^{2+}$ )/polyvalent cation sensing receptor (Car) protein that acts as a magnesium ( $\text{Mg}^{2+}$ ) sensor in the dogfish shark (*Squalus acanthias*). *Am. Soc. Nephrol., Programs and Abstracts*, 30<sup>th</sup> AGM, A0194. 1997
- 85 Massry, SG., and Coburn, JW. : The hormonal and non-hormonal control of renal excretion of calcium and magnesium. *Nephron* 10: 66-112, 1973.
- 86 Quamme, GA., and Dirks, JH.: Magnesium metabolism. In: *Clinical Disorders of Fluid and Electrolyte Metabolism*, edited by R.G. Narins, McGraw-Hill Inc., 1994, p.373-398.
- 87 Dai, L-J., Bapty, B., Ritchie, G., Friedman, PA., Quamme, GA.: Glucagon and arginine vasopressin stimulate  $\text{Mg}^{2+}$  uptake in mouse distal convoluted tubule cells. *Am. J. Physiol* 274(2 pt2):F328-35, 1998
- 88 Bailly, C., and Amiel, C.: Effect of glucagon on magnesium renal reabsorption in the rat. *Pflügers Arch.* 392: 360-365, 1982.
- 89 Bailly, C., Roinel, N., and Amiel, C.: Stimulation by glucagon and PTH of Ca and Mg reabsorption in the superficial distal tubule of the rat kidney. *Pflügers Arch.* 403: 28-34, 1985.
- 90 Koeppen, BM., and Stanton, BA.: Sodium chloride transport: distal nephron. In: *The Kidney: Physiology and Pathophysiology*. Raven Press Ltd. NY. 2nd Edition. Edited by Seldin, D.W., and G. Giebisch. 1992, pp 2003-2039.

- 91 Bouby, N., Trinh-Trang-Tan, M-M., Bankir, L.: Stimulation of tubular reabsorption of magnesium and calcium by antidiuretic hormone in conscious rats: study in Brattleboro rats with hereditary hypothalamic diabetes insipidus. *Pflügers Arch.* 402: 458-464, 1984.
- 92 Elalouf, JM., Roinel, N., de Rouffignac, C.: Effects of antidiuretic hormone on electrolyte reabsorption and secretion in distal tubules of rat kidney. *Pflügers Arch.* 401: 167-173, 1984.
- 93 DeRouffignac, C., Corman, B., N. Roinel.: Stimulation by antidiuretic hormone of electrolyte tubular reabsorption in rat kidney. *Am. J. Physiol.* 244 (Renal Fluid Electrolyte Physiol. 13): F156-F164, 1983.
- 94 Costanzo, LS., and Windhager, EE.: Effect of PTH, ADH and cyclic AMP on distal tubule Ca and Na reabsorption. *Am. J. Physiol.* 239 (Renal Fluid Electrolyte Physiol. 8): F478-F485, 1980.
- 95 Massry, SG., Coburn, JW., Kleeman, CR.: Renal handling of magnesium in the dog. *Am. J. Physiol.* 216: 1460-1467, 1969.
- 96 Arthur, JM.: The calcium-sensing receptor (CaR) inhibits calcium transport in a model of renal distal tubule. *J. Am. Soc. Nephrol.* 8: 557A, 1997 (Abstract).
- 97 Quamme, GA., Dirks, JH.: Effect of intraluminal and contraluminal magnesium on magnesium and calcium transfer in the rat nephron. *Am. J. Physiol.* 238 (Renal Fluid Electrolyte Physiol. 7): F187-F198, 1980.
- 98 Quamme, GA., Effect of furosemide on calcium and magnesium transport in the rat nephron. *Am. J. Physiol.* 241 (Renal Fluid Electrolyte Physiol. 10): F340-F347, 1981.
- 99 Quamme, GA., Carney, SL., Wong, NLM., Dirks, JH.: Effect of parathyroid hormone on renal calcium and magnesium reabsorption in magnesium deficient rats. *Pflügers Arch.* 386: 59-65, 1980.
- 100 Quamme, GA., and J.H. Dirks. Effect of intraluminal and contraluminal magnesium on magnesium and calcium transfer in the rat nephron. *Am. J. Physiol.* 238 (Renal Fluid Electrolyte Physiol. 7): F187-F198, 1980.
- 101 Harris, CA., Burnatowska, MA., Seely, JF., Sutton, RAL., Quamme, GA., Dirks, JH.: Effects of parathyroid hormone on electrolyte transport in the hamster nephron. *Am. J. Physiol.* 246 (Renal Fluid Electrolyte Physiol. 15): F745-F756, 1984.

- 102 deRouffignac, C. , Elalouf, JM., Roinel, N., Bailly, C., and Amiel, C.: Similarity of the effects of antidiuretic hormone, parathyroid hormone, calcitonin and glucagon on rat kidney. In: Nephrology, edited by R.R. Robinson: Springer, 1984, p340-357.
- 103 Poujeol, P., Touvay, C., Roinel, N. and deRouffignac, C.: Stimulation of renal magnesium reabsorption by calcitonin in the rat. *Am. J. Physiol.* 239 (Renal Fluid Electrolyte Physiol. 8): F524-F532, 1980.
- 104 Elalouf, JM., Roinel, N., De Rouffignac, C.: Stimulation by human calcitonin of electrolyte transport in distal tubules of rat kidney. *Pflügers Arch.* 399: 111-118, 1983
- 105 Bailly, C., Imbert-Teboul, M., Chabardés, D., Hus-Citharel, A., Montégut, M., Clique, A., Morel, F.: The distal nephron of rat kidney: a target site for glucagon. *Proc. Natl. Acad. Sci. USA* 77: 3422-3424, 1980.
- 106 Morel, F.: Sites of hormone action in the mammalian nephron. *Am. J. Physiol.* 240 (Renal Fluid Electrolyte Physiol.9): F159-F164, 1981.
- 107 Morel, F., Imbert-Teboul, M., Chabardés, D.: Receptors to vasopressin and other hormones in the mammalian kidney. *Kidney Int.* 31: 512-520, 1987.
- 108 Friedman, PA. and Gesek, FA.: Calcium transport in renal epithelial cells. *Am. J. Physiol.* 264 2(Renal Fluid Electrolyte Physiol. 38): F181-F198, 1993.
- 109 Friedman, PA., Coutermarsh, BA., Kennedy, SM., Gesek, FA.: Parathyroid hormone stimulation of calcium transport is mediated by dual signalling mechanisms involving protein kinase A and renal protein kinase C. *Endocrinology* 137: 13-20, 1996.
- 110 Hilal, G., Claveau, D., Zuo, Q., Brunette, MG.: Interaction of second messengers on  $\text{Ca}^{2+}$  uptake by the renal distal luminal membranes. *J. Am. Soc. Nephrol.* 6: 950, 1995.(Abstract)
- 111 Ahloulay, M., Déchaux, M., Laborde, K., Bankir, L.: Influence of glucagon on GFR and on urea and electrolyte excretion: direct and indirect effects. *Am. J. Physiol.* 269 (Renal Fluid Electrolyte Physiol. 38): F225-F235, 1995.
- 112 Wittner, M., Di Stefano, A.: Effects of antidiuretic hormone, parathyroid hormone and glucagon on the cortical and medullary thick ascending limb of Henle's loop of the mouse nephron. *Pflügers Arch.* 415: 707-712, 1990.

- 113 Friedman, PA., Gesek, FA.: Vitamin D<sub>3</sub> accelerates PTH-dependent calcium transport in distal convoluted tubule cells. *Am. J. Physiol.* 265 (Renal Fluid Electrolyte Physiol. 34): F300-F308, 1993.
- 114 Lajeunesse, D., Bouhtiauy, I., Brunette, M.G.: Parathyroid hormone and hydrochlorothiazide increase calcium transport by the luminal membrane of rabbit distal nephron segments through different pathways. *Endocrinology* 134: 35-41, 1994.
- 115 Bailly, C., Roinel, N., Amiel, M.: PTH-like glucagon stimulation of Ca and Mg reabsorption in Henle's loop of the rat. *Am. J. Physiol.* 246 (Renal Fluid Electrolyte Physiol. 15): F205-F212, 1984.
- 116 Di Stefano, A., Wittner, M., Nischke, R., Braitsch, R., Greger, R., Bailly, C., Amiel, C., Elalouf, JM., Roinel, N., de Rouffignac, C.: Effect of glucagon on Na<sup>+</sup>, Cl, K<sup>+</sup>, Mg<sup>2+</sup> and Ca<sup>2+</sup> transport in cortical and medullary thick ascending limbs of mouse kidney. *Pflügers Arch.* 414: 640-646, 1989.
- 117 deRouffignac, C.: Multihormonal regulation of nephron epithelia: achieved through combinational mode? *Am. J. Physiol.* 269 (Regulatory Integrative Comp. Physiol. 38): R739-R748, 1995.
- 118 Le Grimellec C., Roinel, N., Morel, F.: Simultaneous Mg, Ca, P, K, Na and Cl analysis in rat tubular fluid. II. During acute Mg plasma loading. *Pflügers Arch.* 340: 197-210, 1973.
- 119 Le Grimellec C., Roinel, N., Morel, F.: Simultaneous Mg, Ca, P, K, Na and Cl analysis in rat tubular fluid. III. During acute Ca plasma loading. *Pflügers Arch.* 346: 171-189, 1974.
- 120 Quamme, GA.: Effect of hypercalcemia on renal tubular handling of calcium and magnesium. *Can. J. Physiol. Pharmacol.* 60: 1275-1280, 1980.
- 121 Quamme GA, Dirks JH. : Effect of intraluminal and contraluminal magnesium and calcium transport in the rat nephron. *Am J Physiol* 238:F187-F198, 1980.
- 122 Quamme, GA.: Effect of furosemide on calcium and magnesium transport in the rat nephron. *Am. J. Physiol.* 241 (Renal Fluid Electrolyte Physiol. 10): F340-F347, 1981.
- 123 Hebert SC.: Extracellular calcium-sensing receptor: implications for calcium and magnesium handling in the kidney. *Kidney Int.* 50:2129-2139, 1996

- 124 Wong, NLM., Dirks, JH., Quamme, GA.: Tubular maximum reabsorption capacity for magnesium in the dog. *Am. J. Physiol.* 244 (Renal Fluid Electrolyte Physiol. 13): F78-F83, 1983.
- 125 Di Stefano, A., Roinel, N., de Rouffignac, C., Wittner, M.: Transepithelial  $\text{Ca}^{2+}$  and  $\text{Mg}^{2+}$  transport in the cortical thick ascending limb of Henle's loop of the mouse is a voltage-dependent process. *Renal Physiol. Biochem.* 16: 157-166, 1993.
- 126 Doucet, A, Katz, AI.: Mineralocorticoid receptors along the nephron:  $^3\text{H}$  aldosterone binding in rabbit tubules. *Am. J. Physiol.* 241 (Renal Fluid Electrolyte Physiol. 10): F605-F611, 1981.
- 127 Farman, N., Bonvalet, JP.: Aldosterone binding in isolated tubules. III. Autoradiography along the rat nephron. *Am. J. Physiol.* 245 (Renal Electrolyte Physiol. 15): F606-F614, 1982.
- 128 Farman, N., Vandewalle, A., Bonvalet, JP.: Aldosterone binding in isolated tubules. II. An autoradiography study of concentration dependency in the rabbit nephron. *Am. J. Physiol.* 245 (Renal Fluid Electrolyte Physiol. 12): F69-F77, 1982.
- 129 Krozowski, ZS., Rundle, SE., Wallace, C., Castell, MJ., Shen, JH., Dowling, J., Funder, JW., Smith, AI.: Immunolocalization of renal mineralocorticoid receptor with an antiserum against a peptide deduced from the complementary deoxyribonucleic acid sequence. *Endocrinology* 125 :192-198, 1981.
- 130 Koeppen, BM., Stanton, BA.: Sodium chloride transport: distal nephron. In: *The Kidney: Physiology and Pathophysiology*, edited by D.W. Seldin and G. Giebisch. New York: Raven, 1992, p. 2003-2040.
- 131 Rossier, BC., Palmer, LG.: Mechanisms of aldosterone action on sodium and potassium transport. In: *The Kidney: Physiology and Pathophysiology*, edited by D.W. Seldin, and G. Giebisch. New York, Raven, 1992, p. 1373-1410.
- 132 Chen, Z., Vaughn, DA., Blakeley, P., Fanestil, DD.: Adrenocortical steroids increase renal thiazide diuretic receptor density and response. *J. Am. Soc. Nephrol.* 5: 1361-1368, 1994.
- 133 Velázquez, H., Bartiss, A., Bernstein, P., Ellison, DH.: Adrenal steroids stimulate thiazide-sensitive  $\text{NaCl}$  transport by rat distal tubules. *Am. J. Physiol.* 270 (Renal Fluid Electrolyte Physiol. 39): F211-F219, 1996.

- 134 Doucet, A., Barlet-Bas, C., Siaume-Perez, S., Khadouri, C., Marsy, S.: Gluco-and mineralocorticoids control adenylate cyclase in specific nephron segments. *Am. J. Physiol.* 258 (Renal Fluid Electrolyte Physiol. 27): F812-F820, 1990.
- 135 El Mernissi, G., Barlet-Bas, C., Khadouri, C., Cheval, L., Marsy, S., Doucet, A.: Short-term effect of aldosterone on vasopressin-sensitive adenylate cyclase in rat collecting tubule. *Am. J. Physiol.* 264 (Renal Fluid Electrolyte Physiol. 33): F821-F826, 1993.
- 136 Jackson, B.A., Braun-Werness, J.L., Kusano, E., Dousa, T.P.: Concentrating defect in the adrenalectomized rat. Abnormal vasopressin-sensitive cyclic adenosine monophosphate metabolism in the papillary collecting duct. *J. Clin. Invest.* 72: 997-1004, 1983.
- 137 Rajerison, R.M., Marchetti, J., Roy, C., Bockaert, J., Jard, S.: The vasopressin-sensitive adenylate cyclase of the rat kidney. Effect of adrenalectomy and corticosteroids on hormonal receptor-enzyme coupling. *J. Biol. Chem.* 249: 6390-6400, 1974.
- 138 Schwartz, M.J., Kokko, J.P.: Urinary concentrating defect of adrenal insufficiency. Permissive role of adrenal steroids on the hydroosmotic response across the rabbit cortical collecting tubule. *J. Clin. Invest.* 66: 234-242, 1980.
- 139 Dai, L.-J., Ritchie, G., Bapty, B., Quamme, G.: Aldosterone potentiates hormone-stimulated  $Mg^{2+}$  uptake in distal convoluted tubule cells. *Am. J. Physiol.* 274 (2 Pt 2): F336-341, 1998.
- 140 Schafer, J.A., Hawk, C.T.: Regulation of  $Na^+$  channels in the cortical collecting duct by AVP and mineralocorticoid. *Kidney Int.* 41: 255-268, 1992.
- 141 Dai, L.-J., Friedman, P.A., Quamme, G.A.: Cellular mechanisms of chlorothiazide and potassium depletion on  $Mg^{2+}$  uptake in mouse distal convoluted tubule cells. *Kidney Int.*, 51: 1008-1017, 1997.
- 142 Van OS, C.H.: Transcellular calcium transport in intestinal and renal epithelial cells. *Biochim Biophys Acta* 906:195-222, 1987
- 143 Kumar R.: Vitamin D metabolism and mechanism of calcium transport. *J Am Soc Nephrol* 1:30-42, 1990
- 144 Liu, L.T., Ng, M., Iacopino, A.M., Dunn, S.T., Hughes, M.R., Bourdeau, J.E.: Vitamin D receptor gene expression in mammalian kidney. *J Am Soc Nephrol* 5:1251-1258, 1994

- 145 Roth, J., Brown, D., Norman, AW., Orci, L.: Localization of the vitamin D-dependent calcium-binding protein in mammalian kidney. *Am J Physiol* 243:F243-F252, 1982
- 146 Stumpf, WE., Sar, M., Narbaitz, R., Reid, FA., De Luca, HF., Tanaka, Y. : Cellular and subcellular localization of 1,25(OH)<sub>2</sub>-vitamin D<sub>3</sub> in rat kidney, comparison with localization of parathyroid hormone and oestradiol. *Proc Natl Acad Sci USA* 77:1149-1153, 1980
- 147 Manillier, C., Farman, N., Bonjour, JP., Bonvalet, JP. : 1,25(OH)<sub>2</sub> D<sub>3</sub> binding along the rat nephron: Autoradiographic study in isolated tubular segments. *Am J Physiol* 248:F296-F307, 1985
- 148 Wasserman, RH., Fullmer, CS.: Vitamin D and intestinal calcium transport: facts, speculations and hypotheses. *J Nutr* 125: S1971-S1979, 1995
- 149 Borke, JL., Caride, A., Verma, AK., Penniston, JT., Kumar, R.: Plasma membrane calcium pump and 28-kDa calcium binding protein in cells of rat kidney distal tubules. *Am J Physiol* 257:F842-F849, 1989
- 150 Feher, JJ., Fullmer, CS., Wasserman, RH.: Role of facilitated diffusion of calcium by calbindin in intestinal calcium absorption. *Am J Physiol* 262:C517-C526, 1992
- 151 Bouhtiauy, I., Lajeunesse, D., Brunette, MG.: Effect of vitamin D depletion on calcium transport by the luminal and basolateral membranes of the proximal and distal nephrons. *Endocrinology* 132:115-120, 1993
- 152 Bouhtiauy, L., Lajeunesse, D., Christakos, S., Brunette, MG. : Vitamin-D<sub>3</sub>-dependent calcium binding proteins increase calcium reabsorption by different mechanisms. I. Effect of CaBP-28K. *Kidney Int.* 45:461-468, 1994
- 153 Bouhtiauy, L., Lajeunesse, D., Christakos, S., Brunette, MG. : Two vitamin-D<sub>3</sub>-dependent calcium binding proteins increase calcium reabsorption by different mechanisms. I. Effect of CaBP-9K. *Kidney Int.* 45:469-474, 1994
- 154 Koster, HPG., Hartog, A., Van Os, CH., Bindels, RJM.: Calbindin-D28k facilitates cytosolic calcium transport without interfering with calcium signalling. *Cell Calcium* 18:187-196, 1995

- 155 Timmermans, JAH., Bindels, RJM., Van Os, CH. : Stimulation of plasma membrane  $\text{Ca}^{2+}$  pump by calbindin-D28k and calmodulin is additive in EGTA-free solutions. *J Nutr* 125:S1981-S1986, 1995
- 156 Costanzo, LS., Sheehe, PR., Weiner, IM.: Renal actions of vitamin D in D-deficient rats. *Am J Physiol* 226:864-870, 1974
- 157 Bindels, RJM., Hartog, A., Timmermans, J., Van Os, CH.: Active  $\text{Ca}^{2+}$  transport in primary cultures of rabbit kidney CCD: stimulation by 1,25-dihydroxyvitamin D<sub>3</sub> and PTH. *Am J Physiol* 261:F799-F807, 1991
- 158 Puschett, JB., Beck, WS., Jelonek, A., Fernandez, PC.: Study of the renal tubular interactions of thyrocalcitonin, cyclic adenosine 3'5-monophosphate, 25-hydroxycholecalciferol and calcium ion. *J Clin Invest* 53:756-767, 1974
- 159 Huji, K., Bonjour, J-P., Fleisch, H. : Renal handling of calcium: influence of parathyroid hormone and 1,25-dihydroxyvitamin D<sub>3</sub>. *Am J Physiol* 236:F349-F356, 1979
- 160 Puschett, J.B.: Micropuncture study of the acute renal tubular transport effects of 25-hydroxyvitamin D<sub>3</sub> in the dog. *Miner Electrolyte Metab* 4:178-188, 1980
- 161 Burnatowska, MA., Harris, CA., Sutton, RAL., Seely, JF. : Effects of vitamin D on renal handling of calcium, magnesium, and phosphate in the hamster. *Kidney Int.* 27:864-870, 1985
- 162 Hanna, S. : Influence of large doses of vitamin D on magnesium metabolism in rats. *Metab Clin Exp* 10:735-743, 1961
- 163 Hanne, S., Alcock, N., Lazarus, B., Mallan, B. : Changes in gut and urinary ciliates following low calcium and magnesium diet and administration of vitamin D. *J Lab Clin Med* 61:220-229, 1963
- 164 Miller, ER., Ullrey, HG., Zutan, CL., Hoefer, JA., Luecke, RW. : Mineral balance studies with the baby pig: Effects of dietary vitamin D<sub>3</sub> level on Ca, P, and Mg balance. *J Nutr* 85:255-259, 1965
- 165 Richardson, JA., Welt, LG. : Hypomagnesemia of vitamin D administration. *Proc Soc Exp Med* 118:512-514, 1965

- 166 Lifshitz, F., Harrison, HC., Harrison, HE, : Effects of vitamin D on magnesium metabolism in rats. *Endocrinology* 81:849-853, 1967
- 167 Anast, CS., Gardner, DW. : Magnesium metabolism. *Disorders of Mineral Metabolism* 3:424-506, 1981
- 168 Delvin, EE., Salle, BL., Glorieux, FH., Adeleine, P., David, S.: Vitamin D supplementation during pregnancy: effect on neonatal calcium homeostasis. *J Pediatrics* 109: 328-334, 1986
- 169 Mortensen, L., Hyldstrup, L., Charles, P.: Effect of vitamin D treatment in hypoparathyroid patients: a study on calcium, phosphate and magnesium homeostasis. *European J Endocrinol* 136:25-30 , 1997
- 170 Norman, AW., Nemere, I., Zhou, L-X., Bishop, JE., Lowe, KE., Maiyar, AC., Collins, E., Taoka, T., Sergeev, I., Farach-Carson, MC. : 1,25(OH)<sub>2</sub>-vitamin D<sub>3</sub>, a steroid hormone that produces biologic effects via both genomic and nongenomic pathways. *J Steroid Biochem Mol Biol* 41:231-240, 1992.
- 171 Andersson, M., Malmendal, A., Linse, S., Ivarsson, I., Forsen, S., Svensson, A.:Structural basis for the negative allostery between Ca<sup>2+</sup>- and Mg<sup>2+</sup>-binding in the intracellular Ca<sup>2+</sup>-receptor calbindin D9K. *Protein Sci* 6:1139-1147, 1997.
- 172 Dai, L.-J., Bapty, B., Ritchie, G., Quamme, GA.: PGE<sub>2</sub> stimulates Mg<sup>2+</sup> uptake in mouse distal convoluted tubule cells. *Am. J. Physiol.* 275: 833-839, 1998
- 173 Bailly, C., Imbert-Teboul, M., Chabardés, M., Hus-Citharel, A., Montégut, M., Clique, A., Morel, F.: The distal nephron of rat kidney: a target site for glucagon. *Proc. Natl. Acad. Sci. USA* 77: 3422-3424, 1980.
- 174 Chabardés, D., Imbert-Teboul, M., Gagnon-Burnette, M., Morel, F.: Different hormonal target sites along the mouse and rabbit nephrons: *Biochemical Nephrology*, edited by W.G. Guder, and U. Schmidt, Bern: Huber, 1978, p.447-454.
- 175 Lea, JP., Ertoy, D., Hollis, JL., Marrero, MB., Sands, JM.: Immunolocalization of phospholipase C isoforms in rat kidney. *Kidney Int.* 54(5):1484-90, 1998.
- 176 Hamm, HE.: The many faces of G protein signaling. *J. Biol. Chem.* 273: 669-672, 1998.
- 177 Le Grimellec, C, Roinel, N., Morel, F.: Simultaneous Mg, Ca, P, K, Na and Cl analysis in rat tubular fluid. IV. During acute Mg plasma loading. *Pflügers Arch.* 340: 197-210, 1973.
- 178 Le Grimellec, C, Roinel, N., Morel, F.: Simultaneous Mg, Ca, P, K, Na and Cl analysis in rat tubular fluid. III. During acute Ca plasma loading. *Pflügers Arch.* 346: 171-189, 1974.